

## Copyright Undertaking

This thesis is protected by copyright, with all rights reserved.

**By reading and using the thesis, the reader understands and agrees to the following terms:**

1. The reader will abide by the rules and legal ordinances governing copyright regarding the use of the thesis.
2. The reader will use the thesis for the purpose of research or private study only and not for distribution or further reproduction or any other purpose.
3. The reader agrees to indemnify and hold the University harmless from and against any loss, damage, cost, liability or expenses arising from copyright infringement or unauthorized usage.

If you have reasons to believe that any materials in this thesis are deemed not suitable to be distributed in this form, or a copyright owner having difficulty with the material being included in our database, please contact [lbsys@polyu.edu.hk](mailto:lbsys@polyu.edu.hk) providing details. The Library will look into your claim and consider taking remedial action upon receipt of the written requests.

COLOUR MEASUREMENT CORRECTION MODEL  
FOR  
IMPROVING INTER-INSTRUMENTAL AGREEMENT

A Thesis Presented for the  
Degree of Doctor of Philosophy

CHUNG Yiu-sing

Institute of Textiles and Clothing

The Hong Kong Polytechnic University

2003



Pao Yue-kong Library  
PolyU • Hong Kong

**TO  
MY FAMILY**

## **ACKNOWLEDGEMENT**

I would like to express my very great appreciation to Dr John H. Xin, Associate Professor of the Institute of Textiles and Clothing at The Hong Kong Polytechnic University, for his very valuable and constructive suggestions during the planning and development of this research work. His willingness to spend his time so generously has been very much appreciated.

I would also like to thank Dr K.M. Sin, Associate Professor of the Institute of Textiles and Clothing at The Hong Kong Polytechnic University, for invaluable advice and a sustained interest and encouragement throughout the period of my research work.

In addition, I would like to express my thanks to all the staff and technicians in the textile chemistry laboratory and evaluation and objective laboratory. I would like to express my thanks to all the lecturers especially Ms Gail Taylor, research students and research assistants in the Institute of Textiles and Clothing at The Hong Kong Polytechnic University for their fully support in the past three years.

Finally, I would like to thank my family and Rise for their great support during the whole study period.



**ABSTRACT**

Accurate colour measurement is a very important factor to determine the quality of finished products in the colour-related industries, such as paint, printing or textiles. In the past, visual colour assessment was used to match colours and physical samples played an important role. The drawback of the visual colour assessment is that, even in the case of well trained colourists, performance is influenced by a number of parameters including psychological, medical and environmental factors. In addition, during the transportation and assessment of the physical samples, there is the risk of soiling. These factors may account for mistakes in colour identification, even in the case of well trained and experienced colourists.

The objective colour communication method is an alternative method to enhance both colour matching and colour assessment. Because of advances in spectrophotometry and information technology, colour quality may be expressed in a digital format and communicated to other parties by electronic means. This format of colour communication represents the trend in view of the regionalisation and globalisation of the textile and apparel industries.

The spectrophotometer is one of the important instruments for colour matching and colour measurement. It performs at a finite level of accuracy but, as an electro-mechanical-optical device, it exhibits measurement errors relative to a theoretically error-free instrument that users must accept. Most of the modern spectrophotometers have satisfactory repeatability and the suppliers of these instruments claim that the repeatability of the measurement on the same instrument is lower than 0.01 CIELAB  $\Delta E$  units. In this research project, it was found that the repeatability of the advanced spectrophotometers ranged from 0.044 to 0.112 CIELAB  $\Delta E$  units for the dual beam spectrophotometers while, for the single beam spectrophotometer, the repeatability ranged from 0.115 to 0.377 CIELAB  $\Delta E$  units.

When considering the inter-instrumental agreement of different makes of spectrophotometers, the manufacturers also claim that the inter-instrumental agreement of those of similar design is lower than 0.15 CIELAB  $\Delta E$  units. However, in this research, it was found that the inter-instrumental agreement between the spectrophotometers manufactured by the same manufacturer ranged from 0.526 to 0.611 CIELAB  $\Delta E$  units. The inter-instrumental agreement between the spectrophotometers manufactured by different manufacturers ranged from 0.575 to 0.854 CIELAB  $\Delta E$  units.

Since the inter-instrumental agreement of the spectrophotometers is very low, various mathematical models have been developed in order to improve the inter-instrumental agreement between spectrophotometers. In past research, those mathematical models were developed using calibration data from the GLOSSY Ceramic Tiles which may not be suitable for application to textile and paper samples.

For the above-stated reasons, in this project a new mathematical model, named the R-Model, was developed using both GLOSSY and MATT Ceramic Tiles. Spectral data from 400 – 700 nm was analysed using the concept of bandpass correction as well as the multilinear regression method. The performance of R-Model was found to be better than that of the previous models. The improvement of the inter-instrumental agreement was up to 90% for the ceramic tiles. Moreover, the inter-instrumental agreement for the other coloured samples such as textile and paper samples also improved accordingly, from 26.1% to 57.6% and 13.7% to 61.1% respectively. Using this model, the global colour communication between designers, coloration companies and buyers can be further enhanced, and also the non-physical sample communication method through the use of digital reflectance data can become feasible.

---

**CONTENTS**

---

	<b><u>Page No.</u></b>
<b><u>DEDICATION</u></b>	<b>I</b>
<b><u>ACKNOWLEDGEMENT</u></b>	<b>II</b>
<b><u>ABSTRACT</u></b>	<b>III</b>
<b><u>CONTENTS</u></b>	<b>VI</b>
<b><u>LIST OF FIGURES</u></b>	<b>IX</b>
<b><u>LIST OF TABLES</u></b>	<b>XIII</b>
<b><u>LIST OF PUBLICATION</u></b>	<b>XVIII</b>
<b><u>CHAPTER 1 INTRODUCTION</u></b>	
1.1 Research Background	1
1.2 Objectives	7
1.3 Scope Of Study	8
<b><u>CHAPTER 2 LITERATURE REVIEW</u></b>	
2.1 Introduction	10
2.2 Historical Development Of Colour Measurement Instruments	11
2.3 Classification Of Colour Measurement Instruments	13
2.4 Common Used Types Of Spectrophotometers	28
2.5 Colour Difference Formulae Used In Textile Industries	31
2.6 Colouring By Numbers	38
2.7 Inter-Instrumental Agreement	40
2.8 Band-Pass Correction	49
<b><u>CHAPTER 3 EXPERIMENTAL DESIGN AND METHODOLOGY</u></b>	
3.1 Introduction	51
3.2 Physical Standards	52
3.3 Colour Measuring Instruments	58
3.4 Methodology	61
3.5 Mathematical Model Development	63
<b><u>CHAPTER 4 SPECTROPHOTOMETRIC MEASUREMENT RESULTS</u></b>	
4.1 Introduction	67
4.2 Repeatability	67
4.3 Wavelength Shift	79

4.4 Inter-instrumental agreement	87
4.5 Difference In The Summation Of The Relative Spectral Reflectance Difference Of CCS-II Tiles For Visual Spectrum Measured Using Different Spectrophotometers	92
<b><u>CHAPTER 5 DEVELOPMENT OF THE FIRST MATHEMATICAL MODEL (L-Model)</u></b>	
5.1 Introduction	96
5.2 Development Of The First Mathematical Model (L-Model)	97
5.3 The Improvement Of The Inter-Instrumental Agreement After Applying L-Model	103
<b><u>CHAPTER 6 DEVELOPMENT OF THE SECOND MATHEMATICAL MODEL (R-Model)</u></b>	
6.1 Introduction	117
6.2 Development Of The Second Mathematical Model (R-Model)	118
6.3 The Improvement Of The Inter-Instrumental Agreement After Applying R-Model	120
<b><u>CHAPTER 7 TESTING OF DEVELOPED MODELS</u></b>	
7.1 Introduction	140
7.2 Testing Of The R-Model Using Textile Samples	140
7.3 Testing Of The R-Model Using Paper Samples	145
<b><u>CHAPTER 8 COMPARISON OF THE R-MODEL WITH OTHER INTER-INSTRUMENTAL AGREEMENT MODELS</u></b>	
8.1 Introduction	151
8.2 Comparison Of The R-Model With Other Inter-instrumental Agreement Models Using Tiles	152
8.3 Comparison Of The R-Model With Other Inter-instrumental Agreement Models Using Textile Samples And Paper Samples	155
8.4 Conclusion	158
<b><u>CHAPTER 9 CONCLUSIONS AND RECOMMENDATIONS</u></b>	
9.1 Introduction	159

## **Contents**

---

<b>9.2 Conclusions Of The Research Issue</b>	<b>159</b>
<b>9.3 Recommendations</b>	<b>163</b>
 <b>REFERENCE</b>	 <b>i</b>
<b>APPENDIX I</b>	<b>viii</b>
<b>APPENDIX II</b>	<b>xvii</b>
<b>APPENDIX III</b>	<b>xxx</b>
<b>APPENDIX IV</b>	<b>xxxix</b>

**LIST OF FIGURES**

	<b><u>Page No.</u></b>
Figure 2.1 Burnham Colorimeter With Red, Green And Blue Filters And Aperture Plate	16
Figure 2.2 Simplified Optical Diagram Of The Dual-Beam Spectrophotometer (Source: Colour Physics For Industry, 2 <sup>nd</sup> Edition)	24
Figure 2.3 CIE Illuminating And Viewing Geometries (Source: Colour Physics For Industry, 2 <sup>nd</sup> Edition)	25
Figure 3.1 The Standard Calibrated Reflectance Curve Of The GLOSSY Type Standard Tiles Measured Using Specular Component Included Mode By CE-7000A	56
Figure 3.2 The Standard Calibrated Reflectance Curve Of The MATT Type Standard Tiles Measured Using Specular Component Included Mode By CE-7000A	56
Figure 3.3 The CIE L*, a* And b* Space Distribution Of The Textile Samples	57
Figure 3.4 The CIE L*, a* And b* Space Distribution Of The ColorCurve Samples	58
Figure 3.5 Optical Block Diagram For Dual Beam Spectrophotometer (Source: Datacolor International, Spectraflash® 600 PLUS Operators Manual, April 1997)	61
Figure 3.6 The Regression Method Used To Develop The Mathematical Model	65
Figure 4.1 The Repeatability Of The CCS-II Tiles Measured Using CE-2180 Over A Period Of 60 Weeks	77
Figure 4.2 The Repeatability Of The CCS-II Tiles Measured Using CE-7000A Over A Period Of 60 Weeks	78
Figure 4.3 The Repeatability Of The CCS-II Tiles Measured Using SF600 Over A Period Of 60 Weeks	78
Figure 4.4 The Wavelength Shift Of The GLOSSY Tiles Measured Using The Specular Component Excluded Mode Of CE-2180	80
Figure 4.5 The Wavelength Shift Of The GLOSSY Tiles Measured Using The Specular Component Included Mode Of CE-2180	81
Figure 4.6 The Wavelength Shift Of The MATT Tiles Measured Using The Specular Component Excluded Mode Of CE-2180	81
Figure 4.7 The Wavelength Shift Of The MATT Tiles Measured Using The	81

	<b>Specular Component Included Mode Of CE-2180</b>	
<b>Figure 4.8</b>	<b>The Wavelength Shift Of The GLOSSY Tiles Measured Using The Specular Component Excluded Mode Of CE-7000A</b>	<b>82</b>
<b>Figure 4.9</b>	<b>The Wavelength Shift Of The GLOSSY Tiles Measured Using The Specular Component Included Mode Of CE-7000A</b>	<b>82</b>
<b>Figure 4.10</b>	<b>The Wavelength Shift Of The MATT Tiles Measured Using The Specular Component Excluded Mode Of CE-7000A</b>	<b>83</b>
<b>Figure 4.11</b>	<b>The Wavelength Shift Of The MATT Tiles Measured Using The Specular Component Included Mode Of CE-7000A</b>	<b>83</b>
<b>Figure 4.12</b>	<b>The Wavelength Shift Of The GLOSSY Tiles Measured Using The Specular Component Excluded Mode Of SF-600</b>	<b>84</b>
<b>Figure 4.13</b>	<b>The Wavelength Shift Of The GLOSSY Tiles Measured Using The Specular Component Included Mode Of SF-600</b>	<b>84</b>
<b>Figure 4.14</b>	<b>The Wavelength Shift Of The MATT Tiles Measured Using The Specular Component Excluded Mode Of SF-600</b>	<b>84</b>
<b>Figure 4.15</b>	<b>The Wavelength Shift Of The MATT Tiles Measured Using The Specular Component Included Mode Of SF-600</b>	<b>85</b>
<b>Figure 4.16</b>	<b>The Distribution Of The Summation Of The Relative Spectral Reflectance Difference For The CCS-II Tiles Comparing SF-600 And CE-7000A</b>	<b>93</b>
<b>Figure 4.17</b>	<b>The Distribution Of The Summation Of The Relative Spectral Reflectance Difference For The CCS-II Tiles Comparing CE-2180 And CE-7000A</b>	<b>93</b>
<b>Figure 5.1</b>	<b>The Comparison Of The DE Between The Original DE and L-Model For SF-600 And CE-7000A (GLOSSY Tiles Measured Using Specular Component Excluded Mode)</b>	<b>109</b>
<b>Figure 5.2</b>	<b>The Comparison Of The DE Between The Original DE and L-Model For SF-600 And CE-7000A (GLOSSY Tiles Measured Using Specular Component Included Mode)</b>	<b>110</b>
<b>Figure 5.3</b>	<b>The Comparison Of The DE Between The Original DE and L-Model For SF-600 And CE-7000A (MATT Tiles Measured Using Specular Component Excluded Mode)</b>	<b>110</b>
<b>Figure 5.4</b>	<b>The Comparison Of The DE Between The Original DE and L-Model For SF-600 And CE-7000A (MATT Tiles Measured Using Specular Component Included Mode)</b>	<b>111</b>
<b>Figure 5.5</b>	<b>The Comparison Of The DE Between The Original DE and L-Model For CE-2180 And CE-7000A (GLOSSY Tiles Measured Using Specular Component Excluded Mode)</b>	<b>113</b>



Figure 5.6	The Comparison Of The DE Between The Original DE and L-Model For CE-2180And CE-7000A (GLOSSY Tiles Measured Using Specular Component Included Mode)	113
Figure 5.7	The Comparison Of The DE Between The Original DE and L-Model For CE-2180And CE-7000A (MATT Tiles Measured Using Specular Component Excluded Mode)	114
Figure 5.8	The Comparison Of The DE Between The Original DE and L-Model For CE-2180And CE-7000A (MATT Tiles Measured Using Specular Component Included Mode)	114
Figure 6.1	The Comparison Of The DE Between The Two Different Developed Models (GE) For SF-600 And CE-7000A	125
Figure 6.2	The Comparison Of The DE Between The Two Different Developed Models (GI) For SF-600 And CE-7000A	126
Figure 6.3	The Comparison Of The DE Between The Two Different Developed Models (ME) For SF-600 And CE-7000A	126
Figure 6.4	The Comparison Of The DE Between The Two Different Developed Models (MI) For SF-600 And CE-7000A	127
Figure 6.5	The Comparison Of The DE Between The Two Different Developed Models (GE) ForCE-2180 And CE-7000A	129
Figure 6.6	The Comparison Of The DE Between The Two Different Developed Models (GI) For CE-2180 And CE-7000A	129
Figure 6.7	The Comparison Of The DE Between The Two Different Developed Models (ME) For CE-2180 And CE-7000A	130
Figure 6.8	The Comparison Of The DE Between The Two Different Developed Models (MI) For CE-2180 And CE-7000A	130
Figure 6.9	The Comparison Of The DE Between SF-600 And CE-2180 Before After Applying R-Model (GE)	136
Figure 6.10	The Comparison Of The DE Between SF-600 And CE-2180 Before After Applying R-Model (GI)	137
Figure 6.11	The Comparison Of The DE Between SF-600 And CE-2180 Before After Applying R-Model (ME)	137
Figure 6.12	The Comparison Of The DE Between SF-600 And CE-2180 Before After Applying R-Model (MI)	138
Figure 8.1	The Comparison Of The DE For MATT Tiles Measured Using Specular Component Excluded Mode	154
Figure 8.2	The Distribution Of The DE For The Textile Samples By Applying To Different Models Using Matt Tiles Measured Using Specular Component Excluded Mode	155

Figure 8.3	The Distribution Of The DE For The Paper Samples By Applying To Different Models Using Matt Tiles Measured Using Specular Component Excluded Mode	156
------------	---	-----

**LIST OF TABLES**

		<b><u>Page No.</u></b>
Table 2.1	General Classification Of Colour Measurement Instruments (Source: Modern Concepts Of Color And Appearance)	13
Table 3.1	Comparison Of Three Different Types Of Spectrophotometer Used In This Research	60
Table 4.1	Summary Of The Repeatability Of The CCS-II Tiles Measured Using GretagMacbeth CE-7000A	70
Table 4.2	Summary Of The Repeatability Of The CCS-II Tiles Measured Using GretagMacbeth CE-2180	72
Table 4.3	Summary Of The Repeatability Of The CCS-II Tiles Measured Using Datacolor SF-600	74
Table 4.4	Summary Of The Inter-Instrumental Agreement Of SF-600 And CE-7000A Using CCS-II Tiles	88
Table 4.5	Summary Of The Inter-Instrumental Agreement Of CE-2180 And CE-7000A Using CCS-II Tiles	90
Table 5.1	Summary Of The Inter-Instrumental Agreement For The CCS-II GLOSSY Tiles Using Specular Component Excluded Mode Between SF-600 And CE-7000A	104
Table 5.2	Summary Of The Inter-Instrumental Agreement For The CCS-II GLOSSY Tiles Using Specular Component Included Mode Between SF-600 And CE-7000A	104
Table 5.3	Summary Of The Inter-Instrumental Agreement For The CCS-II MATT Tiles Using Specular Component Excluded Mode Between SF-600 And CE-7000A	105
Table 5.4	Summary Of The Inter-Instrumental Agreement For The CCS-II MATT Tiles Using Specular Component Included Mode Between SF-600 And CE-7000A	105
Table 5.5	Summary Of The Inter-Instrumental Agreement For The CCS-II GLOSSY Tiles Using Specular Component Excluded Mode Between CE-2180 And CE-7000A	106
Table 5.6	Summary Of The Inter-Instrumental Agreement For The CCS-II GLOSSY Tiles Using Specular Component Included Mode Between CE-2180 And CE-7000A	106
Table 5.7	Summary Of The Inter-Instrumental Agreement For The CCS-II MATT Tiles Using Specular Component Excluded Mode Between CE-2180 And CE-7000A	107

Table 5.8	Summary Of The Inter-Instrumental Agreement For The CCS-II MATT Tiles Using Specular Component Included Mode Between CE-2180 And CE-7000A	107
Table 6.1	Summary Of The Inter-Instrumental Agreement For The CCS-II GLOSSY Tiles Using Specular Component Excluded Mode Between SF-600 And CE-7000A After Applying The R-Model	120
Table 6.2	Summary Of The Inter-Instrumental Agreement For The CCS-II GLOSSY Tiles Using Specular Component Included Mode Between SF-600 And CE-7000A After Applying The R-Model	121
Table 6.3	Summary Of The Inter-Instrumental Agreement For The CCS-II MATT Tiles Using Specular Component Excluded Mode Between SF-600 And CE-7000A After Applying The R-Model	121
Table 6.4	Summary Of The Inter-Instrumental Agreement For The CCS-II MATT Tiles Using Specular Component Included Mode Between SF-600 And CE-7000A After Applying The R-Model	122
Table 6.5	Summary Of The Inter-Instrumental Agreement For The CCS-II GLOSSY Tiles Using Specular Component Excluded Mode Between CE-2180 And CE-7000A After Applying The R-Model	122
Table 6.6	Summary Of The Inter-Instrumental Agreement For The CCS-II GLOSSY Tiles Using Specular Component Included Mode Between CE-2180 And CE-7000A After Applying The R-Model	123
Table 6.7	Summary Of The Inter-Instrumental Agreement For The CCS-II MATT Tiles Using Specular Component Excluded Mode Between CE-2180 And CE-7000A After Applying The R-Model	123
Table 6.8	Summary Of The Inter-Instrumental Agreement For The CCS-II MATT Tiles Using Specular Component Included Mode Between CE-2180 And CE-7000A After Applying The R-Model	124
Table 6.9	Summary Of The Inter-Instrumental Agreement For The CCS-II GLOSSY Tiles Using Specular Component Excluded Mode Between CE-2180 And SF-600 Before And After Applying The R-Model	134
Table 6.10	Summary Of The Inter-Instrumental Agreement For The CCS-II GLOSSY Tiles Using Specular Component Included Mode Between CE-2180 And SF-600 Before And After Applying The R-Model	135
Table 6.11	Summary Of The Inter-Instrumental Agreement For The CCS-II MATT Tiles Using Specular Component Excluded Mode Between CE-2180 And SF-600 Before And After Applying The	135

	<b>R-Model</b>	
<b>Table 6.12</b>	<b>Summary Of The Inter-Instrumental Agreement For The CCS-II MATT Tiles Using Specular Component Included Mode Between CE-2180 And SF-600 Before And After Applying The R-Model</b>	<b>136</b>
<b>Table 7.1</b>	<b>Inter-Instrumental Agreement In Terms Of <math>\Delta E</math> Using GLOSSY Tiles Measured Using Specular Component Excluded Mode R-Model SF-600 Vs CE-7000A To Test The Performance Of Selected Textile Samples</b>	<b>141</b>
<b>Table 7.2</b>	<b>Inter-Instrumental Agreement In Terms Of <math>\Delta E</math> Using GLOSSY Tiles Measured Using Specular Component Included Mode R-Model SF-600 Vs CE-7000A To Test The Performance Of Selected Textile Samples</b>	<b>141</b>
<b>Table 7.3</b>	<b>Inter-Instrumental Agreement In Terms Of <math>\Delta E</math> Using MATT Tiles Measured Using Specular Component Excluded Mode R-Model SF-600 Vs CE-7000A To Test The Performance Of Selected Textile Samples</b>	<b>142</b>
<b>Table 7.4</b>	<b>Inter-Instrumental Agreement In Terms Of <math>\Delta E</math> Using MATT Tiles Measured Using Specular Component Included Mode R-Model SF-600 Vs CE-7000A To Test The Performance Of Selected Textile Samples</b>	<b>142</b>
<b>Table 7.5</b>	<b>Inter-Instrumental Agreement In Terms Of <math>\Delta E</math> Using GLOSSY Tiles Measured Using Specular Component Excluded Mode R-Model CE-2180 Vs CE-7000A To Test The Performance Of Selected Textile Samples</b>	<b>143</b>
<b>Table 7.6</b>	<b>Inter-Instrumental Agreement In Terms Of <math>\Delta E</math> Using GLOSSY Tiles Measured Using Specular Component Included Mode R-Model CE-2180 Vs CE-7000A To Test The Performance Of Selected Textile Samples</b>	<b>143</b>
<b>Table 7.7</b>	<b>Inter-Instrumental Agreement In Terms Of <math>\Delta E</math> Using MATT Tiles Measured Using Specular Component Excluded Mode R-Model CE-2180 Vs CE-7000A To Test The Performance Of Selected Textile Samples</b>	<b>144</b>
<b>Table 7.8</b>	<b>Inter-Instrumental Agreement In Terms Of <math>\Delta E</math> Using MATT Tiles Measured Using Specular Component Included Mode R-Model CE-2180 Vs CE-7000A To Test The Performance Of Selected Textile Samples</b>	<b>144</b>
<b>Table 7.9</b>	<b>Inter-Instrumental Agreement In Terms Of <math>\Delta E</math> Using GLOSSY</b>	<b>146</b>

	Tiles Measured Using Specular Component Excluded Mode R-Model SF-600 Vs CE-7000A To Test The Performance Of Selected ColorCurve Paper Samples	
Table 7.10	Inter-Instrumental Agreement In Terms Of $\Delta E$ Using GLOSSY Tiles Measured Using Specular Component Included Mode R-Model SF-600 Vs CE-7000A To Test The Performance Of Selected ColorCurve Paper Samples	146
Table 7.11	Inter-Instrumental Agreement In Terms Of $\Delta E$ Using MATT Tiles Measured Using Specular Component Excluded Mode R-Model SF-600 Vs CE-7000A To Test The Performance Of Selected ColorCurve Paper Samples	146
Table 7.12	Inter-Instrumental Agreement In Terms Of $\Delta E$ Using MATT Tiles Measured Using Specular Component Included Mode R-Model SF-600 Vs CE-7000A To Test The Performance Of Selected ColorCurve Paper Samples	147
Table 7.13	Inter-Instrumental Agreement In Terms Of $\Delta E$ Using GLOSSY Tiles Measured Using Specular Component Excluded Mode R-Model CE-2180 Vs CE-7000A To Test The Performance Of Selected ColorCurve Paper Samples	148
Table 7.14	Inter-Instrumental Agreement In Terms Of $\Delta E$ Using GLOSSY Tiles Measured Using Specular Component Included Mode R-Model CE-2180 Vs CE-7000A To Test The Performance Of Selected ColorCurve Paper Samples	148
Table 7.15	Inter-Instrumental Agreement In Terms Of $\Delta E$ Using MATT Tiles Measured Using Specular Component Excluded Mode R-Model CE-2180 Vs CE-7000A To Test The Performance Of Selected ColorCurve Paper Samples	148
Table 7.16	Inter-Instrumental Agreement In Terms Of $\Delta E$ Using MATT Tiles Measured Using Specular Component Included Mode R-Model CE-2180 Vs CE-7000A To Test The Performance Of Selected ColorCurve Paper Samples	149
Table 8.1	Inter-instrumental Agreement In Terms Of $\Delta E$ Using 12 MATT BCRA-NPL Series II Tiles Using Specular Component Excluded Mode	153
Table 8.2	The Distribution Of The DE For The Textile Samples By Applying To Different Models Using Matt Tiles Measured Using Specular Component Excluded Mode	156

Table 8.3	The Distribution Of The DE For The Paper Samples By Applying To Different Models Using Matt Tiles Measured Using Specular Component Excluded Mode	157
-----------	---	-----

**LIST OF PUBLICATION**

1. "Study of Reproducibility of state-of-art of Spectrophotometer". Sidney Y.S. Chung, John H. Xin, and Patrick T.F. Chong, "AIC Midterm Meeting 99"
2. "顏色量度的準確性", 宗耀昇, 忻浩忠, 莊德虎, "全國染色專業委員會年會"
3. "New Regression Models For the Measurement of Textiles by Spectrophotometer", Sidney Y.S. Chung, John H. Xin, and Patrick T.F. Chong, "The 5<sup>th</sup> Asian Textiles Conference"
4. "Comparison of The Different Mathematical Models For Inter-instrument Agreement Between Spectrophotometers", Sidney Y.S. Chung, John H. Xin, and Patrick T.F. Chong, "Colour and Visual Scales 2000, National Physical Laboratory, United Kingdom, 3-5 April, 2000"
5. "Study of New Regression Model For Inter-instrument Agreement", Sidney Y.S. Chung, John H. Xin, and K. M. Sin, "2000 AIC Meeting Seoul"
6. "Comprehensive Comparison Between Different Mathematical Models for Inter-instrument Agreement of Reflectance Spectrophotometers", Sidney Y.S. Chung, John H. Xin, and K.M. Sin, "AIC Color 01 Rochester"
7. "The Factors Affecting the Accuracy of Instrument Colour Measurement", Sidney Y.S. Chung, John H. Xin, K.M. Sin, "The 6<sup>th</sup> Asian Textiles Conference"
8. "The Application of Modern Colour Measurement Services In Coloration"



- Industries", Y. S. Chung, John H. Xin and K. M. Sin, Submitted to Journal of China Textile University**
- 9. "The Study of the Repeatability and Reproducibility of the State-of-Art Spectrophotometers", Yiu-sing CHUNG, John H. XIN and K. M. SIN, Submitted to Coloration Technology**
- 10. "The Development of the New Inter-instrumental Agreement For Reflectance Spectrophotometers, Part I – Development of The Model", Yiu-sing CHUNG, John H. XIN and K. M. SIN, Submitted to Coloration Technology**
- 11. "The Development of the New Inter-instrumental Agreement For Reflectance Spectrophotometers, Part II – Testing of The Model", Yiu-sing CHUNG, John H. XIN and K. M. SIN, Submitted to Coloration Technology**

## **CHAPTER 1**

### **INTRODUCTION**

#### **1.1 Research Background**

#### **1.2 Objectives**

#### **1.3 Scope Of Study**

#### **1.1 Research Background**

It is often difficult to achieve accurate colour communication because the perception of colour is subject to the influence of at least three different elements: the light source, the object and the visual system. The variation in either the radiant quantity or the spectral distribution of the source can alter the observed colour. For this reason, the objective quantitative tools and communication method are highly significant when evaluating colour. Using advanced computer systems and electronic devices, colour measurement has become increasingly more accurate, especially in the case of spectrophotometric measurement.

Traditionally, physical samples played an important role in colour matching and communication. Unfortunately, sample soiling and notoriously unreliable visual assessments account for 17% of “wrong decisions” made by both trained and experienced colourists<sup>[44]</sup>. In addition, the performance of the trained colourist can be influenced by a number of parameters such as psychological, medical and environment factors. There are also factors such as the variability between visual observers and within observers, the variability between light cabinets and light sources<sup>[44]</sup>. All these influences make colour matching and communication more difficult.

An alternative method for achieving colour quality assessment is using a colour measuring system. Because of advances in spectrophotometry and information technology, colour quality may be expressed in digital format and communicated to the opposite parties by electronic means. This form of colour communication or “colour by number” represents the trend in view of the regionalisation and globalisation of the textile and apparel industry, as well as other colour related industries. A clear message from the leading retailer Marks & Spencer plc to the suppliers in this region is that instrumental results and digital data exchange are a necessity.

In general, spectrophotometers for colour measurement perform at a finite level of accuracy but, being electro-mechanical-optical devices, they exhibit measurement errors relative to a theoretical error-free instrument that users must accept. Most modern spectrophotometers have satisfactory repeatability, but the measurements are not necessarily accurate. In a research study carried out by the Spectrophotometry and Colorimetry Club of the National Physical Laboratory (NPL) of the UK<sup>[106,107]</sup>, twenty-four participants were asked to measure the colour of a set of NPL ceramic colour standards using their in-house spectrophotometers. Even the state-of-art instruments showed variance from the standard in the region of 0.7 to 1.6 CIELAB units. Larger differences in excess of 3 CIELAB units were also obtained for some instruments. However, the human eye can identify differences in colour of between 0.5 and 1.0 CIELAB units, depending on the colour. This result strongly suggests that the accuracy of the instrument and the inter-instrumental agreement between spectrophotometers present problems where meeting the requirements for industrial digital colour communication is concerned.

If measurement errors can be quantified and corrected, then the accuracy of the measurement task can be improved. In the design of the spectrophotometer, there are inherent problems which lead to both systematic and random error, affecting the

accuracy of results. As a consequence, such errors must be analysed and quantified mathematically in order to improve the accuracy and to promote globalised digital colour communication for a variety of commercial and industrial applications. The colour measurement spectrophotometers have performed satisfactorily and provided useful colour information for over 10 years. However they exhibit several deficiencies, primarily due to age, poor inter-instrumental agreement and limited software flexibility and capabilities.

Earlier researchers have shown the effectiveness of the improvement of the inter-instrumental agreement<sup>[2,8,9,84]</sup>. However, systematic studies which focus on the requirement of digital colour communication have not yet been conducted. The research project described served to develop a methodology and an algorithm aiming at improving the accuracy of the colour communication based on spectrophotometric measurement so that commerce and industry may gain immediate benefits from the results obtained.

In surface colour measurement related industries, colour measurement systems are widely used to both measure colour and evaluate colour quality. Reflectance

spectrophotometers are one of the popular instruments used in colour measurement related industries in order to measure the surface colour accurately. Spectral reflectance data of a colour can be measured using reflectance spectrophotometers. In addition, the spectrophotometer can provide higher accuracy with its high precision sensor and measure colour for a variety of illuminant conditions.

In the textile or other colour related industries, for example textile coloration and printing *et al.*, objective colour difference evaluation is now far more important than ever before. Colour quality control is one of the most important parameters to determine whether the finished goods are acceptable or not in textile or other colour related industries. In addition, objective colour difference specification for quantitative colour comparison is also very important to promote quick response to the market place and is an efficient means of in-house colour quality control. Reflectance spectrophotometers are one of the most important devices for checking the colour quality of textile products.

With the development in electronic devices and machine design, the repeatability of spectrophotometric measurements has become more and more accurate in practice. For this reason, different manufacturers claim that the repeatability of measurement on the

same instrument is lower than 0.01 CIELAB  $\Delta E$  units<sup>[29,70,71]</sup>. The manufacturers also claim that the inter-instrumental agreement of the spectrophotometers of similar design is lower than 0.15 CIELAB  $\Delta E$  units<sup>[29,70,71]</sup>. However, in the investigation under discussion, it was found that even the reflectance spectrophotometers produced by the same manufacturers had an inter-instrumental agreement range from 0.526 to 0.611 CIELAB  $\Delta E$  units. In the case of instruments produced by different manufacturers, the inter-instrumental agreement ranged from 0.575 to 0.854 CIELAB  $\Delta E$  units. For this reason, the first objective of this research project was to study the inter-instrumental agreement of the commercial reflectance spectrophotometers using Ceramic Colour Standards – Series II tiles (CCS-II Tiles). Both the GLOSSY and MATT types of the CCS-II tiles were chosen for use in the experimental work. The results of this study illustrate that improvement in the communication between instruments should be achieved in order to enhance inter-instrumental agreement.

In previous studies, the development and the tests for the mathematical models were based on GLOSSY type ceramic tiles. For this reason, both GLOSSY and MATT types of ceramic tiles were used to develop the mathematical models separately in this project. In addition to ceramic tiles, textile samples and also paper samples were used to test the newly developed mathematical models.

## **1.2 Objectives**

The objectives of this research study are summarized as follows:

- I. To study the repeatability and inter-instrumental agreement of spectrophotometers.
- II. To analyse the causes of the poor inter-instrumental agreement between spectrophotometers.
- III. To develop a mathematical model in order to improve inter-instrumental agreement between spectrophotometers.
- IV. To test the new developed mathematical models using different types of samples.



### **1.3 Scope Of Study**

This research project focused on the study of the measurement results of spectrophotometers and the development of new mathematical models to improve inter-instrumental agreement. Experiments were carried out to develop the appropriate mathematical models. A comparison between the newly developed mathematical models and the previously reported mathematical models was also carried out in this research project. The emphasis of the research was to develop a new mathematical model in order to improve the inter-instrumental agreement of the reflectance spectrophotometers. In addition, the performance of the newly developed models was of major importance, thus the testing of the previously reported and newly developed mathematical models are also summarised in this thesis.

## **CHAPTER 2**

### **LITERATURE REVIEW**

#### **2.1 Introduction**

#### **2.2 Historical Development Of Colour Measurement Instruments**

#### **2.3 Classification Of Colour Measurement Instruments**

#### **2.4 Commonly Used Types Of Spectrophotometers**

#### **2.5 Colour Difference Formulae Used In Textile Industry**

#### **2.6 Colouring By Numbers**

#### **2.7 Inter-Instrumental Agreement**

#### **2.8 Band-Pass Correction**

## 2.1 Introduction

Colorimetry<sup>[85,95]</sup> is the science of measuring or evaluating colour and colour is defined as the sensation experienced or caused by light reflected from or transmitted through objects. The appearance of colour is subject to the influence of three different phenomena: the light source, the object and the visual system. If the above three factors can be quantified, the sensation of colour can be measured and finally calculated even though the perceived colour cannot be directly measured. In the textile industries, especially in textile coloration, it would be very beneficial if the colour properties of textile materials could be quantified.

Colour measurement is achieved using instruments such as the tristimulus colorimeter and spectrophotometer. Video cameras<sup>[21,22]</sup> have also been employed in the field of colour measurement and control. The tristimulus colorimeter measures the CIE tristimulus data directly<sup>[18]</sup>; the spectrophotometer measures the spectral reflectance factors or transmittance factors, and the video camera is mainly used for on-line colour monitoring.

In general, the tristimulus colorimeter<sup>[17]</sup> is easy to use and cheaper than the

spectrophotometer. Although it is less accurate in practical application than the modern spectrophotometer, the tristimulus colorimeter can also express colours numerically according to international standards, for example as seen in the CIE system<sup>[7,18]</sup>. For this reason, the tristimulus colorimeter is primarily used for colour quality monitoring.

In order to measure colour accurately, the modern spectrophotometer<sup>[17]</sup> is widely used in colour science related industries. Using spectrophotometers, not only the numerical data obtained from the tristimulus colorimeters, but also the spectral reflectance graph for the colour can be obtained. The spectrophotometer also offers greater accuracy with its high precision sensor and the inclusion of data for a variety of illuminant conditions.

## 2.2 Historical Development Of Colour Measurement Instruments

Colour quality control has become far more important recently, since colour is the first parameter in evaluating the quality of coloured, finished goods. Visual assessment is the traditional method to evaluate the colour quality, but this method has many drawbacks. For instance, sample soiling and notoriously unreliable visual assessment account for 17% of “wrong decisions” made by colour experts<sup>[44]</sup>. In addition, visual assessments are qualitative, debatable, vary according to viewing conditions and are

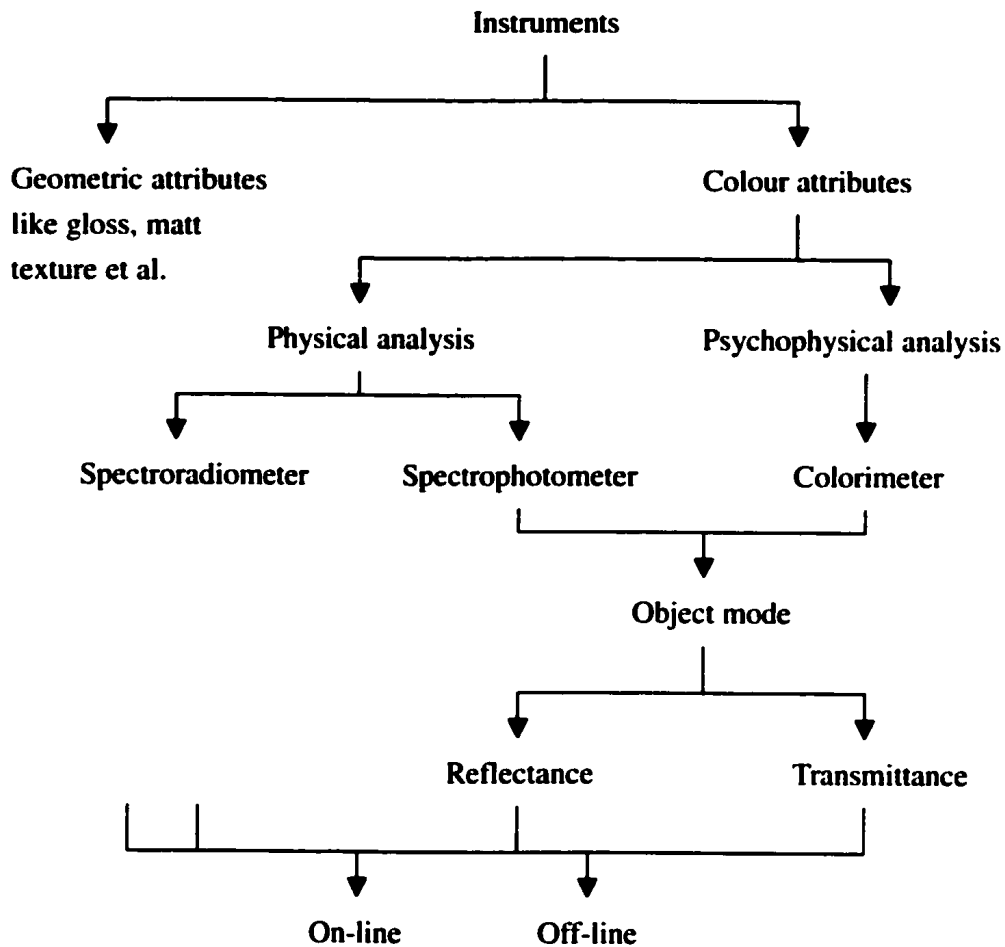
observer-dependent.

In 1931 CIE<sup>[18]</sup> defined the standard observer and illuminants, which became the basis for instrumental colour measurement. The first generation instrument for this task measured point-to-point reflectance, and the results were calculated using conventional techniques available at the time. Between 1936 and 1946, Prof A.C. Hardy introduced automatic mechanical calculators, and these became known as the second-generation instruments. The commercialisation of the analog computer led to the third generation of the instruments. With the development of personal computers, the measurement speed and calculation time became progressively faster and the fourth generation of colour measurement instruments arrived.

### **2.3 Classification Of Colour Measurement Instruments**

Colorimetric instruments can be divided into three basic types, these being the colorimeter, spectroradiometer and spectrophotometer. The classification of those three types of machines are summarised in the table below:

**Table 2.1 General Classification Of Colour Measurement Instruments (Source: Modern Concepts Of Color And Appearance)**



### 2.3.1 Colorimeter

Colorimeters<sup>[17]</sup> were the first colour measurement instruments to be used in the colour related industries. Colorimeters were also known as “Three-filter Colour Measurement Instruments”. The three-filters simulated the human eye’s cone cell, red, green and blue photo-detectors, measuring the tristimulus values. The light source for these

colorimeters was a quartz halogen bulb, which illuminated the sample at 45° to the norm.

The colorimeter is primarily used for measuring CIE tristimulus values (CIE colorimetric coordinates) for a stimulus. In general, there are two different types of colorimeter, one being visual and the other photoelectric<sup>[64]</sup>. Visual colorimeters were traditionally of two types, the earliest ones being visual absorptionmeters or colour comparators. Such instruments are mainly used to measure liquid colour and they are employed for chemical analysis, concentration determination or grading on the basis of colour. The other type of colorimeter was a true colorimeter that emphasised visual equivalence or psychophysical estimation. This type of visual colorimeter compared the colour of the samples with the colour of the standard and matched the two. The other type was a true colorimeter that emphasised visual equivalent or psychophysical estimation.

True colorimeters define colours in terms of their own primaries. A number of colorimeters were specially developed for colour vision research. These were very complex, costly and highly specialised to serve one or a limited number of purposes.

The earliest true colorimeter was Clerk Maxwell's colour box, which consisted of a prism unit with adjustable slits in the appropriate parts of a light path to independently control the amount of red, green and blue light beams viewed as a homogeneous colour in an optical viewing unit to match the colour of the sample shown in the other half of the optical unit. The relative aperture areas  $x$ ,  $y$  and  $z$  were recorded as the amount of the three primaries,  $x$ ,  $y$  and  $z$ .

The earliest tristimulus colorimeters, such as those developed by Guild<sup>[49]</sup>, Wright<sup>[109]</sup>, Donaldson<sup>[31,32]</sup>, MacAdam<sup>[69]</sup> and Wyszecki<sup>[110,111]</sup>, were used mainly for research purposes where more than two visual fields were necessary to examine colour difference matching, colour matching ellipses, hue matching etc. The Burnham colorimeter<sup>[12]</sup> was relatively simple in construction and utilized additive mixing of primary stimuli made up of coloured filters and a light source. Figure 2.1 shows the arrangement of the three filters and aperture plate. The lower two adjacent filters are red and green, while the upper filter is blue. The horizontal and vertical movements of the filter control the proportion of red-green and yellow-blue components respectively. The scales actuated by the two movements gave the proportion of the three primary colours. A shutter on the test field allowed the luminosity of the two fields to be equalised.





***Figure 2.1 Burnham Colorimeter With Red, Green And Blue Filters And Aperture Plate***

The Lovibond colorimeter<sup>[16,65]</sup> was a popular commercial visual colorimeter even 100 years after its use and development. This colorimeter was based on the subtractive colour mixing of coloured glass filters. For each of the three primaries, magenta, yellow and cyan, there were 250 Lovibond glass filters. The filters are graduated in the way that two "1.0" glasses match a "2.0" glass plus a colorless glass. An equal value of all three together gave a grey series down to the black. There are around nine million colours of varying brightness which can be matched by putting suitable Lovibond filters in the light filters in the light path for whole visible colour or saturation.

Modern colorimeters directly measure colorimetric quantities, and the detector system of the colorimeters consists of a glass filter and a photodetector, usually a silicon photodiode.

In common practise, the measurement results of the tristimulus colorimeter are less accurate when compared with the modern reflectance spectrophotometer. The tristimulus colorimeter expresses colours numerically according to CIE standards<sup>[18]</sup> and it is mainly used in colour quality monitoring.

### 2.3.2 Spectroradiometer

The spectroradiometer is mainly used to measure self-illuminant objects such as television and video displays. Inside the spectroradiometer, the light source is integral and shielded from external light sources whereas a spectroradiometer can accept light from external sources. Spectroradiometers measure radiometric quantities of light sources as a function of wavelength. The measurement involves the comparison of the test source with a suitable reference source of known spectral power distribution. Standardised tungsten filament lamps are the most often-used reference source. In the case of a tungsten or tungsten-halogen lamp, the bandwidth can be large ( $\Delta\lambda = 5$  or 10 nm) for light sources with continuous spectra, but for discontinuous line spectra, such as fluorescent lamps, the interval should not be more than 2 nm. However if the wavelength of emission lines is known, separate measurements can be made at those wavelengths and then the data combined with those taken at 10 nm bandwidth. An

elaborate spectroradiometer and sophisticated illumination standards can provide accurate colorimetric information for coloured samples. However some good estimates of chromaticity values can be obtained from a broad band device such as a colour video camera, provided it is properly calibrated by measuring R, G and B values of suitably chosen colour standards and by reconstructing reflectance accordingly<sup>[64]</sup>.

### 2.3.3 Spectrophotometer

The spectrophotometer<sup>[17]</sup> mainly measures reflectance, transmittance, or absorbance at different wavelengths in the spectrum. The quantity of reflectance measured is referred to as the reflectance factor (RF) and is defined as the reflectance of the sample at a specific wavelength range compared to the reflectance of the perfect diffuse white measured under the exact same conditions. The mathematical expression is as follows:

$$RF(\lambda) = R(\lambda)_{(sample)} / R(\lambda)_{(standard)} \text{ ----- E.Q. 2.1}$$

In common practice, the reflectance factors are expressed as a percentage, %R.

Some important principle components of the spectrophotometer are discussed in the

following paragraphs.

#### **2.3.3.1 Spectral Range<sup>[5,13,51,89,96,97]</sup>**

According to the Sandoz Colorimetry Manual, the reflectance factor is the ratio of the reflected to the incident light at a given wavelength. Based on the CIE recommendations<sup>[18,87]</sup>, it is preferable that the measurement data of spectrophotometer should have a spectral range from 380 to 780 nm available at 5-nm intervals. In general practice, the spectral range from 400 to 700 nm with minimum data available at 10-nm intervals is sufficient.

#### **2.3.3.2 Illuminating System<sup>[5,13,51,59,89,96,97,98]</sup>**

The primary considerations for the illuminating system, also the light sources, for spectrophotometers are stability, life, directibility and spectral energy distribution.

Incandescent lamps are mostly preferred because of the following features:

- i. Low cost
- ii. Continuous SPD as sunlight

- iii. **Steady output of light**
- iv. **Output controllable by changing electrical input**
- v. **Small compact size allowing concentrated light beam that can be directed by mirror etc.**

No specifications are made for the light source used in the spectrophotometer because they measure the ratio of incident to reflected light due to the size as well as the absence of a concentrated light beam.

Quartz halogen lamps are used only for illuminant A. Such lamps emit very limited UV hence they do not excite a fluorescent brightening agent to the same extent as daylight. On the other hand, these lamps produce too much energy in the IR region but many colorants are sensitive to light (known as photochromic) or to heat (known as thermochromic). Thus the samples are heated by the emitted energy, potentially leading to errors in the measurements of thermochromic samples. In addition, colour fading may occur after prolonged exposure to the strong light beam.

In order to overcome these problems, pulsed xenon light sources are employed in modern spectrophotometers, since the physical characteristics of the pulsed xenon light are almost ideal and have a spectral power distribution (SPD) close to daylight. The pulsed xenon lights are easily filtered to approximate illuminant D<sub>65</sub> from the UV to the IR end of the spectrum. Pulsed xenon light releases a flash of light of a few nanoseconds duration during each measurement instead of supplying a constantly illuminating light source. This kind of light is used for electrical discharge lamps that emit a large quantity of radiant power for a very short duration of time. The drawback is that the pulsed xenon light provides a line spectrum of discontinuous nature and the output stability is poor. Fluorescent samples can also be measured by such sources and the samples may not be heated by such sources. In addition, pulsed xenon light is suitable for the measurement of dark colours.

### 2.3.3.3 *Monochromator*<sup>[5,13,51,89,96,97]</sup>

The monochromator, or so-called spectral analyser, is a device that splits light into its spectral components so that it can be measured. It is a key component of the spectrophotometer, setting most of the performance characteristics.

In the earliest spectrophotometer, a photomultiplier tube was commonly used as a monochromator. It used mechanical techniques to scan the spectrum over a single light detector. Thus the measurements were made sequentially, and it could take several minutes to scan from 400 to 700 nm.

Prisms, the classic devices for splitting white light into its component colours, were the most popular monochromator used in many early spectrophotometers. They consisted of an entrance slit, a collimator lens for producing parallel beam, a prism for dispersion of light and a second telescopic lens for focusing in the plane of the exit slit. As the exit slit is in a fixed position, monochromatic radiation can be selected by moving a narrow exit slit or by rotating the prism.

Both the entrance and the exit slit should be extremely narrow, but a compromise can be made by allowing a minimum amount of monochromatic light to pass into the detector.

In addition the exit slit should be of adjustable width because the separation of equal wavelength intervals is inconstant. Most importantly the bandwidth of radiation depends on the construction of the monochromator and varies between different spectrophotometers. In most of the modern spectrophotometers, the manufacturers will

not use prism monochromators because of the limited supply of natural materials required to make them.

Diffraction grating is one substitute for the prism. A grating is a film or surface containing close equidistant and parallel lines used for producing spectra by diffraction.

The price for diffraction grating monochromators is lower than that for prism monochromators and their dispersion power is independent of wavelength, therefore the wavelength selection is much simpler than in the case of the prism.

#### 2.3.3.4 *Equipment Mode*<sup>[5,13,51,89,96,97]</sup>

There are two equipment modes for colour measurement, one being polychromatic and the other monochromatic.

In the polychromatic mode, the light source is directed onto the sample first and the reflected light is then monochromated. In monochromatic mode, the light source is monochromated first and the selected monochromatic light is then directed onto the



sample. In principle, the monochromatic mode is suitable for the measurement of the nonfluorescent sample but not for the fluorescent sample and vice versa.

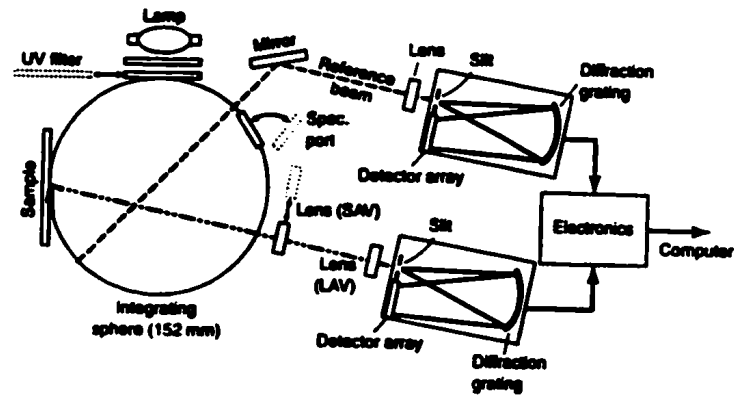


**Fig. 2.2 Simplified Optical Diagram Of The Dual-Beam Spectrophotometer (Source: Colour Physics For Industry, 2<sup>nd</sup> Edition)**

#### 2.3.3.5 Illumination and Viewing Geometries<sup>[5,13,51,89,96,97]</sup>

The term geometry refers to the placement of a sample relative to the light source and measuring lens in a spectrophotometer. There are four geometries defining the direction of the incident light and the direction of detecting the reflected light based on the recommendation of CIE. In general, the four geometries can be further divided into two groups, these being the bi-direction type and sphere type.

The bi-direction type is suitable for the measurement of a sample with a smooth surface.

In this type of geometry, the light beam at one angle illuminates the sample and the reflected beam is detected at an angle of 45/0 or 0/45 geometries. If the samples used in the measurement process do not have a smooth surface, circumferential 45/0 or 0/circumferential 45 are preferred.

The geometry of the sphere type is designated as Diffuse/0 (D/0) or 0/Diffuse (0/D) according to CIE recommendation. These two geometries are suitable for the measurement of textile samples since they generally have matt surface. The Diffuse/8 (D/8) or 8/Diffuse (8/D) sphere type provides the option to include or exclude the specular port measurement of the flat samples.

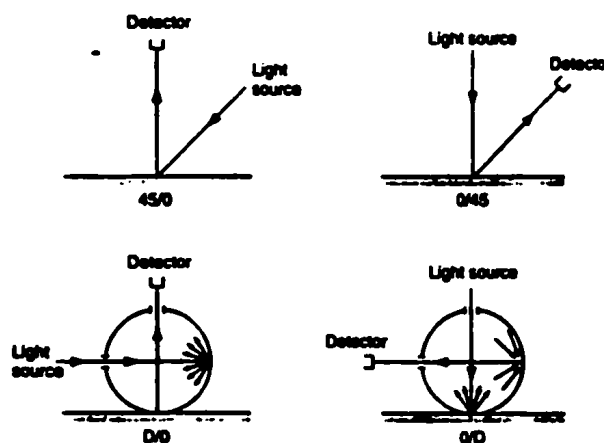


**Figure 2.3 CIE Illuminating And Viewing Geometries (Source: Colour Physics For Industry, 2<sup>nd</sup> Edition)**

**2.3.3.6 Detector System<sup>[5,13,51,89,96,97]</sup>**

The spectral analyser is a device that splits light into its spectral components so that they can be measured.

The photomultiplier is a traditional type of light-detecting device updated using the tiny solid-state silicon diode photodetector array. An array of silicon diodes ensures that measurements can be made in a few seconds and, since there are no moving parts, the reliability is greater.

MC90 is a dual-channel, holographic grating based spectrometer which uses two custom photodiode linear arrays for the reference and sample beams.

In order to enhance the measurement accuracy, the hardware has been progressively modified<sup>[20]</sup>. The first modification was the addition of a motorised adjustable UV control. The UV content should be automatically adjusted once the UV calibration has been achieved and the UV filter adjustment made accordingly.

In order to measure dark or highly saturated colours, a high intensity pulsed xenon light was adopted for the purpose of improving the accuracy of readings. In addition, a removable thin film sample holder was added to the instrument for the measurement of diffusion or transmission of the liquid or solution. It is advantageous for the spectrophotometer to adjust the lens automatically once the aperture is changed, and to measure the reflectance of the surface coloured objects with greater accuracy. Recently, video cameras have also used for colour measurement, mainly in the course of on-line colour monitoring.

The performance of an instrument is important when obtaining measurement data which is consistent, repeatable or error free. Regular checks can help to ensure the accuracy of the measurement results. Documentation also assists the user to compare experimentally-derived data with the standard data provided by the manufacturer, or data obtained at an early stage after purchase of the apparatus.

## **2.4 Commonly Used Types Of Spectrophotometers**

There are four different types of spectrophotometers commonly in use, these being the

Single-Beam Spectrophotometer<sup>[96,97]</sup>, Dual-Beam Spectrophotometer<sup>[96,97]</sup>,  
Double-Beam Spectrophotometer<sup>[96,97]</sup> and Portable Hand-Held  
Spectrophotometer<sup>[26,27,90,91]</sup>.

### **2.4.1 Single-Beam Spectrophotometer<sup>[96,97]</sup>**

In the case of the single-beam spectrophotometer, two measurements must be made in sequence. For this reason, time is required between the two measurements in order to keep the measurement system stable. The time requirement is mainly for the stabilisation of the light sources and conversion of the small electrical signals coming from various detectors into large signals which may be collected by the amplifiers. Although the single-beam spectrophotometer is simpler in its construction, it is harder to calibrate. The long-term repeatability is inferior to that of the dual-beam and also the double-beam spectrophotometers if calibration is not done carefully and on a regular basis.

### **2.4.2 Dual-Beam Spectrophotometer<sup>[96,97]</sup>**

The reference beam of the dual-beam spectrophotometer measures light that is reflected from the integrating sphere wall. This gives a measurement of light in the sphere that is incident on the sample. The measurement is generally more accurate because both the incident and reflected light from the sample is measured. The measurement stability of instrument is increased with the use of a reference beam so that any drift of the electronics or light source intensity is cancelled out as both beams will be equally affected. A dual-beam spectrophotometer is less sensitive to the dis-colouring of barium sulphate in the integrating sphere with age. Errors caused by the drift of the measurement electronics or variation in the light source is eliminated because dual-beam measurement mainly involves the measurement of a ratio rather than an absolute value.

### **2.4.3 Double-Beam Spectrophotometer<sup>[96,97]</sup>**

There are two types of double-beam spectrophotometers. The main difference between the two instruments is that one uses two detectors while the other uses one only. The light beam from the monochromator is split to follow two paths in the former type of spectrophotometer. The sample is placed in one, whilst the other contains all the

components except the sample. The light intensity/response curves of the two detectors must be accurately matched and two signals are obtained by electrical switching between the two detectors or by using a chopping device to interrupt the light beam alternately in the two beams. The requirement to match the two detectors is obviously in the single detector systems. In these, a chopper is used to allow the light to traverse the sample and solvent paths alternately. There should be identical components in each path.

### **2.4.4 Portable Hand-Held Colour Measuring Instruments<sup>[26,27,90,91]</sup>**

As a consequence of advances in integrated electronics and smaller optical components, portable, hand-held colour measuring instruments<sup>[90,91]</sup> have been introduced into the market in recent years. Assisting in the matter of quality control, portable hand-held colour measuring instruments become increasingly more popular for simple colour measurement and communication. The advantages of the portable hand-held colour measuring instrument are that the computer is not required as the communication interface. The built-in microprocessors can calculate colour differences, pass/fail, shade sorting, whiteness, grades of fastness, and many other indices of colour and appearance. Besides, the prices for the portable models are lower than those for the laboratory. According to D. Scott Reininger<sup>[26,27]</sup>, there are four requirements for portable hand-held

colour measuring instruments; these being accuracy, precision, durability and lastly functionality.

Of the four different spectrophotometers, portable hand-held machines are the most commonly used in quality control because of their light weight (two to four pounds) and ease of use. Bench top models have better functions than portable ones, but because of their size and the requirement of a computer as the communication interface, they are more commonly used in laboratories or factories.

## **2.5 Colour Difference Formulae Used In Textile Industry**

In this project, colour difference was used to evaluate both the colour measurement and inter-instrumental agreement results. There are many colour difference formulae and those most commonly used in the textile industry are CIELAB Color Space<sup>[1]</sup>, CMC(l:c)<sup>[10,11,19,72]</sup> and CIE 1994( $\Delta L^*$   $\Delta C^*_{ab}$   $\Delta H^*_{ab}$ ) colour-difference formula<sup>[73,83]</sup>.



### 2.5.1 CIELAB Color Space<sup>[1]</sup>

CIELAB is the modification of the Adams-Nickerson formula (ANLAB)<sup>[4,64]</sup>, and it was recommended by CIE in 1976. This color space included three attributes  $L^*$ ,  $a^*$  and  $b^*$  which are calculated based on the CIE tristimulus values, CIE X, Y and Z.  $L^*$  represents the lightness,  $a^*$  represents the redness and greenness and  $b^*$  represents the yellowness and blueness.

The general CIELAB colour difference formula is as follows:

$$\Delta E^*_{ab} = [(\Delta L^*)^2 + (\Delta a^*)^2 + (\Delta b^*)^2]^{1/2} \text{ ----- EQ 2.2}$$

or

$$\Delta E^*_{ab} = [(\Delta L^*)^2 + (\Delta C^*_{ab})^2 + (\Delta H^*)^2]^{1/2} \text{ ----- EQ. 2.3}$$

Where

$$L^* = 116(Y/Y_n)^{1/3} - 16 \text{ if } Y/Y_n > 0.008856$$

$$a^* = 500 [(X/X_n)^{1/3} - (Y/Y_n)^{1/3}] \text{ if } X/X_n > 0.008856$$

$$b^* = 0.4 \times 500 [(Y/Y_n)^{1/3} - (Z/Z_n)^{1/3}] \text{ if } Z/Z_n > 0.008856$$

OR

$$L^* = 903.3(Y/Y_n) \text{ if } Y/Y_n \leq 0.008856$$

$$a^* = 500 \times [7.787 \times (X/X_n - Y/Y_n) + 16/116] \text{ if } X/X_n \leq 0.008856$$

$$b^* = 500 \times [7.787 \times (Y/Y_n - Z/Z_n) + 16/116] \text{ if } Z/Z_n \leq 0.008856$$

$$C^*_{ab} = [(a^*)^2 + (b^*)^2]^{1/2}$$

$$h_{ab} = \tan^{-1} (b^*/a^*)$$

$$\Delta L^* = L^*_{\text{sample}} - L^*_{\text{standard}}$$

$$\Delta a^* = a^*_{\text{sample}} - a^*_{\text{standard}}$$

$$\Delta b^* = b^*_{\text{sample}} - b^*_{\text{standard}}$$

$$\Delta C^*_{ab} = C^*_{ab, \text{sample}} - C^*_{ab, \text{standard}}$$

$$\Delta H^* = [(\Delta E^*_{ab})^2 - (\Delta L^*)^2 - (\Delta C^*_{ab})^2]^{1/2}$$

OR

$$\Delta H^* = 2(C^*_1 \times C^*_2)^{1/2} \times \sin (\Delta h/2) \text{ [87,102]}$$

### 2.5.2 CMC(l:c) Colour-Difference Formula

The CMC(l:c) colour-difference formula was derived from the JPC79 colour-difference formula, developed by J & P Coats<sup>[19]</sup>. The general formula of CMC(l:c) is as follows:

$$\Delta E_{\text{CMC}(l:c)} = [(\Delta L^*/S_L)^2 + (\Delta C^*_{ab}/S_C)^2 + (\Delta H^*_{ab}/S_H)^2]^{1/2} \text{ ----- EQ. 2.4}$$

Where

$$S_L = 0.040975 L^*_{\text{standard}} / (1 + 0.01765 L^*_{\text{standard}}) \text{ if } L^* \geq 16$$

$$S_L = 0.511 \text{ if } L^* < 16$$

$$S_C = 0.638 + 0.0638 C^*_{ab, \text{standard}} / (1 + 0.0131 C^*_{ab, \text{standard}})$$

$$S_H = S_C (TF + 1 - F)$$

$$F = \{(C^*_{ab, \text{standard}})^4 / [(C^*_{ab, \text{standard}})^4 + 1900]\}$$

$$T = 1 \text{ when } C^*_{ab, \text{standard}} < 0.638 \text{ or}$$

$$T = 0.56 + |0.2 \cos (\theta + 168^\circ)| \text{ or}$$

$$T = 0.56 + |0.4 \cos (\theta + 35^\circ)| \text{ when } 164^\circ < \theta < 345^\circ$$

### 2.5.3 CIE 1994( $\Delta L^*$ $\Delta C^*_{ab}$ $\Delta H^*_{ab}$ ) Colour-Difference Formula

In 1995, the CIE Technical Committee (TCI-29) recommended a new colour difference formula CIE94<sup>[73]</sup>, which was a modification of CMC(l:c) formula and CIE Color Space.

In this new colour-difference formula, there was a new term ( $\Delta V$ ) for the visually perceived magnitude of a colour difference.

$$\Delta V = k_E^{-1} \Delta E^*_{94} \text{ ----- EQ. 2.5}$$

Where  $k_E$  is an overall visual sensitivity factor, set to unity under the conditions usually applying in industrial assessment.

The basic conditions are as follows:

- i. The specimens are homogeneous in colour
- ii. The colour difference between them is such that  $\Delta E^*_{ab} \leq 5$
- iii. They are placed in direct edge contact
- iv. Each subtends an angle greater than  $4^\circ$  to the assessor

- v. The assessor's colour vision is normal
- vi. They are illuminated at 1000 lux and viewed in object mode, against a uniform neutral grey background of  $L^* = 50$ , under illumination simulating D65

The general formula of CIE94 colour-difference formula is as follows:

$$\Delta E^*_{94} = [(\Delta L^*/k_L S_L)^2 + (\Delta C^*_{ab}/k_C S_C)^2 + (\Delta H^*_{ab}/k_H S_H)^2]^{1/2} \text{----- EQ. 2.6}$$

Where

$\Delta L^*$ ,  $\Delta C^*_{ab}$  and  $\Delta H^*_{ab}$  are the components of the CIELAB formula,

$k_L$ ,  $k_C$  and  $k_H$  are parameters factors - under usual condition,  $k_L = k_C = k_H = 1$ , while in textile assessment  $k_L = 2$  and  $k_C = k_H = 1$

$S_L$ ,  $S_C$  and  $S_H$  are the weighting functions, where

$$S_L = 1$$

$$S_C = 1 + 0.045C^*_{ab,X}$$

$$S_H = 1 + 0.014C_{ab,X}^*$$

Where

$C_{ab,X}^* = C_{ab,standard}^*$  if there is a clear difference distinguished between the sample and standard, and

$C_{ab,X}^* = (C_{ab,standard}^* \times C_{ab,sample}^*)^{1/2}$  when there is no difference distinguished between the standard and sample.

In general, CMC(l:c) seems similar to CIE94, which is to define ellipsoids in CIELAB space, but the ways in which the two formula are expressed are different<sup>[83]</sup>. The differences are:

- i. In the CMC(l:c) formula,  $S_L$  increases with the  $L_{standard}^*$ , but this is not recommended in the case of the CIE94 formula.
- ii. CMC(l:c) formula shows non-linear expansion of  $S_C$  and  $S_H$  with  $C_{ab}^*$  but in the case of CIE94 formula the relationship is linear.
- iii. In CMC(l:c) formula,  $S_H$  shows systematic variation with  $h_{ab}$ , but in the case of CIE94, it is independent.

There are still many different colour difference formulae, such as ANLAB Color Space<sup>[4]</sup>, CIELUV Color Space<sup>[1]</sup>, M&S colour-difference formula and BFD(l:c) Color-difference Formula<sup>[66,67]</sup>, and all of these are specially designed to fit a particular set of data, which may result in poor correlation between  $\Delta E$  and other visual data.

In this project CIELAB Color Space was selected to evaluate the colour difference of the measured data and also the inter-instrumental agreement. This is because CIELAB is one of the colour difference formulae that approximate uniform colour spaces and colour-difference calculations.

## 2.6 Colouring By Numbers

Traditionally, physical samples played an important role in colour matching and communication, but even experienced colourists make errors in their visual assessment<sup>[44]</sup>. Their performance is affected by medical, psychological and environmental factors such as the light booth, lighting and so forth.

As a result of advances in the development of personal computers and networked systems, as well as spectrophotometry and information technology, objective colour judgement<sup>[28,41,42,45,46]</sup> has become more useful and important in monitoring the colour acceptability of a product by customers and sellers during the various stages of the production cycle. In addition, colour quality may be assessed in digital format, i.e., spectral reflectance factors, and sent to another party by electronic means rather than physical samples. This communication format is commonly known as "Colouring by Numbers".

Although "Colouring by Numbers" has become popular in colour measuring and colour matching, there are still many difficulties to be overcome. One problem is that a spectrophotometer performs at a finite level of accuracy but it exhibits measurement errors relative to a theoretically error free instrument that the user must accept<sup>[39,40,52,61,62]</sup>. The other problem is the repeatability<sup>[23,24,47,93]</sup> and inter-instrumental agreement<sup>[24,47,86]</sup> of the spectrophotometer. Repeatability and inter-instrumental agreement can be checked using the Ceramic Colour Standards (CCS)<sup>[14,15]</sup> developed by the National Physical Laboratory (NPL) in the UK<sup>[82,106,107]</sup>. Besides repeatability and inter-instrumental agreement, CCS can also be used to diagnose the spectrophotometer and improve inter-instrumental agreement.



## **2.7 Inter-Instrumental Agreement<sup>[105]</sup>**

Inter-instrumental agreement is the agreement between two or more spectrophotometers achieved using the same measuring and operation system.

In a study conducted by the NPL in 1995<sup>[82,106,107]</sup>, it was found that colour measurement results ranged from 0.1 to 3.0 CIELAB units among twenty participants. In another research project conducted by NPL, it was discovered that only 50% of measurements made by four national laboratories agreed to within a range of 0.5 CIELAB units.

According to James Rodgers, Kaye Wolf, Norm Willis, Don Hamilton, Ralph Ledbetter and Curtis Stewart<sup>[57,58]</sup>, the major studies of inter-instrumental agreement were the development of inter-instrumental agreement, software development and computer interface. The inter-instrumental systems were compared with an instrument matrix, a decision matrix, and a product matrix.

In 1987, A. R. Robertson<sup>[2]</sup> proposed a mathematical model for inter-instrumental agreement. He divided the errors into the categories of Photometric Zero Error,

**Photometric Scale Error, Wavelength Shift Error, Bandwidth Error and lastly other Error.**

**According to Robertson's definition, the errors can be summarised as follows:**

**Photometric Zero Error:**

$$R_i(\lambda) - R(\lambda) = e_1 \text{ ----- EQ. 2.7}$$

**Photometric Scale Error:**

$$R_i(\lambda) - R(\lambda) = e_2 R(\lambda) \text{ ----- EQ. 2.8}$$

**Wavelength Shift Error:**

$$R_i(\lambda) - R(\lambda) = e_3 R'(\lambda) \text{ ----- EQ. 2.9}$$

**Bandwidth Error:**

$$R_i(\lambda) - R(\lambda) = e_4 R''(\lambda) \text{ ----- EQ. 2.10}$$

**Other Error:**

$$R_i(\lambda) - R(\lambda) = e_j F_j \text{ ----- EQ. 2.11}$$

### Symbols:

$\lambda$	=	Wavelength
$R(\lambda)$	=	True or standard value of spectral reflectance factor at wavelength, $\lambda$
$R_i(\lambda)$	=	Spectral reflectance factor measured in the instrument to be tested
$R'(\lambda)$	=	First derivative of $R(\lambda)$ with respect to $\lambda$ . This is the slope of the reflectance factor curve
$R''(\lambda)$	=	Second derivative of $R(\lambda)$ with respect to $\lambda$ . This is a measure of the curvature of the reflectance factor curve
$e_j$	=	A measure of the magnitude of a particular type of error. Photometric zero error are indicated by $j=1$ , photometric scale error by $j=2$ , wavelength shift error by $j=3$ <i>et al</i>
$F_j$	=	Any function of $\lambda$ , $R$ , $R'$ , $R''$

Where  $R'(\lambda)$  and  $R''(\lambda)$  can be estimated by 1). Matrix Method or 2). Selection Method.

Based on their research results, both the matrix method and the selection method performed well, and the matrix was preferable if it could be inverted accurately.

In 1988, Roy S. Berns and Kelvin H. Peterson<sup>[8]</sup> modified Robertson's equation adding more detail to describe the errors of inter-instrumental agreement. Besides the above-mentioned errors, Photometric Nonlinear Scale Error and Wavelength Nonlinear Scale Error were included, and each of the errors was represented by one equation.

Photometric Nonlinear Scale Error:

$$R_i(\lambda) - R(\lambda) = e_5[100 - R(\lambda)]R(\lambda) \text{ ---- EQ. 2.12}$$

**Wavelength Nonlinear Scale Error:**

$$R_i(\lambda) - R(\lambda) = e_6 w_1(\lambda) R'(\lambda) \text{ ---- EQ. 2.13}$$

$$w_1(\lambda) = [(\lambda - \lambda_{\text{first}})/(\lambda_{\text{last}} - \lambda_{\text{first}})] \{ 1 - [(\lambda - \lambda_{\text{first}})/(\lambda_{\text{last}} - \lambda_{\text{first}})] \} \text{ ---- EQ. 2.14}$$

$$R_i(\lambda) - R(\lambda) = e_7 w_2(\lambda) R'(\lambda) \text{ ---- EQ. 2.15}$$

$$w_2(\lambda) = \sin 2\pi (\lambda / 200) \text{ ---- EQ. 2.16}$$

Where  $e_6$  and  $e_7$  are non-linear wavelength scale errors. Weighting function  $w_1(\lambda)$  is identical to the quadratic function described in EQ. 2.9, except scaled to wavelength. Weighting function  $w_2(\lambda)$  is a one-and one-half-cycle sine wave. This would represent an instrument with both positive and negative wavelength errors.

In 1994, Lisa Reniff<sup>[63]</sup> successfully applied the equations to transfer the 45/0 reflectance factor and the average  $\Delta E^*_{ab}$  was about 0.2 units. The average reflectance factor error consistently found between the corrected measurement of the National Institute of Standards and Technology (NIST) standards and their certificate values was 0.0006.

In 1997, further studies by Roy S. Berns and Lisa Reniff<sup>[9]</sup>, resulted in the integration of all the equations, and the Abridged Technique to Diagnose Spectrophotometric Errors was developed. The integrated equation is as follows:

$$R_s(\lambda) = R(\lambda) - \beta_o - \beta_1 R(\lambda) - \beta_2 d R(\lambda)/d\lambda \text{ ----- EQ. 2.17}$$

Symbols:

$R_s(\lambda)$	=	Simulated error
$R(\lambda)$	=	True or standard value of spectral reflectance factor at wavelength, $\lambda$
$\beta_o$	=	Black photometric error
$\beta_1$	=	White photometric error
$\beta_2$	=	Wavelength error

For reference white error ( $\beta_1$ ) affects the upper portion of photometric scale more and for reference black error ( $\beta_o$ ) affects the photometric scale equally. EQ. 2.17 defining a straight line, reference white affects the slope while reference black affects the intercept. Wavelength errors ( $\beta_2$ ) affect the portion of the reflectance factor curve where there is the greatest rate of change  $d R(\lambda)/d\lambda$ .

Based on EQ. 2.17, if a flat curve occurs there is no error, if a slight curve occurs there is a small error and, once a steep curve occurs, a large error is evident.

There was the limitation for EQ. 2.17 and once applied, there was an assumption: three errors equally throughout the spectrum -----  $\beta_0$ ,  $\beta_1$ ,  $\beta_2$  assumed to be wavelength independent, but the assumption failed when the white calibration plaque was wavelength dependent because of soiling, yellowing and abrasion

Morovic and et. al<sup>[84]</sup>, proposed three modifications to the Berns and Petersen's model to calculate the inter-instrumental agreement. According to their model, the errors could be summarised as follows:

Zero-offset

$$e_0(\lambda) = 1 \text{ ----- EQ. 2.18}$$

Linearity

$$e_1(\lambda) = Rm(\lambda) \text{ ----- EQ. 2.19}$$

### Non-linearity

$$E_2(\lambda) = (100 - R_m(\lambda))R_m(\lambda) \text{ ----- EQ. 2.20}$$

For correcting wavelength scale, equations 2.21 – 2.23 were used

### Linearity

$$e_3(\lambda) = dR_m(\lambda) / d\lambda \text{ ----- EQ. 2.21}$$

### Non-linearity (Quadratic)

$$e_4(\lambda) = w_1(\lambda)dR_m(\lambda) / d\lambda \text{ ----- EQ.2.22}$$

Where  $w_1(\lambda)$  is a quadratic weighting function

### Non-linearity (Sine Wave)

$$E_5(\lambda) = w_2(\lambda)dR_m(\lambda) / d\lambda \text{ ----- EQ.2.23}$$

Where  $w_2(\lambda)$  is a sine wave weighting function

### **Bandwidth Error**

$$e_6(\lambda) = d^2 R_m(\lambda) / d\lambda^2 \text{ ----- EQ. 2.24}$$

In order to solve the coefficients, they proposed three different methods:

**Method I: The same seven coefficients for all wavelengths (7 x 1)**

7 coefficients were obtained by the use of EQ. 2.18 to EQ. 2.24, and those coefficients were used to correct the reflectance for all wavelengths.

**Method II: Seven coefficients for each wavelength (7 x 31 or 16)**

A different set of seven coefficients was obtained to correct the reflectance for each wavelength by the use of EQ. 2.18 to EQ. 2.24.



**Method III: Three coefficients for each wavelength (3 x 31 or 16)**

A different set of three coefficients was obtained to correct the photometric scale by the use of EQ. 2.18 to EQ. 2.20. This set of coefficients was used to correct reflectance at each wavelength.

The performance of Model II was expected to be the best because of the higher number of degree of freedom than that found in the case of the other models. Model I assumed the same degree of discrepancy across all wavelengths. Model III assumed that a majority of discrepancies occurred as a result of photometric error. According to their reported data, their method and their model resulted in approximately forty percent improvement in the inter-instrumental agreement.

In 1998, the neural networks method was developed to calibrate the spectrophotometer. According to H. P. Lee, G. Qiu and M. R. Luo<sup>[50]</sup>, the experimental result for two different spectrophotometers are presented which show good improvement in inter-instrumental agreement for both the training and testing samples. Using this neural networks method, the systemic errors proposed by Berns and Petersen were included in the study and the results showed a significant improvement in the inter-instrumental

agreement. The results show that after the eight hidden training process, the average colour difference was lowered from 0.65 to 0.24 CIELAB units.

## 2.8 Band-Pass Correction<sup>[6,33, 34, 35]</sup>

In 1981<sup>[34]</sup>, Stearns proposed the influence of spectrophotometer slits on the tristimulus calculations. The slit function is defined as photoreceptor response as a function of wavelength during a single radiance-factor measurement. In 1987 and 1988, Stearns<sup>[33,35]</sup> proposed another factor affecting the accuracy of tristimulus data ----- Band-pass. Based on Stearns' report, there was a significance of the difference in tristimulus values with CIELAB colour difference formula. In this project, the concept of the mathematical models was based on Band-Pass Correction.

Stearns' equation is shown as follows:

$$ZR_a = 1.2MR_a - 0.1MR_{a-1} - 0.1MR_{a+1} \text{ ----- EQ. 2.25}$$

The method of application of EQ. 2.25 is to take 1.2 times the measured radiance at any wavelength and subtract from it a tenth of radiance at the adjoining wavelengths. This gives an estimate of the zero bandwidth radiance at the central wavelength.

## **CHAPTER 3**

### **EXPERIMENTAL DESIGN AND METHODOLOGY**

#### **3.1 Introduction**

#### **3.2 Physical Standards**

#### **3.3 Colour Measuring Instruments**

#### **3.4 Methodology**

#### **3.5 Mathematical Model Development**

#### **3.1 Introduction**

In this chapter, the physical standards used for colour measurement and colour measuring instruments are discussed. The method of selection of experimental standard<sup>[30]</sup>, experimental sample<sup>[36]</sup>, and also the selection of the spectrophotometers are also outlined<sup>[94,99]</sup>. The concept of the mathematical models used to predict the colour measurement results are also described.

### 3.2 Physical Standards

The first Ceramic Colour Standard was produced in 1968<sup>[38,39]</sup>. It was mainly used to meet the demand for permanent reflectance standards. To date, the British Ceramic Research Association - National Physical Laboratory (BCRA-NPL) Ceramic Colour Standard Series II (CCS-II) is one of the most common and popularly used standards for the colour-related industries<sup>[37]</sup>. British Ceramic Research Ltd and the National Physical Laboratory developed a collaborative project for this set of standards, with the supporting work on colour difference pairs from the Society of Dyers and Colourists<sup>[75]</sup>. CCS-II tiles are mainly used to check the consistency of operation and accuracy of the colour-measuring instruments over a long period of time. The tiles are commonly divided into two types, "GLOSSY" and "MATT".

"GLOSSY" tiles are the ceramic tiles that have the whole smooth surface on the whole area, while "MATT" tiles are the ceramic tiles that have the smooth surface on the edge of the tiles but have the non-smooth surface in the center position of the tile.

### **3.2.1 Production of Ceramic Measurement Standards<sup>[14,15,101]</sup>**

These two sets of CCS-II Tiles contain three neutral grey standards that are used to test the linearity of response, and seven chromatic standards for checking the spectral response of the instruments. All of these standards are sealed into black protective trays. Two colour difference standards, one grey and one green completes the sets and which are sealed into white protective trays. They are used to compare with the middle grey standard and the green standard to provide the two colour difference pairs respectively. All the tiles of the same colour should be produced in the same batch in order to minimize the variation in the spectral properties of the standard. When subsequent batches are needed, they must be clearly labeled, and treated as separate colours for calibration purposes.

During production, careful control is applied to preserve a smooth, slightly convex surface profile, to ensure that the standard fits the aperture of an instrument precisely.

### **3.2.2 Care of Standards<sup>[54,100]</sup>**

The standards should be held by the edges in order to avoid touching the face with the fingers as this may leave marks on the surface. If the standard becomes soiled, it should

be cleaned by breathing on the surface and wiping it gently with a clean cloth or tissue. If it becomes badly finger-marked or soiled, the glazed surface may be wiped with a pad of tissue moistened with mild detergent solution or a solution of laboratory grade detergent that contains no additives such as bleaching agents, thickeners or colouring agents. After cleaning, the standard can be wiped with a pad moistened with clean water and given a final wipe dry. If this is not sufficient, a pad of tissue lightly moistened with Propanol can be applied and then dried off<sup>[14,15]</sup>. Most importantly, the standard should not be immersed in water. Care should be taken in handling and cleaning the standard to avoid scratching the glazed surface. At all times, care should be taken not to apply undue pressure when cleaning, to avoid a polishing action or the deposition of lint from the tissue onto the surface.

### **3.2.3 Use of Standards<sup>[53]</sup>**

In order to obtain the most reproducible results, measurements should be restricted to the central 60mm region of the standard. Ideally a jig should be used to locate the standard centrally over the measuring aperture of instrument. However, the back pattern on each standard is designed to help in locating it in the same position for each measurement.

A strongly coloured standard shows the effect of thermochromism or photochromism<sup>[56,68]</sup>, therefore the standard should always be allowed to stabilise at room temperature before measurement, and care should be taken to avoid undue heating during measurement. Thermochromism is a reversible change of transmittance, reflectance or absorptance caused by a change of temperature, and photochromism is the corresponding effect induced by optical radiation. Such effects can occur when the reflectance standard is used, because they may undergo a considerable temperature rise when subjected to the polychromatic irradiation used by many measuring instruments. A neutral standard does not exhibit thermochromism<sup>[56,68]</sup>. According to past research<sup>[59,92]</sup>, the red and orange tiles show significant colour change when the temperature changes, and the colour difference is in the range of 1.18 CIELAB  $\Delta E$  units when the temperature increases from 25°C to 35°C.

The effects of thermochromism and photochromism can occur in the use of reflectance standards, as they may undergo a considerable temperature rise when subjected to the polychromatic irradiation used by many measuring instruments.

After the measurement of standards, the reflectance curves of the standards were plotted



as follows:

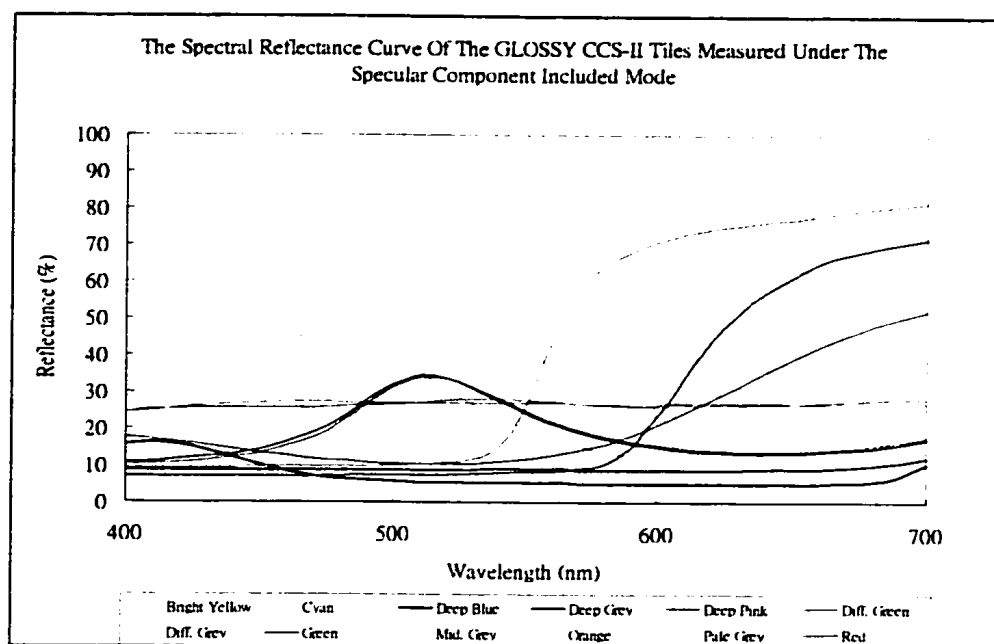


**Figure 3.1 The Standard Calibrated Reflectance Curve Of The GLOSSY Type Standard Tiles Measured Using Specular Component Included Mode By CE-7000A**

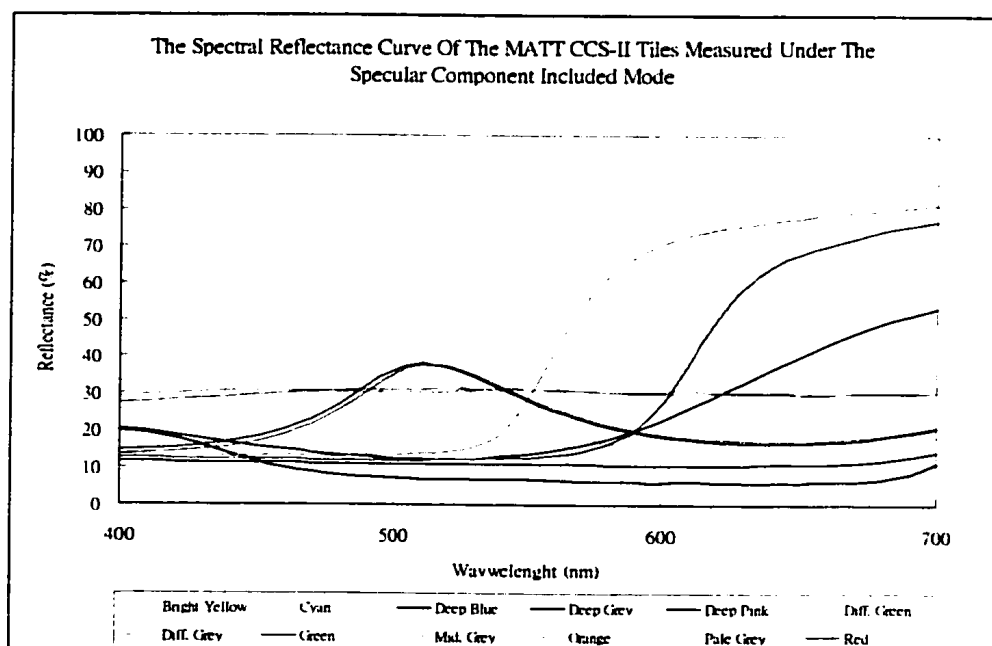


**Figure 3.2 The Standard Calibrated Reflectance Curve Of The MATT Type Standard Tiles Measured Using Specular Component Included Mode By CE-7000A**

### 3.2.4 Other Testing Samples

In this project, BCRA-NPL CCS-II tiles were the main calibrating standards and the data input for building up the mathematical models. After the development of mathematical models, two different types of samples were selected to test the performance of the mathematical models. One was a textile sample and the other was a selected ColorCurve sample.

The distribution of the textile samples and ColorCurve samples are plotted as follows:

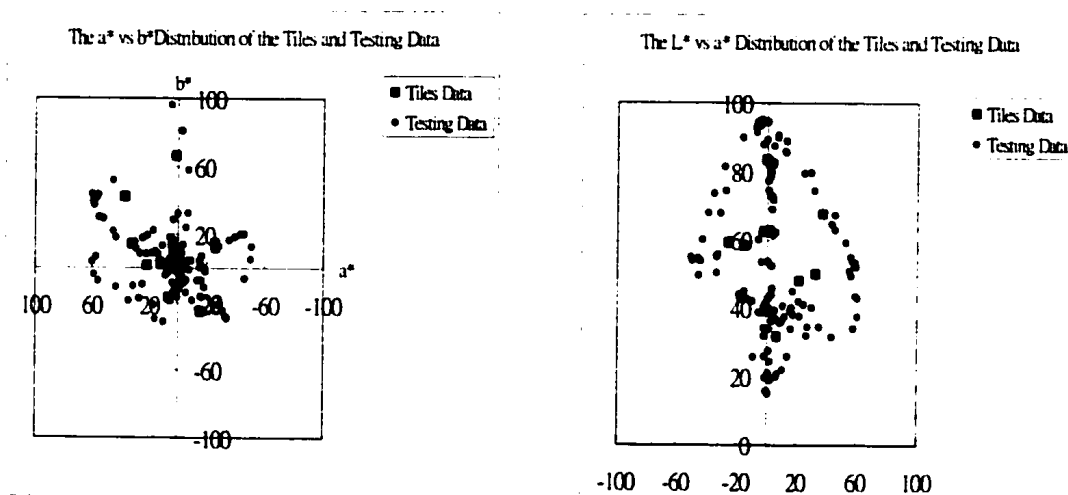


**Figure 3.3 The CIE L\*, a\* And b\* Space Distribution Of The Textile Samples**

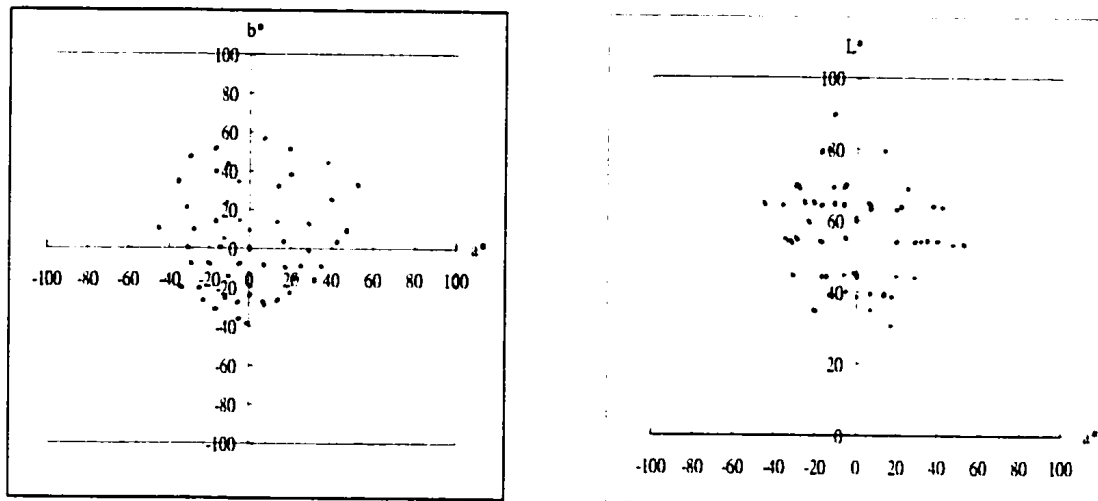


**Figure 3.4 The CIE  $L^*$ ,  $a^*$  And  $b^*$  Space Distribution Of The ColorCurve Samples**

### 3.3 Colour Measuring Instruments<sup>[55,102]</sup>

The objective of this project was to determine the inter-instrumental agreement between different reflectance spectrophotometers, thus the colour measurement instruments were the most important control during the whole study period.

The historical development and the internal parts and designs of spectrophotometers were discussed in the previous chapter.

In this project, three different spectrophotometers were used to study inter-instrumental agreement. They were:

-Spectraflash 600 PLUS (SF-600) from Datacolor International<sup>[29]</sup>

-COLOR-EYE 7000A (CE-7000A) from GretagMacbeth<sup>[71]</sup>

-COLOR-EYE 2180 (CE-2180) from GretagMacbeth<sup>[70]</sup>

All of three different reflectance spectrophotometers work on the principles of sphere type measuring geometry. Both SF-600 and CE-7000A are dual-beam type spectrophotometers, while CE-2180 is a single-beam type spectrophotometer. Table 3.1 describes the major features of these three instruments in terms of their optical design, illumination, optical geometry configuration, spectral range, aperture size, wavelength interval, dynamic range, baud rate and working environment.

**Table 3.1: Comparison Of the Three Different Types Of Spectrophotometer Used In This Research**

	<b>CE-2180</b>	<b>CE-7000A</b>	<b>SF-600</b>
<b>Optical Design</b>	Single-beam	Dual-beam	Dual-beam
<b>Illumination</b>	Pulsed Xenon Flashlamp	Pulsed Xenon Flashlamp	Pulsed Xenon Flashlamp
<b>Optical Geometry Configuration</b>	D/8 (diffuse)	D/8 (diffuse)	D/8 (diffuse)
<b>Spectral Range</b>	360 – 750 nm	360 – 750 nm	360 – 700 nm
<b>Aperture Size</b>	LAV – 14 mm SAV 5 mm	LAV – 25.4 mm MAV – 15 mm SAV – 10 mm USAV – 3 mm	LAV – 26 mm SAV – 5 mm USAV 2.5 mm
<b>Wavelength Interval</b>	10 nm	10 nm	10 nm
<b>Photometric Range / Dynamic Range</b>	0% - 150%	0% - 200%	0% - 200%
<b>Baud Rate</b>	9600	9600	9600 / 19200
<b>Measurement Cycle Time</b>	-----	1 second	<= 4 sec
<b>Operating Environment</b>	15 to 32°C, 0 – 80%Relative Humidity, non-condensing	15 to 32°C, 25 – 80%Relative Humidity, non-condensing	5 to 40°C, 20 – 85%Relative Humidity, non-condensing

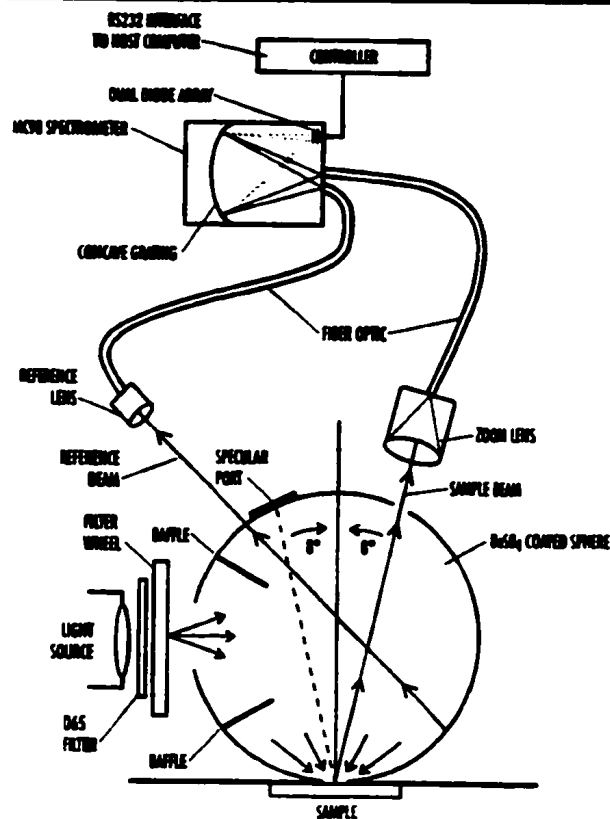


**Figure 3.5 Optical Block Diagram For Dual Beam Spectrophotometer (Source: Datacolor International, Spectraflash® 600 PLUS Operators Manual, April 1997)**

## 3.4 Methodology

### 3.4.1 Instrument Setting

All the colour measuring instruments were set according to the following:

- large area of view;
- wavelength range: 400nm to 700nm at 10nm intervals.

Since all spectrophotometers are of sphere type, the specular component excluded (SCE) or specular component included (SCI) should be specified in advance of the measurement process.

### **3.4.2 Sample Conditioning**

All the CCS II tiles, textile sample, Color Curve sample and reflectance spectrophotometers were conditioned according to standard temperature and humidity levels in the laboratory ( $20\pm1^{\circ}\text{C}$  and 68% relative humidity) 24 hours before the measurements took place to eliminate variables caused by temperature and humidity change.

### **3.4.3 Instrument Calibration<sup>[60]</sup>**

Before measuring the tiles, all colour measuring instruments were warmed up for a period of 30 to 60 minutes, according to the recommendation provided by the instrumental suppliers. In the research under discussion, all the colour measurement instruments were left to warm up for 30 minutes before measurement and then calibrated according to the manufacturer's guide using both the black and the white standard.

#### **3.4.4 Measurement Procedure**

Each tile, textile sample and Color Curve sample was measured once at the centre position for spectral reflectance factor from 400nm to 700nm at 10nm intervals using the advanced colour control software, SCOPE.

#### **3.4.5 Evaluation of the Performance of the Models**

After the measurement of tiles, textile samples and Color Curve samples, the average  $\Delta E^*_{ab}$  units were reported in order to evaluate the performance of the colour measuring instruments. (All the colorimetric data<sup>[18]</sup> used in this project was calculated by use of the CIELAB colour difference formula under  $D_{65}$  and CIE 1964 standard observer conditions).

### **3.5 Mathematical Model Development<sup>[92]</sup>**

In order to enhance the inter-instrumental agreement among spectrophotometers, many different mathematical models have been developed in the past years but, to date, no reliable mathematical models have been proposed for inter-instrumental agreement. In Bern's and Petersen's mathematical models, cyan tiles were used as the calibrating



standards and the other eleven tiles were used for the tested samples. Their model did not cover other physical samples. In this project, a new mathematical model was developed based on the concept of band-pass correction<sup>[6,33,34,35]</sup> and using the computer programme SPSS<sup>[79,80,81]</sup>. The twelve ceramic tiles were used as the calibration standards and the textile samples and the paper samples were used as the tested samples in this newly developed model.

The reflectance data for the twelve tiles at specific wavelength measured by CE-7000A were fitted as the dependent valuable for the purpose of SPSS application. The reflectance data for the twelve tiles at specific wavelength, and the reflectance data for the twelve tiles at 10nm before and after specific wavelength for the twelve tiles for SF-600 or CE-2180 were fitted as the independent valuable. Using the “Stepwise” method, a set of the coefficients was calculated, and the regression coefficient was used to evaluate the goodness of fit.

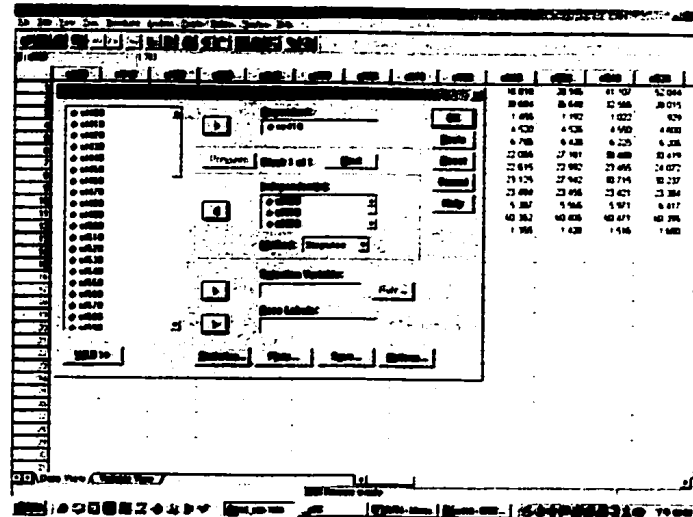


**Figure 3.6 The Regression Method Used To Develop The Mathematical Model**

## **CHAPTER 4**

### **SPECTROPHOTOMETRIC MEASUREMENT RESULTS**

#### **4.1 Introduction**

#### **4.2 Repeatability**

#### **4.3 Wavelength Shift**

#### **4.4 Inter-Instrumental Agreement**

#### **4.5 Differences In The Summation Of The Relative Spectral Reflectance Difference Of CCS-II Tiles For Visual Spectrum Measured Using Different Spectrophotometers**

## **4.1 Introduction**

This chapter provides preliminary findings on the different spectral reflectance results for Ceramic Tiles within the visual spectrum measured using different spectrophotometers. The repeatability and the inter-instrumental agreement of the spectrophotometers are also reported here.

## **4.2 Repeatability**

Repeatability is the closeness of agreement between the results of successive measurements of the same test specimen, or of test specimens taken at random from a homogeneous supply, carried out using a single instrument, the same method of measurement, operator, and measurement method, with repetition over a specified period of time.

CCS-II tiles were used to evaluate the repeatability and inter-instrumental agreement of the reflectance spectrophotometers. In this research project, long-term repeatability was studied for a period of three years. Repeatability and inter-instrumental agreement were quantified by evaluating their lightness difference ( $\Delta L^*$ ),  $a^*$  difference ( $\Delta a^*$ ),  $b^*$

difference ( $\Delta b^*$ ), chroma difference ( $\Delta C^*$ ), Hue difference ( $\Delta H^*$ ) and also colour difference values  $\Delta E^*_{ab}$ . The results are summarized below.

The lightness difference,  $a^*$  difference,  $b^*$  difference, chroma difference and hue difference and colour difference of the repeatability is the difference between the average of the measurement data and measurement results taken at weekly intervals.

The average of the lightness difference,  $a^*$  difference,  $b^*$  difference, chroma difference, hue difference and colour difference for the last 60 weeks was calculated using the following equation and the results were reported in Appendix II:

$$\text{Sample avge} = \Sigma \Delta p / 60 \text{ where } p = L^*, a^*, b^*, C^*, H^* \text{ or } E^*_{ab} \text{ ----- EQ. 4.1}$$

$$\Delta p = P_{\text{late Measurement}} - P_{\text{Average Measurement}} \text{ ----- EQ. 4.2}$$

The average  $\Delta E^*_{ab}$  is the average of the summation of average colour difference values for the twelve tiles.

$$\text{Average } \Delta E^*_{ab} = \Sigma \Delta E^*_{ab} / 12 \text{ ---- EQ. 4.3}$$

Those values and standard derivation are summarized as follows:

## Chapter 4 Spectrophotometric Measurement Results

**Table 4.1: Summary Of The Repeatability Of The CCS-II Tiles Measured Using Gretag Macbeth CE-7000A**

<i>Tile</i>	<i>GE<sup>1</sup></i>	<i>SD<sup>5</sup></i>	<i>GI<sup>2</sup></i>	<i>SD</i>	<i>ME<sup>3</sup></i>	<i>SD</i>	<i>MI<sup>4</sup></i>	<i>SD</i>
<i>Pale Grey</i>								
<i>Sample avge</i>	0.024	0.010	0.018	0.011	0.024	0.018	0.030	0.017
<i>Mid Grey</i>								
<i>Sample avge</i>	0.020	0.009	0.018	0.007	0.023	0.009	0.019	0.010
<i>Diff Grey</i>								
<i>Sample avge</i>	0.020	0.008	0.021	0.009	0.031	0.013	0.025	0.010
<i>Deep Grey</i>								
<i>Sample avge</i>	0.083	0.015	0.038	0.012	0.045	0.015	0.035	0.013
<i>Deep Pink</i>								
<i>Sample avge</i>	0.046	0.016	0.030	0.012	0.047	0.012	0.037	0.011
<i>Red</i>								
<i>Sample avge</i>	0.332	0.081	0.045	0.020	0.056	0.019	0.068	0.020
<i>Orange</i>								
<i>Sample avge</i>	0.120	0.032	0.080	0.022	0.109	0.039	0.067	0.024
<i>Bright Yellow</i>								
<i>Sample avge</i>	0.155	0.041	0.102	0.033	0.052	0.024	0.055	0.019
<i>Green</i>								
<i>Sample avge</i>	0.047	0.019	0.033	0.020	0.047	0.016	0.054	0.016
<i>Diff Green</i>								
<i>Sample avge</i>	0.054	0.015	0.035	0.019	0.036	0.016	0.037	0.013
<i>Cyan</i>								
<i>Sample avge</i>	0.054	0.015	0.043	0.013	0.050	0.021	0.047	0.017
<i>Deep Blue</i>								
<i>Sample avge</i>	0.389	0.109	0.100	0.021	0.068	0.017	0.057	0.017
<b>Average <math>\Delta E^*_{ab}</math></b>								
	<b>0.112</b>		<b>0.047</b>		<b>0.049</b>		<b>0.044</b>	

1 = GLOSSY Tiles Measured using Specular Component Excluded Mode

2 = GLOSSY Tiles Measured using Specular Component Included Mode

3 = MATT Tiles Measured using Specular Component Excluded Mode

4 = MATT Tiles Measured using Specular Component Included Mode

5 = Standard Deviation

Table 4.1 shows that the repeatability of the CCS-II tiles measured using Gretag Macbeth CE-7000A, except in the case of GLOSSY tiles measured under specular component excluded mode, was satisfactory for the measurement combinations. In the case of GLOSSY tiles measured using the specular component excluded mode, the repeatability for the red, orange, bright yellow and deep blue was larger than 0.1 CIELAB  $\Delta E$  units. In those cases, the poor repeatability may have been caused by the high reflection inside the integrated sphere, in addition to which some of the reflected beam may have been lost through the opening of the specular component port. The repeatability for deep blue was also poor as a result of the low signal-to-noise ratio, which reduced the repeatability.



#### Chapter 4 Spectrophotometric Measurement Results

**Table 4.2: Summary Of The Repeatability Of The CCS-II Tiles Measured Using Gretag Macbeth CE-2180**

<i>Tile</i>	<i>GE<sup>1</sup></i>	<i>SD<sup>5</sup></i>	<i>GI<sup>2</sup></i>	<i>SD</i>	<i>ME<sup>3</sup></i>	<i>SD</i>	<i>MI<sup>4</sup></i>	<i>SD</i>
<i>Pale Grey</i>								
<i>Sample avge</i>	0.118	0.042	0.124	0.032	0.120	0.039	0.123	0.034
<i>Mid Grey</i>								
<i>Sample avge</i>	0.133	0.088	0.057	0.077	0.173	0.048	0.093	0.023
<i>Diff Grey</i>								
<i>Sample avge</i>	0.071	0.087	0.073	0.074	0.237	0.055	0.106	0.024
<i>Deep Grey</i>								
<i>Sample avge</i>	0.342	0.333	0.140	0.217	0.363	0.085	0.073	0.063
<i>Deep Pink</i>								
<i>Sample avge</i>	0.272	0.247	0.097	0.195	0.336	0.076	0.083	0.050
<i>Red</i>								
<i>Sample avge</i>	0.802	1.494	0.197	0.357	0.364	0.085	0.104	0.070
<i>Orange</i>								
<i>Sample avge</i>	0.269	0.498	0.272	0.315	0.236	0.119	0.228	0.086
<i>Bright Yellow</i>								
<i>Sample avge</i>	0.187	0.467	0.156	0.320	0.101	0.084	0.116	0.080
<i>Green</i>								
<i>Sample avge</i>	0.190	0.245	0.146	0.195	0.186	0.062	0.090	0.052
<i>Diff Green</i>								
<i>Sample avge</i>	0.250	0.271	0.136	0.198	0.151	0.059	0.141	0.061
<i>Cyan</i>								
<i>Sample avge</i>	0.127	0.153	0.110	0.150	0.271	0.061	0.175	0.045
<i>Deep Blue</i>								
<i>Sample avge</i>	0.806	1.822	0.150	0.388	0.582	0.114	0.081	0.120
<b><i>Average <math>\Delta E^*_{ab}</math></i></b>	<b>0.297</b>		<b>0.140</b>		<b>0.260</b>		<b>0.118</b>	

1 = GLOSSY Tiles Measured using Specular Component Excluded Mode

2 = GLOSSY Tiles Measured using Specular Component Included Mode

3 = MATT Tiles Measured using Specular Component Excluded Mode

4 = MATT Tiles Measured using Specular Component Included Mode

5 = Standard Deviation

Table 4.2 shows the repeatability of the CCS-II tiles measured using Gretag Macbeth CE-2180, and the repeatability of the four measurement combinations ranged from 0.118 to 0.297 CIELAB  $\Delta E$  units. The repeatability results show that the stability of the CE-2180 was inferior. The results were affected by either the drift of the measurement electronics or variation in the light sources.

When the GLOSSY tiles were measured using the specular component excluded mode, the repeatability for the red and deep blue was larger than 1 CIELAB  $\Delta E$  unit. In the case of red, the repeatability result may have been caused by the high reflection inside the integrated sphere, and some of the reflected beam may have been lost through the opening of the specular component port. The deep blue result was also disappointing because of the low signal to noise ratio, thus the repeatability was unsatisfactory.

## Chapter 4 Spectrophotometric Measurement Results

**Table 4.3: Summary Of The Repeatability Of The CCS-II Tiles Measured Using Datacolor SF-600**

<i>Tile</i>	<i>GE<sup>1</sup></i>	<i>SD<sup>5</sup></i>	<i>GI<sup>2</sup></i>	<i>SD</i>	<i>ME<sup>3</sup></i>	<i>SD</i>	<i>MI<sup>4</sup></i>	<i>SD</i>
<i>Pale Grey</i>								
<i>Sample ave</i>	0.038	0.023	0.035	0.012	0.039	0.022	0.024	0.017
<i>Mid Grey</i>								
<i>Sample ave</i>	0.047	0.024	0.035	0.020	0.039	0.022	0.028	0.016
<i>Diff Grey</i>								
<i>Sample ave</i>	0.053	0.025	0.044	0.019	0.035	0.020	0.039	0.020
<i>Deep Grey</i>								
<i>Sample ave</i>	0.099	0.055	0.043	0.015	0.050	0.036	0.041	0.021
<i>Deep Pink</i>								
<i>Sample ave</i>	0.083	0.033	0.041	0.019	0.063	0.033	0.054	0.020
<i>Red</i>								
<i>Sample ave</i>	0.254	0.190	0.052	0.024	0.057	0.029	0.051	0.019
<i>Orange</i>								
<i>Sample ave</i>	0.116	0.055	0.060	0.023	0.081	0.045	0.067	0.028
<i>Bright Yellow</i>								
<i>Sample ave</i>	0.125	0.071	0.075	0.036	0.060	0.040	0.066	0.036
<i>Green</i>								
<i>Sample ave</i>	0.050	0.031	0.048	0.020	0.057	0.028	0.053	0.025
<i>Diff Green</i>								
<i>Sample ave</i>	0.059	0.033	0.048	0.019	0.042	0.029	0.049	0.017
<i>Cyan</i>								
<i>Sample ave</i>	0.042	0.013	0.033	0.010	0.045	0.010	0.032	0.013
<i>Deep Blue</i>								
<i>Sample ave</i>	0.250	0.099	0.048	0.019	0.052	0.033	0.050	0.020
<i>Average <math>\Delta E^*_{ab}</math></i>								
	<b>0.101</b>		<b>0.047</b>		<b>0.052</b>		<b>0.046</b>	

1 = GLOSSY Tiles Measured using Specular Component Excluded Mode

2 = GLOSSY Tiles Measured using Specular Component Included Mode

3 = MATT Tiles Measured using Specular Component Excluded Mode

4 = MATT Tiles Measured using Specular Component Included Mode

5 = Standard Deviation

Table 4.3 shows that the repeatability of the CCS-II tiles measured using Datacolor International SF-600, except in the case of GLOSSY tiles measured using specular component excluded mode, was satisfactory for the measurements combination. The repeatability for the red, orange, bright yellow, deep grey and deep blue of the GLOSSY tiles measured using specular excluded mode was larger than 0.1 CIELAB  $\Delta E$  units. In the case of red, orange and bright yellow, the poor repeatability may have been caused by the high reflection inside the integrated sphere and some of the reflected beam may have been lost through the opening of the specular component port. The repeatability for deep blue and deep grey was also very poor because of the low signal-to-noise ratio.

According to the results shown in Table 4.2, it may be concluded that the stability of the CE-2180 was poor because the average  $\Delta E^*_{ab}$  values ranged from 0.115 to 0.377 units. The other two measurement results, shown in Tables 4.1 and 4.3, show that the stability was good because the average  $\Delta E^*_{ab}$  values for SF-600 ranged from 0.046 to 0.101 units and the average  $\Delta E^*_{ab}$  values for CE-7000A ranged from 0.044 to 0.112 units. The good repeatability of the SF-600 and CE-7000A was due to the presence of a second beam, the reference beam, in these two dual-beam spectrophotometers. The second beam was used to allow direct measurement of the reflectance between the ratio of reflected and incident light. Dual-beam measurements are preferred for use in

industry as a result of their inherent stability, as the measurement is of a ratio rather than an absolute value.

Of the three spectrophotometers, red, orange and bright yellow, had the higher  $\Delta E^*_{ab}$  values ( $>0.1 \Delta E^*_{ab}$ ) even though the measurements were carried out inside a room with controlled temperature and humidity. This was because of the different size of the integrated sphere and the position of the specular component port. During the measurement of the tiles, some of the reflected beam was emitted through the opening of the specular component port. In addition, the random reflectance resulted in poor measurement results for sensitive colours.

Based on the average  $\Delta E^*_{ab}$  values of the three spectrophotometers, it was concluded that the repeatability of the CE-2180 needed further improvement using better calibration procedures. The repeatability of the other two spectrophotometers was satisfactory and the colorimetric values were further used to evaluate the inter-instrumental agreement. According to the results shown in Table 4.1, the repeatability for CE-7000A was the best of all the three spectrophotometers;

CE-7000A was used as the reference instrument to evaluate the inter-instrumental agreement of three spectrophotometers.

In addition to the above repeatability results, long term repeatability was important in this study. The results of the long term repeatability are plotted in the following figures.

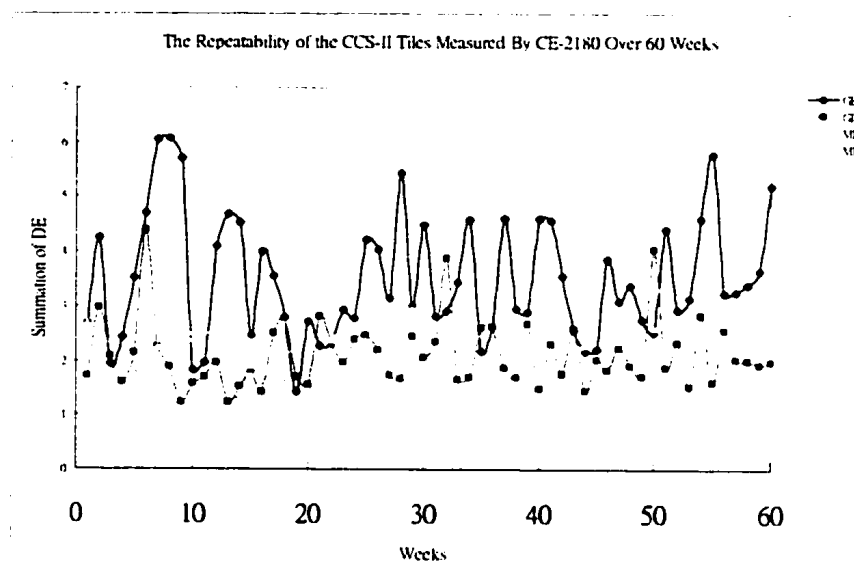


**Figure 4.1 The Repeatability Of The CCS-II Tiles Measured Using CE-2180 Over A Period of 60 Weeks**

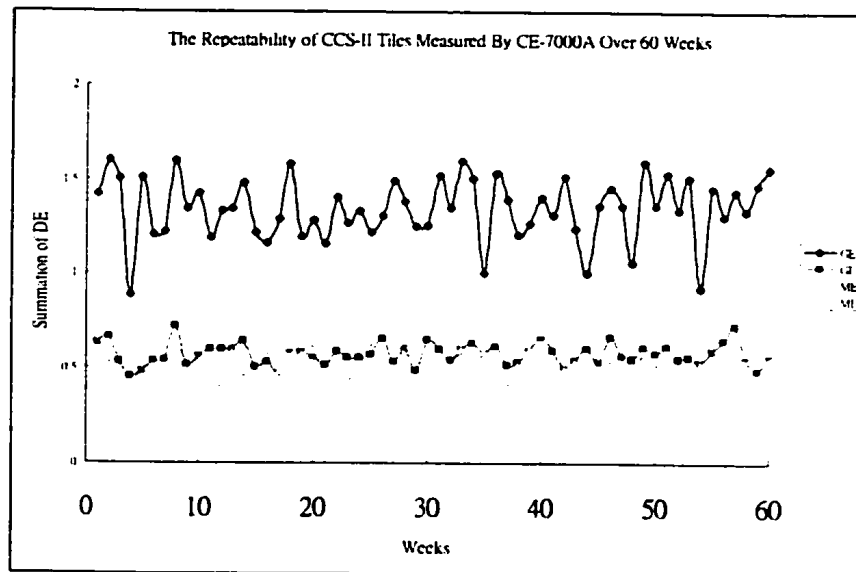


**Figure 4.2 The Repeatability Of The CCS-II Tiles Measured Using CE-7000A Over A Period of 60 Weeks**

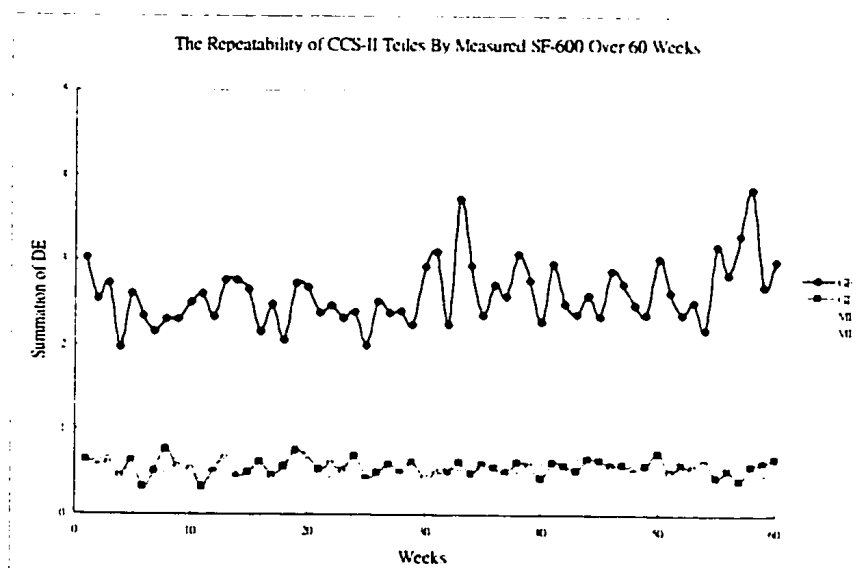


**Figure 4.3 The Repeatability Of The CCS-II Tiles Measured Using SF600 Over A Period of 60 Weeks**

The three figures above, which show results for the repeatability of the CCS-II tiles measured using different spectrophotometers, indicate that long-term repeatability was satisfactory over a long period of time. The results imply that the three spectrophotometers were stable for the duration of the whole study period.

### 4.3 Wavelength Shift

In addition to the colour difference of the spectrophotometer, wavelength shift is another parameter to determine repeatability. The equations used for wavelength calculation are shown as follows:

$$\text{Wavelength shift} = dR_{(\lambda)}/d\lambda \text{ ----- EQ. 4.4}$$

Difference of Wavelength Shift between spectrophotometric measurement =

$$(dR_{(\lambda)}/d\lambda)_{\text{last measurement}} - (dR_{(\lambda)}/d\lambda)_{\text{initial measurement}} \text{ ----- EQ. 4.5}$$



Where,

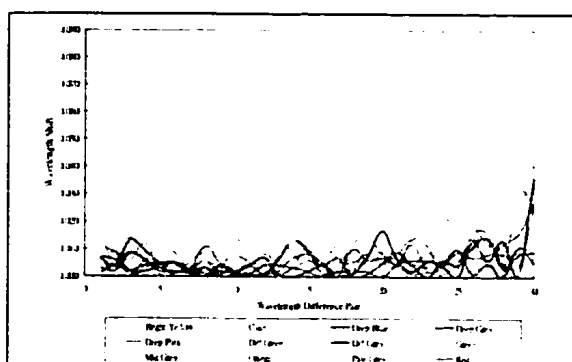
initial measurement is the measurement results measured at the beginning of the repeatability study,

while,

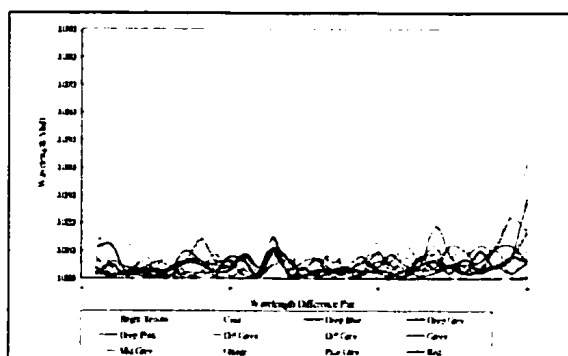
last measurement is the measurement results at the end of the repeatability study.

The wavelength shift for the visual spectrum was obtained using equations 4.4 and 4.5.

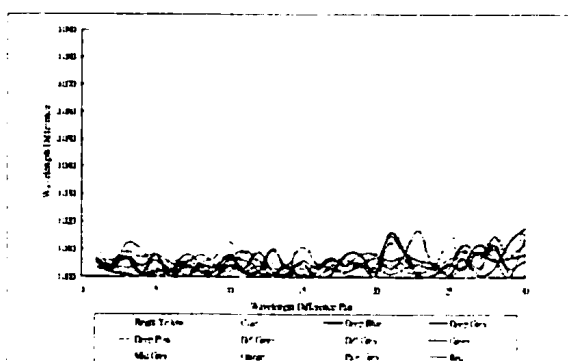
The wavelength shift results of the three different spectrophotometers were plotted as follows:



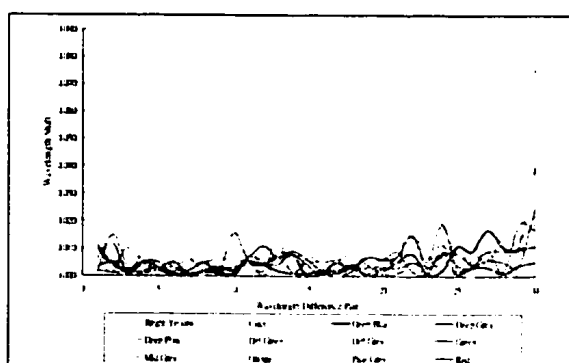
**Figure 4.4 The Wavelength Shift Of The GLOSSY Tiles Measured Using The Specular Component Excluded Mode Of CE-2180**



**Figure 4.5 The Wavelength Shift Of The GLOSSY Tiles Measured Using The Specular Component Included Mode Of CE-2180**

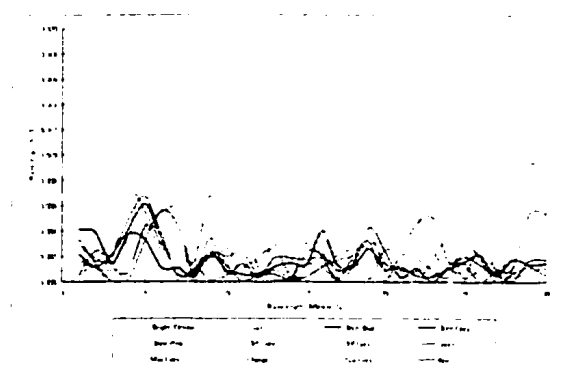


**Figure 4.6 The Wavelength Shift Of The MATT Tiles Measured Using The Specular Component Excluded Mode Of CE-2180**

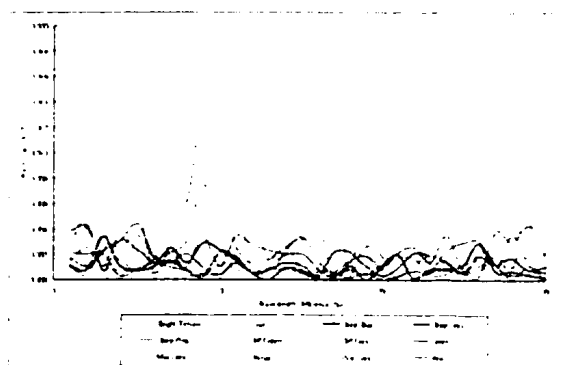


**Figure 4.7 The Wavelength Shift Of The MATT Tiles Measured Using The Specular Component Included Mode Of CE-2180**

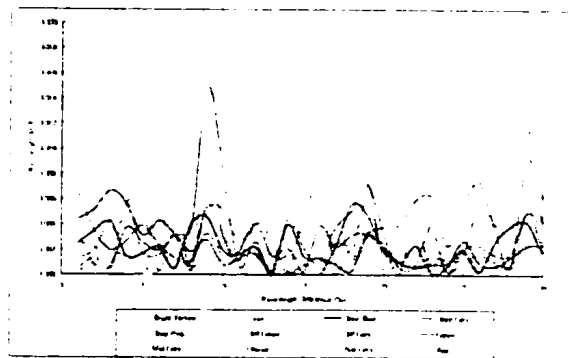
From Figures 4.3 – 4.7, showing the wavelength shift of the CCS-II tiles, it may be seen that the difference in wavelength between the initial and the last measurement of CE-2180 did not exceed 0.09 units. This indicates that the repeatability along the whole experience period was within an acceptable range. In addition to Table 4.2, those results imply the repeatability was poor when results are compared with the other two spectrophotometers.



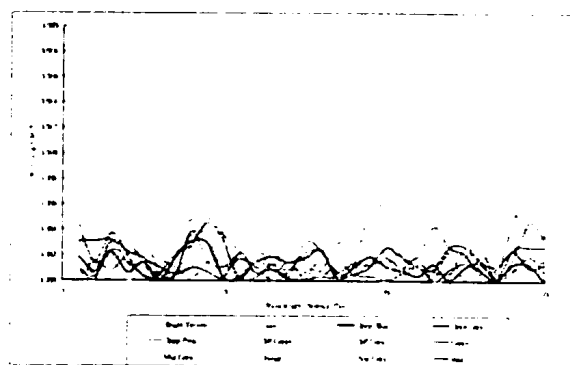
**Figure 4.8 The Wavelength Shift Of The GLOSSY Tiles Measured Using The Specular Component Excluded Mode Of CE-7000A**



**Figure 4.9 The Wavelength Shift Of The GLOSSY Tiles Measured Using The Specular Component Included Mode Of CE-7000A**

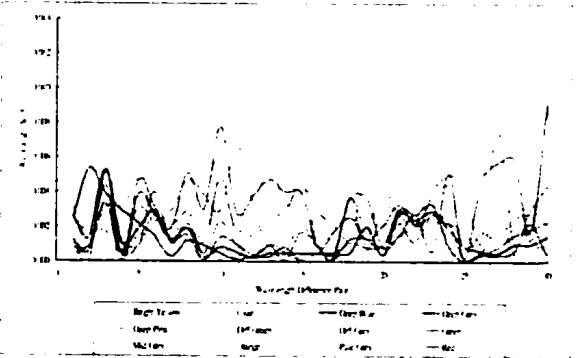
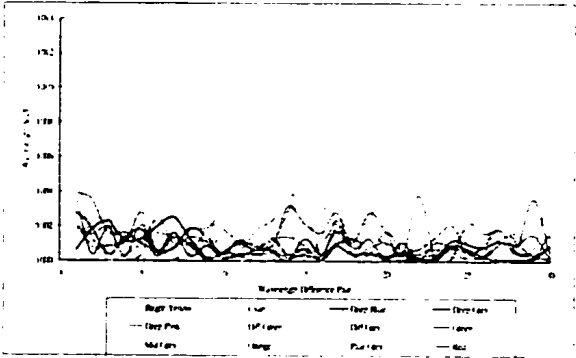
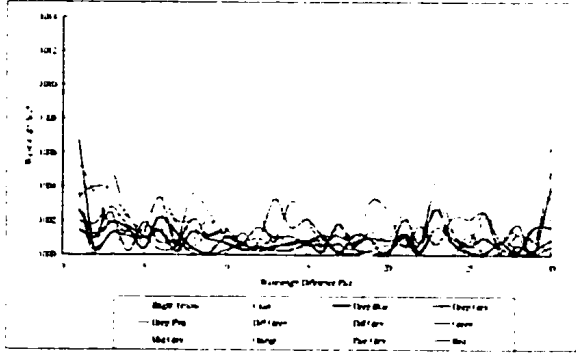


**Figure 4.10 The Wavelength Shift Of The MATT Tiles Measured Using The Specular Component Excluded Mode Of CE-7000A**



**Figure 4.11 The Wavelength Shift Of The MATT Tiles Measured Using Specular Component Included Mode Of CE-7000A**

Figures 4.8 – 4.11, showing the wavelength shift of the CCS-II tiles, demonstrate that the different wavelength between the initial measurement of CE-7000A and the last measurement of CE-7000A did not exceed 0.02 units. The repeatability for the whole experience period was considered to be satisfactory. In addition to results shown in Table 4.1, those results imply that the repeatability was good when compared with the other CE-2180.



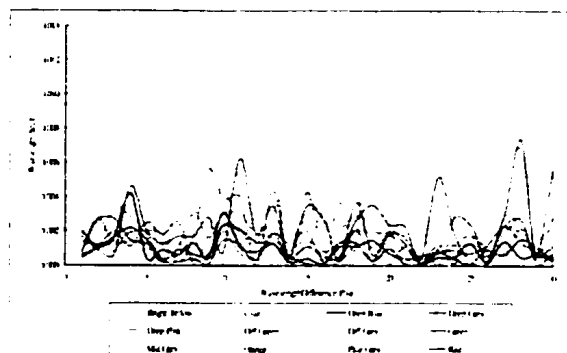


**Figure 4.15 The Wavelength Shift Of The MATT Tiles Measured Using Specular Component Included Mode Of SF-600**

Figures 4.12 – 4.15, which show the wavelength shift of the CCS-II tiles, demonstrate that the difference in wavelength between the initial measurement of SF-600 and the last measurement of SF-600 did not exceed 0.014 units. The repeatability for the whole experience period is seen to be satisfactory. In addition to Table 4.3, the results imply that the repeatability was good compared with those for CE-2180 but similar to those of CE-7000A.

Tables 4.1 – 4.3 and Figures 4.4 – 4.15 shows that the colour difference and the wavelength shift were satisfactory for CE-7000A. CE-7000A was selected as the reference spectrophotometer to evaluate the inter-instrumental agreement by comparing the measurement results with CE-2180 and SF-600.

#### **4.4 Inter-Instrumental Agreement**

Inter-instrumental agreement is the closeness of agreement between the results of successive measurements of the same test specimen, or of test specimens between two or more spectrophotometers achieved using the same measuring and operation system.

As discussed, the repeatability for CE7000A was found to be satisfactory, therefore CE-7000A was selected as a reference spectrophotometer to evaluate the inter-instrumental agreement of CE-7000A and SF-600 as well as CE-7000A and CE-2180.

The lightness difference,  $a^*$  difference,  $b^*$  difference, chroma difference and hue difference and colour difference of the inter-instrumental agreement was the difference between average of the measurement data measured against each week's measurement results. The average of the lightness difference,  $a^*$  difference,  $b^*$  difference, chroma difference, hue difference and colour difference across the last 60 weeks of the experimental work was calculated using the equation below and the results were reported in Appendix III.

$$\text{Sample avge} = \Sigma \Delta p / 60 \text{ where } p = L^*, a^*, b^*, C^*, H^* \text{ or } E^*_{ab} \text{ ----- EQ. 4.6}$$

$$\Delta p = P_{\text{Late Measurement from SF-600 or 2180}} - P_{\text{Average Measurement from CE7000A}} \text{ ----- EQ. 4.7}$$

Average  $\Delta E^*_{ab}$  is the average of the summation of average colour difference values for the twelve tiles.

$$\text{Average } \Delta E^*_{ab} = \Sigma \Delta E^*_{ab} / 12 \text{ ----- EQ. 4.8}$$



## 4.4.1 The Inter-Instrumental Agreement of SF-600 compared to CE-7000A

**Table 4.4: Summary Of The Inter-Instrumental Agreement Of SF-600 And CE-7000A Using CCS-II Tiles**

<i>Tile</i>	<i>GE<sup>1</sup></i>	<i>GI<sup>2</sup></i>	<i>ME<sup>3</sup></i>	<i>MI<sup>4</sup></i>
<i>Pale Grey</i>				
<i>Sample avge</i>	0.690	0.428	0.590	0.361
<i>Mid Grey</i>				
<i>Sample avge</i>	0.459	0.269	0.422	0.182
<i>Diff Grey</i>				
<i>Sample avge</i>	0.495	0.293	0.395	0.166
<i>Deep Grey</i>				
<i>Sample avge</i>	0.196	0.217	0.183	0.074
<i>Deep Pink</i>				
<i>Sample avge</i>	0.756	0.737	0.633	0.603
<i>Red</i>				
<i>Sample avge</i>	0.650	1.263	0.713	0.890
<i>Orange</i>				
<i>Sample avge</i>	1.050	1.084	0.874	0.968
<i>Bright Yellow</i>				
<i>Sample avge</i>	1.437	0.930	0.749	0.768
<i>Green</i>				
<i>Sample avge</i>	1.120	0.775	0.867	0.762
<i>Diff Green</i>				
<i>Sample avge</i>	1.095	0.749	0.788	0.652
<i>Cyan</i>				
<i>Sample avge</i>	1.232	1.004	0.903	0.824
<i>Deep Blue</i>				
<i>Sample avge</i>	1.028	0.849	0.890	0.677
<b><i>Average <math>\Delta E^*_{ab}</math></i></b>	<b>0.851</b>	<b>0.717</b>	<b>0.667</b>	<b>0.577</b>

1 = GLOSSY Tiles Measured using Specular Component Excluded Mode

2 = GLOSSY Tiles Measured using Specular Component Included Mode

3 = MATT Tiles Measured using Specular Component Excluded Mode

4 = MATT Tiles Measured using Specular Component Included Mode

As may be seen in Table 4.4, which shows the inter-instrumental agreement between SF-600 and CE-7000A of the CCS-II tiles, the average  $\Delta E^*_{ab}$  values ranged from 0.577 to 0.851 units. The results were poor because, in past research, the  $\Delta E^*_{ab}$  value of different spectrophotometers was found to range from 0.1 to 3 units<sup>[82]</sup>. The main reason for the poor inter-instrumental agreement was that instrumental design of spectrophotometers varied according to different manufacturers.

The optical design for both CE-7000A and SF-600 is the same: both are dual-beam in nature, but the size of integrated sphere differs. In addition, the position of the specular component port and the detector is also different. For these reasons, the difference between the measurement results for each tile also varies and the inter-instrumental agreement between these two machines is disappointing.

#### 4.4.2 The Inter-Instrumental Agreement of CE-2180 compared with CE-7000A

**Table 4.5: Summary Of The Inter-Instrumental Agreement Of CE-2180 And CE-7000A Using CCS-II Tiles**

<i>Tile</i>	<i>GE<sup>1</sup></i>	<i>GI<sup>2</sup></i>	<i>ME<sup>3</sup></i>	<i>MI<sup>4</sup></i>
<i>Pale Grey</i>				
<i>Sample avge</i>	0.666	0.795	0.928	0.952
<i>Mid Grey</i>				
<i>Sample avge</i>	0.707	0.758	0.535	0.576
<i>Diff Grey</i>				
<i>Sample avge</i>	0.453	0.280	0.760	0.361
<i>Deep Grey</i>				
<i>Sample avge</i>	0.239	0.100	0.446	0.352
<i>Deep Pink</i>				
<i>Sample avge</i>	0.700	0.723	0.713	0.718
<i>Red</i>				
<i>Sample avge</i>	0.719	0.634	0.680	0.755
<i>Orange</i>				
<i>Sample avge</i>	0.119	0.114	0.414	0.436
<i>Bright Yellow</i>				
<i>Sample avge</i>	0.689	0.628	0.516	0.552
<i>Green</i>				
<i>Sample avge</i>	0.130	0.143	0.444	0.500
<i>Diff Green</i>				
<i>Sample avge</i>	0.790	1.023	0.852	0.997
<i>Cyan</i>				
<i>Sample avge</i>	0.140	0.195	0.454	0.428
<i>Deep Blue</i>				
<i>Sample avge</i>	1.134	1.285	0.679	0.968
<b><i>Average <math>\Delta E^*_{ab}</math></i></b>	<b><i>0.541</i></b>	<b><i>0.557</i></b>	<b><i>0.618</i></b>	<b><i>0.633</i></b>

1 = GLOSSY Tiles Measured using Specular Component Excluded Mode

2 = GLOSSY Tiles Measured using Specular Component Included Mode

3 = MATT Tiles Measured using Specular Component Excluded Mode

4 = MATT Tiles Measured using Specular Component Included Mode

With reference to Table 4.5, showing the inter-instrumental agreement for CE-2180 and CE-7000A using CCS-II tiles, it was found that the average  $\Delta E^*_{ab}$  values ranged from 0.541 to 0.633 units. The results were better than those for SF-600 and CE-7000A because the same manufacturer manufactures both the CE-2180 and CE-7000A. Although the optical design is different, the overall design principles are similar, thus their inter-instrumental agreement between CE-2180 and CE-7000A is better than in the case of CE-7000A and SF-600.

Different spectrophotometers have their own systemic errors, therefore a series of new regression models were developed in this study in order to improve the inter-instrumental measurement agreement.

#### **4.5 Differences In The Summation Of The Relative Spectral Reflectance Difference Of CCS-II Tiles For Visual Spectrum Measured Using Different Spectrophotometers**

Irrespective of the inter-instrumental agreement of CE-2180 or SF-600 and CE-7000A, the worst results were obtained when the GLOSSY tiles were measured using the specular component excluded mode. Beside the CIELAB colour difference values ( $\Delta E^*_{ab}$ ), the summation of the relative spectral reflectance difference is an alternative method to evaluate the inter-instrumental agreement of different spectrophotometers.

Summation of Relative Spectral Reflectance Difference:

$$\Sigma [(R_{\lambda \text{CE-2180 or SF-600A}} - R_{\lambda \text{CE-7000A}}) / R_{\lambda \text{CE-7000A}}] \text{----- EQ. 4.9}$$

The plot of the summation of the relative spectral reflectance difference values against the tiles is shown as follows:

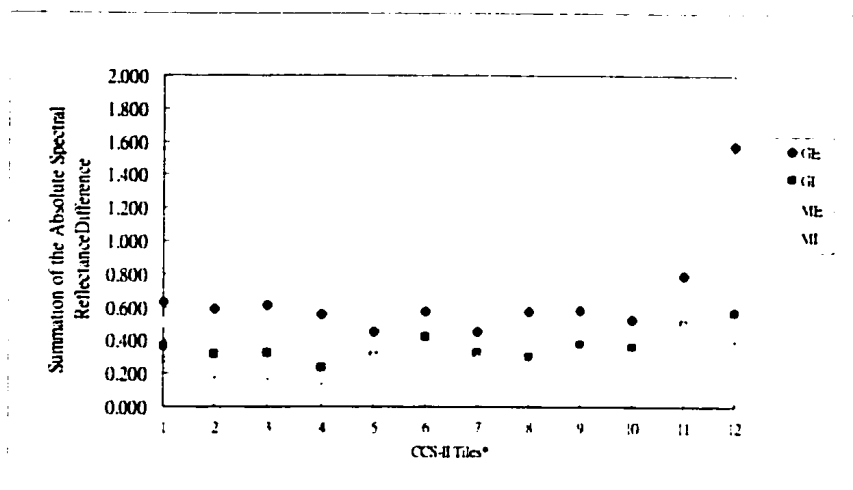


**Figure 4.16 The Distribution Of The Summation Of The Relative Spectral Reflectance Difference For The CCS-II Tiles Comparing SF-600 And CE-7000A**

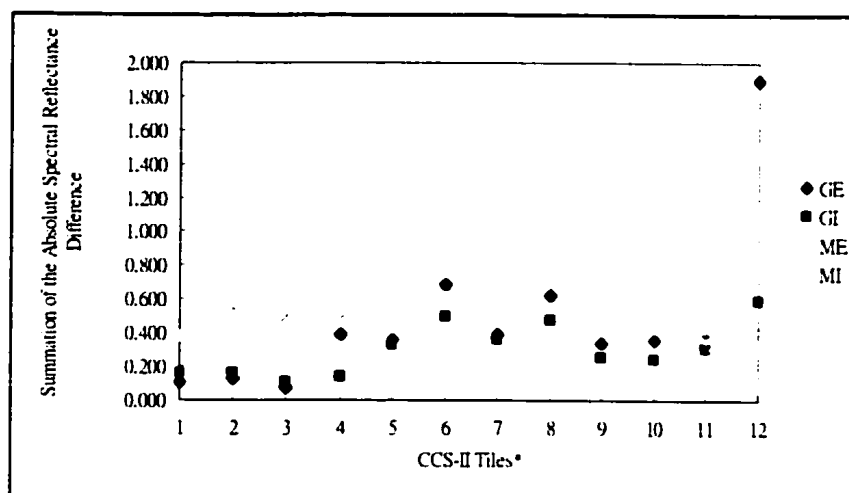


**Figure 4.17 The Distribution Of The Summation Of The Relative Spectral Reflectance Difference For The CCS-II Tiles Comparing CE-2180 And CE-7000A**

**\*Note:**

- |              |                |               |                  |
|--------------|----------------|---------------|------------------|
| 1. Pale Grey | 2. Middle Grey | 3. Diff. Grey | 4. Deep Grey     |
| 5. Deep Pink | 6. Red         | 7. Orange     | 8. Bright Yellow |
| 9. Green     | 10. Diff Green | 11. Cyan      | 12. Deep Blue    |

From Figure 4.16, it may be seen that GLOSSY tiles measured according to the specular component excluded mode showed the greater summation of the relative spectral reflectance difference. With reference to Table 4.4, which provides a summary of the inter-instrumental agreement when comparing SF-600 and CE-7000A using CCS-II tiles, a similar trend may be observed: that the higher the summation of the relative spectral reflectance difference, the higher the CIELAB colour difference,  $\Delta E^*_{ab}$ .

From Figure 4.17, it may be seen that MATT tiles measured under specular component included mode show the greater summation of the relative spectral reflectance difference. With reference to Table 4.5, which shows the summary for the inter-instrumental agreement between CE-2180 and CE-7000A of the CCS-II tiles, a similar trend may be observed, that being that the higher the summation of the relative spectral reflectance difference, the higher the CIELAB colour difference,  $\Delta E^*_{ab}$ .

Based on the results shown in Tables 4.4 and 4.5 and results in Figures 4.13 and 4.14, it may be concluded that the summation of the relative spectral reflectance difference is a good indication of colour difference. The higher the summation of the summation of the relative spectral reflectance, the higher the colour difference.



## **CHAPTER 5**

### **DEVELOPMENT OF THE FIRST MATHEMATICAL MODEL**

#### **(L-Model)**

##### **5.1 Introduction**

##### **5.2 Development Of The First Mathematical Model (L-Model)**

##### **5.3 The Improvement Of The Inter-Instrumental Agreement After Applying L-Model**

##### **5.1 Introduction**

In this chapter, the development of the first mathematical model (L-Model) is outlined.

L-Model was developed based on the colorimetric data,  $L^*$ ,  $a^*$  and  $b^*$ . The inter-instrumental agreement showed improvement after applying the mathematical model.

## **5.2 Development Of The First Mathematical Model (L-Model)**

As the inter-instrumental agreement was poor for the three different models of spectrophotometers, SF-600 vs CE-7000A and CE-2180 vs CE-7000A, a series of new mathematical models was developed in order to improve the inter-instrumental agreement. The simplest way to develop the mathematical models was the correction of the colorimetric data, CIE  $L^*$ ,  $a^*$  and  $b^*$  values for the spectrophotometers. SPSS was used to analyse the data for the  $L^*$ ,  $a^*$  and  $b^*$  values and a series of mathematical models were developed using linear regression.

For GLOSSY samples, two different series of mathematical models were developed. One series was for specular component included measurement, while the other series was for specular component excluded measurement. In addition, another two series of models were developed for "MATT" samples. As the spectral reflectance is different for "GLOSSY" and "MATT" samples, different models were developed for each in order to meet the requirements for different types of materials. As a result, the inter-instrumental agreement of the different samples became more concise and accurate.

### 5.2.1 SF-600 vs CE-7000

For GLOSSY samples measured using the specular component excluded mode, three different equations were formulated:

$$\text{Predicted } L^*_{600} \text{ value (PL}^*_{600}\text{)} = 1.008L^*_{600} - 0.008a^*_{600} - 0.006b^*_{600} + 0.061 \text{ ---- EQ.5.1}$$

$$\text{Predicted } a^*_{600} \text{ value (Pa}^*_{600}\text{)} = 1.008a^*_{600} + 0.006b^*_{600} - 0.074 \text{ ---- EQ. 5.2}$$

$$\text{Predicted } b^*_{600} \text{ value (Pb}^*_{600}\text{)} = -0.005L^*_{600} - 0.024a^*_{600} + 1.014b^*_{600} + 0.17 \text{ ---- EQ. 5.3}$$

Where

PL<sup>\*</sup><sub>600</sub>, Pa<sup>\*</sup><sub>600</sub> and Pb<sup>\*</sup><sub>600</sub> are the predicted value which is calculated by substituting the original data measured by the SF-600, L<sup>\*</sup><sub>600</sub>, a<sup>\*</sup><sub>600</sub> and b<sup>\*</sup><sub>600</sub> into the above equations.

For GLOSSY samples measured using the specular component included mode, a further three different equations were formulated:

$$\text{Predicted } L^*_{600} \text{ value (PL}^*_{600}\text{)} = 1.006L^*_{600} - 0.005a^*_{600} - 0.003b^*_{600} - 0.086 \text{ ---- EQ. 5.4}$$

$$\text{Predicted } a^*_{600} \text{ value (Pa}^*_{600}\text{)} = -0.007L^*_{600} + 1.001a^*_{600} + 0.008b^*_{600} - 0.252 \text{ ---- EQ. 5.5}$$

$$\text{Predicted } b^*_{600} \text{ value (Pb}^*_{600}\text{)} = -0.016a^*_{600} + 1.012b^*_{600} - 0.086 \text{ ---- EQ. 5.6}$$

For MATT samples measured using the specular component excluded mode, three different equations were formulated:

$$\text{Predicted } L^*_{600} \text{ value (PL}^*_{600}\text{)} = 1.009L^*_{600} - 0.009a^*_{600} - 0.006b^*_{600} - 0.219 \text{ ---- EQ. 5.7}$$

$$\text{Predicted } a^*_{600} \text{ value (Pa}^*_{600}\text{)} = -0.004L^*_{600} + 1.005a^*_{600} + 0.009b^*_{600} + 0.161 \text{ ---- EQ. 5.8}$$

$$\text{Predicted } b^*_{600} \text{ value (Pb}^*_{600}\text{)} = -0.024a^*_{600} + 1.011b^*_{600} - 0.175 \text{ ---- EQ. 5.9}$$

For MATT samples measured using the specular component included mode, another three different equations were formulated:

$$\text{Predicted } L^*_{600} \text{ value (PL}^*_{600}\text{)} = 1.007L^*_{600} - 0.008a^*_{600} - 0.005b^*_{600} - 0.257 \text{ ---- EQ. 5.10}$$

$$\text{Predicted } a^*_{600} \text{ value (Pa}^*_{600}\text{)} = -0.005L^*_{600} + 1.001a^*_{600} - 0.011b^*_{600} + 0.180 \text{ ---- EQ. 5.11}$$

$$\text{Predicted } b^*_{600} \text{ value (Pb}^*_{600}\text{)} = 0.002L^*_{600} - 0.023a^*_{600} + 1.018b^*_{600} - 0.203 \text{ ---- EQ. 5.12}$$

### 5.2.2 CE-2180 vs CE-7000

For GLOSSY samples measured using the specular component excluded mode, three different equations were formulated:

$$\text{Predicted } L^*_{2180} \text{ value (PL}^*_{2180}\text{)} = 1.010L^*_{2180} - 0.007a^*_{2180} - 0.01b^*_{2180} + 0.059 \text{ ---- EQ.5.13}$$

$$\text{Predicted } a^*_{2180} \text{ value (Pa}^*_{2180}\text{)} = 1.009a^*_{2180} + 0.057b^*_{2180} - 0.085 \text{ ---- EQ. 5.14}$$

$$\text{Predicted } b^*_{2180} \text{ value (Pb}^*_{2180}\text{)} = -0.068L^*_{2180} - 0.035a^*_{2180} + 1.007b^*_{2180} + 0.098 \text{ ---- EQ. 5.15}$$

Where

$PL^*_{2180}$ ,  $Pa^*_{2180}$  and  $Pb^*_{2180}$  are the predicted value which is calculated by substituting the original data measured by the CE-2180,  $L^*_{2180}$ ,  $a^*_{2180}$  and  $b^*_{2180}$  into the above equations.

For GLOSSY samples measured using the specular component included mode, a further three different equations were formulated:

$$\text{Predicted } L^*_{2180} \text{ value (} PL^*_{2180} \text{)} = 1.015L^*_{2180} - 0.058a^*_{2180} - 0.001b^*_{2180} - 0.096 \text{ ---- EQ. 5.16}$$

$$\text{Predicted } a^*_{2180} \text{ value (} Pa^*_{2180} \text{)} = -0.011L^*_{2180} + 1.045a^*_{2180} + 0.007b^*_{2180} - 0.053 \text{ ---- EQ. 5.17}$$

$$\text{Predicted } b^*_{2180} \text{ value (} Pb^*_{2180} \text{)} = -0.027a^*_{2180} + 1.048b^*_{2180} - 0.075 \text{ ---- EQ. 5.18}$$

For MATT samples measured using the specular component excluded mode, three different equations were formulated:

$$\text{Predicted } L^*_{2180} \text{ value (PL}^*_{2180}) = 1.014L^*_{2180} - 0.018a^*_{2180} - 0.001b^*_{2180} - 0.157 \text{ ---- EQ. 5.19}$$

$$\text{Predicted } a^*_{2180} \text{ value (Pa}^*_{2180}) = -0.007L^*_{2180} + 1.027a^*_{2180} + 0.008b^*_{2180} + 0.297 \text{ ---- EQ. 5.20}$$

$$\text{Predicted } b^*_{2180} \text{ value (Pb}^*_{2180}) = -0.009a^*_{2180} + 1.027b^*_{2180} - 0.398 \text{ ---- EQ. 5.21}$$

For MATT samples measured using the specular component included mode, another three different equations were formulated:

$$\text{Predicted } L^*_{2180} \text{ value (PL}^*_{2180}) = 1.024L^*_{2180} - 0.014a^*_{2180} - 0.009b^*_{2180} - 0.168 \text{ ---- EQ. 5.22}$$

$$\text{Predicted } a^*_{2180} \text{ value (Pa}^*_{2180}) = -0.005L^*_{2180} + 1.008a^*_{2180} - 0.001b^*_{2180} + 0.098 \text{ ---- EQ. 5.23}$$

$$\text{Predicted } b^*_{2180} \text{ value (Pb}^*_{2180}) = -0.036a^*_{2180} + 1.058b^*_{2180} - 0.169 \text{ ---- EQ. 5.24}$$

Based on equations 5.1 – 5.24, a series of predicted  $L^*_{600}$ ,  $a^*_{600}$  and  $b^*_{600}$  values (i.e.  $PL^*_{600}$ ,  $Pa^*_{600}$  and  $Pb^*_{600}$ ) and a series of predicted  $L^*_{2180}$ ,  $a^*_{2180}$  and  $b^*_{2180}$  values (i.e.  $PL^*_{2180}$ ,  $Pa^*_{2180}$  and  $Pb^*_{2180}$ ) was calculated. Those values were then compared with

the actual measured values of CE-7000A by calculating the CIE colour difference value  $\Delta E^*_{ab}$  (EQ. 5.25).

$$\Delta E^*_{ab} = ((L^*_{\text{sample}} - L^*_{\text{standard}})^2 + (a^*_{\text{sample}} - a^*_{\text{standard}})^2 + (b^*_{\text{sample}} - b^*_{\text{standard}})^2)^{1/2} \text{ ---- EQ. 5.25}$$

$$\text{i.e. } \Delta E^*_{ab} = ((PL^*_x - L^*_{\text{CE-7000A}})^2 + (Pa^*_x - a^*_{\text{CE-7000A}})^2 + (b^*_x - b^*_{\text{CE-7000A}})^2)^{1/2} \text{ ---- EQ. 5.26}$$

where x= 600 or 2180

### 5.3 The Improvement Of The Inter-Instrumental Agreement After Applying L-Model

After the mathematical models had been developed, the measurement data of the CCS-II tiles from SF-600 and CE-2180 were then substituted into the equations and the corrected  $\Delta E^*_{ab}$  were calculated. In addition, comparisons between the original  $\Delta E^*_{ab}$  and the corrected  $\Delta E^*_{ab}$  were also calculated and expressed as the percentage improvement of the inter-instrumental agreement. All the results are summarised in the tables below:



**Table 5.1: Summary Of The Inter-Instrumental Agreement For The CCS-II GLOSSY Tiles Using Specular Component Excluded Mode Between SF-600 And CE-7000A**

	<i>Original <math>\Delta E^*_{ab}</math></i>	<i>Corrected <math>\Delta E^*_{ab}</math></i>	<i>% Improvement</i>
<i>Pale Grey</i>	0.690	0.387	43.913
<i>Middle Grey</i>	0.459	0.26	43.355
<i>Diff. Grey</i>	0.495	0.286	42.222
<i>Deep Grey</i>	0.196	0.228	-16.327
<i>Deep Pink</i>	0.650	0.508	21.846
<i>Red</i>	0.650	0.892	-37.231
<i>Orange</i>	1.046	0.599	42.734
<i>Bright Yellow</i>	1.437	0.649	54.836
<i>Green</i>	1.120	0.312	72.143
<i>Diff. Green</i>	1.095	0.329	69.954
<i>Cyan</i>	1.232	0.552	55.195
<i>Deep Blue</i>	1.028	0.649	36.868
<i>Average*</i>	0.842	0.471	44.038

**Table 5.2: Summary Of The Inter-Instrumental Agreement For The CCS-II GLOSSY Tiles Using Specular Component Included Mode Between SF-600 And CE-7000A**

	<i>Original <math>\Delta E^*_{ab}</math></i>	<i>Corrected <math>\Delta E^*_{ab}</math></i>	<i>% Improvement</i>
<i>Pale Grey</i>	0.428	0.274	35.981
<i>Middle Grey</i>	0.269	0.158	41.264
<i>Diff. Grey</i>	0.293	0.288	1.706
<i>Deep Grey</i>	0.217	0.158	27.189
<i>Deep Pink</i>	0.737	0.356	51.696
<i>Red</i>	1.263	0.497	60.649
<i>Orange</i>	1.084	0.311	71.310
<i>Bright Yellow</i>	0.930	0.277	70.215
<i>Green</i>	0.775	0.203	73.806
<i>Diff. Green</i>	0.749	0.153	79.573
<i>Cyan</i>	1.004	0.630	37.251
<i>Deep Blue</i>	0.849	0.583	31.331
<i>Average*</i>	0.717	0.324	54.780

**Table 5.3: Summary Of The Inter-Instrumental Agreement For The CCS-II MATT Tiles Using Specular Component Excluded Mode Between SF-600 And CE-7000A**

	<i>Original <math>\Delta E^*_{ab}</math></i>	<i>Corrected <math>\Delta E^*_{ab}</math></i>	<i>% Improvement</i>
<i>Pale Grey</i>	0.590	0.227	61.525
<i>Middle Grey</i>	0.422	0.153	63.744
<i>Diff. Grey</i>	0.395	0.113	71.392
<i>Deep Grey</i>	0.183	0.100	45.355
<i>Deep Pink</i>	0.633	0.109	82.780
<i>Red</i>	0.713	0.695	2.525
<i>Orange</i>	0.874	0.248	71.625
<i>Bright Yellow</i>	0.749	0.088	88.251
<i>Green</i>	0.867	0.206	76.240
<i>Diff. Green</i>	0.788	0.106	86.548
<i>Cyan</i>	0.903	0.394	56.368
<i>Deep Blue</i>	0.890	0.610	31.461
<i>Average*</i>	0.667	0.254	61.921

**Table 5.4: Summary Of The Inter-Instrumental Agreement For The CCS-II MATT Tiles Using Specular Component Included Mode Between SF-600 And CE-7000A**

	<i>Original <math>\Delta E^*_{ab}</math></i>	<i>Corrected <math>\Delta E^*_{ab}</math></i>	<i>% Improvement</i>
<i>Pale Grey</i>	0.361	0.225	37.673
<i>Middle Grey</i>	0.182	0.154	15.385
<i>Diff. Grey</i>	0.166	0.109	34.337
<i>Deep Grey</i>	0.074	0.101	-36.486
<i>Deep Pink</i>	0.603	0.103	82.919
<i>Red</i>	0.890	0.701	21.236
<i>Orange</i>	0.968	0.286	70.455
<i>Bright Yellow</i>	0.768	0.066	91.406
<i>Green</i>	0.762	0.192	74.803
<i>Diff. Green</i>	0.652	0.111	82.975
<i>Cyan</i>	0.824	0.373	54.733
<i>Deep Blue</i>	0.677	0.553	18.316
<i>Average*</i>	0.577	0.248	57.067

**Table 5.5: Summary Of The Inter-Instrumental Agreement For The CCS-II GLOSSY Tiles Using Specular Component Excluded Mode Between CE-2180 And CE-7000A**

	<i>Original <math>\Delta E^*_{ab}</math></i>	<i>Corrected <math>\Delta E^*_{ab}</math></i>	<i>% Improvement</i>
<i>Pale Grey</i>	0.666	0.723	-8.559
<i>Middle Grey</i>	0.707	0.625	11.598
<i>Diff. Grey</i>	0.453	0.667	-47.241
<i>Deep Grey</i>	0.239	0.444	-85.774
<i>Deep Pink</i>	0.700	0.302	56.857
<i>Red</i>	0.719	0.457	36.439
<i>Orange</i>	0.119	0.416	-249.580
<i>Bright Yellow</i>	0.689	0.397	42.380
<i>Green</i>	0.130	0.394	-203.077
<i>Diff. Green</i>	0.790	0.265	66.456
<i>Cyan</i>	0.140	0.497	-255.000
<i>Deep Blue</i>	1.134	0.425	62.522
<i>Average*</i>	0.541	0.468	13.475

**Table 5.6: Summary Of The Inter-Instrumental Agreement For The CCS-II GLOSSY Tiles Using Specular Component Included Mode Between CE-2180 And CE-7000A**

	<i>Original <math>\Delta E^*_{ab}</math></i>	<i>Corrected <math>\Delta E^*_{ab}</math></i>	<i>% Improvement</i>
<i>Pale Grey</i>	0.795	0.057	92.830
<i>Middle Grey</i>	0.758	0.414	45.383
<i>Diff. Grey</i>	0.280	0.066	76.429
<i>Deep Grey</i>	0.100	0.091	9.000
<i>Deep Pink</i>	0.723	0.407	43.707
<i>Red</i>	0.634	0.631	0.473
<i>Orange</i>	0.114	0.387	-239.474
<i>Bright Yellow</i>	0.628	0.623	0.796
<i>Green</i>	0.143	0.320	-123.776
<i>Diff. Green</i>	1.023	0.349	65.885
<i>Cyan</i>	0.195	0.545	-179.487
<i>Deep Blue</i>	1.285	1.078	16.109
<i>Average*</i>	0.557	0.414	25.606

**Table 5.7: Summary Of The Inter-Instrumental Agreement For The CCS-II MATT Tiles Using Specular Component Excluded Mode Between CE-2180 And CE-7000A**

	<i>Original <math>\Delta E^*_{ab}</math></i>	<i>Corrected <math>\Delta E^*_{ab}</math></i>	<i>% Improvement</i>
<i>Pale Grey</i>	0.928	0.220	76.293
<i>Middle Grey</i>	0.535	0.282	47.290
<i>Diff. Grey</i>	0.760	0.503	33.816
<i>Deep Grey</i>	0.446	0.165	63.004
<i>Deep Pink</i>	0.713	0.421	40.954
<i>Red</i>	0.680	0.372	45.294
<i>Orange</i>	0.414	0.093	77.536
<i>Bright Yellow</i>	0.516	0.362	29.845
<i>Green</i>	0.444	0.055	87.613
<i>Diff. Green</i>	0.852	0.215	74.765
<i>Cyan</i>	0.454	0.155	65.859
<i>Deep Blue</i>	0.679	0.354	47.865
<i>Average*</i>	0.618	0.266	56.920

**Table 5.8: Summary Of The Inter-Instrumental Agreement For The CCS-II MATT Tiles Using Specular Component Included Mode Between CE-2180 And CE-7000A**

	<i>Original <math>\Delta E^*_{ab}</math></i>	<i>Corrected <math>\Delta E^*_{ab}</math></i>	<i>% Improvement</i>
<i>Pale Grey</i>	0.952	0.156	83.613
<i>Middle Grey</i>	0.576	0.225	60.938
<i>Diff. Grey</i>	0.361	0.324	10.249
<i>Deep Grey</i>	0.352	0.140	60.227
<i>Deep Pink</i>	0.718	0.256	64.345
<i>Red</i>	0.755	0.236	68.742
<i>Orange</i>	0.436	0.079	81.881
<i>Bright Yellow</i>	0.552	0.231	58.152
<i>Green</i>	0.500	0.077	84.600
<i>Diff. Green</i>	0.997	0.093	90.672
<i>Cyan</i>	0.428	0.127	70.327
<i>Deep Blue</i>	0.968	0.310	67.975
<i>Average*</i>	0.633	0.188	70.323

Note \* = (Average Original  $\Delta E^*_{ab}$  – Average Corrected  $\Delta E^*_{ab}$ ) / Average Original  $\Delta E^*_{ab}$  × 100

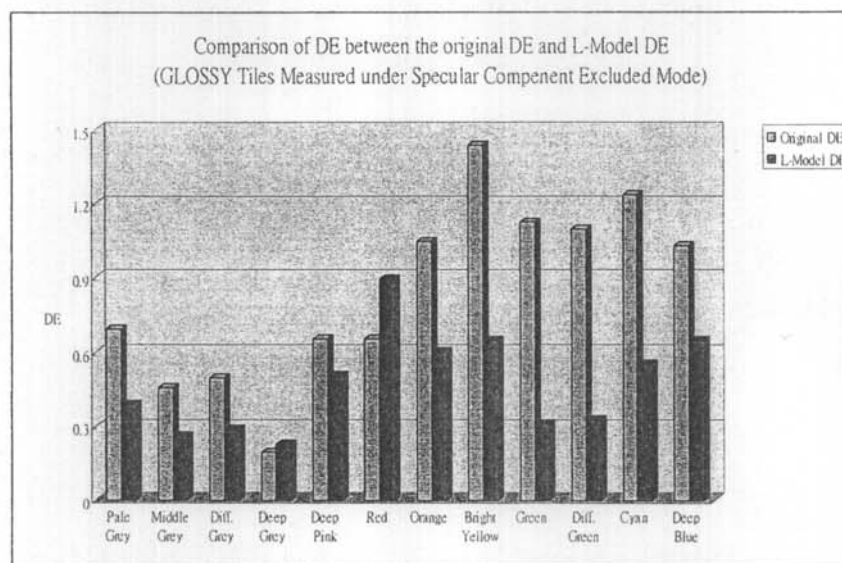
Tables 5.1 – 5.4, which show the summary of the inter-instrumental agreement for the CCS-II Tiles when comparing SF-600 and CE-7000A indicate that after application of the mathematical models to calculate the predicted  $L^*$ ,  $a^*$  and  $b^*$  values, the colour difference improved. The average percentage improvement of the colour difference ranged from 44.0 – 61.9%.

Tables 5.5 – 5.8, summarizing the inter-instrumental agreement for the CCS-II Tiles for CE-2180 and CE-7000A show that, after applying the mathematical models to calculate the predicted  $L^*$ ,  $a^*$  and  $b^*$  values, the colour difference also improved accordingly. The average percentage of the colour difference improved in the range from 13.5 – 70.3%.

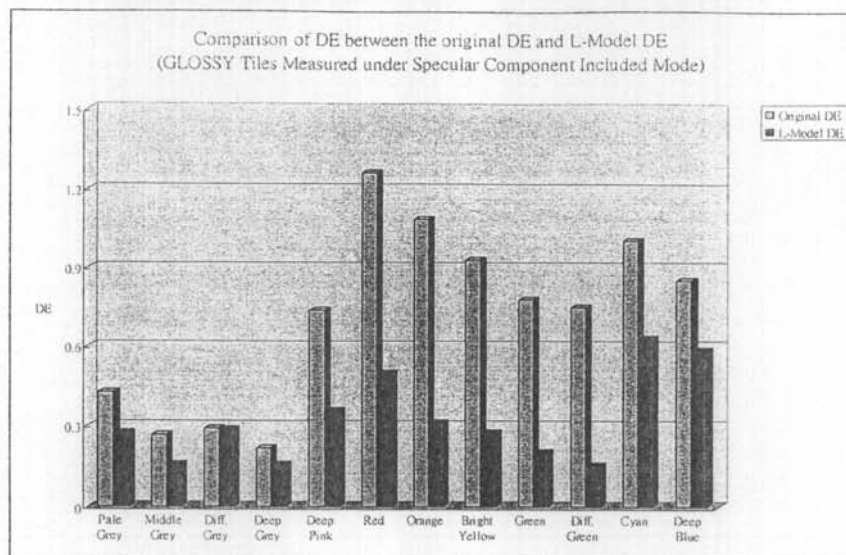
Regardless of whether “GLOSSY” tiles were measured using the specular component excluded mode or not, the percentage improvement for the inter-instrumental agreement between CE-2180 and CE-7000A was less than that for SF-600 and CE-7000A. This was due to the fact that measurements of the spectral reflectance of the “GLOSSY” tiles are depended more on the optical system of the spectrophotometer, especially when using a single-beam spectrophotometer, if the calibration procedure is

not good. For "MATT" Tiles, the inter-instrumental agreements between CE-2180 and CE-7000A and between SF-600 and CE-7000A were satisfactory because the measurements were easier to obtain compared to the "GLOSSY" tiles.

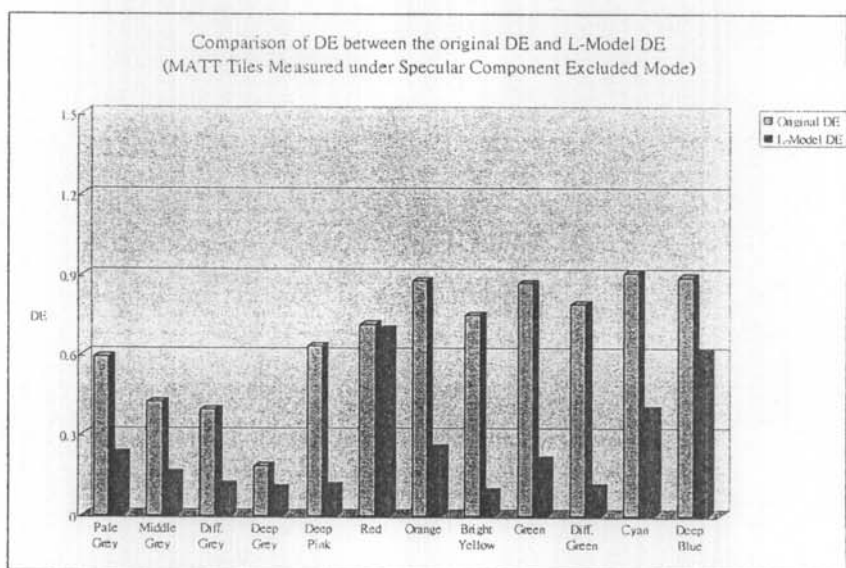
The poor measurement results for the GLOSSY tiles were due to the high reflection inside the integrated sphere. Besides the size of the integrated sphere, the position of the specular component port and the signal receiver are factors which may have affected the measurement results.



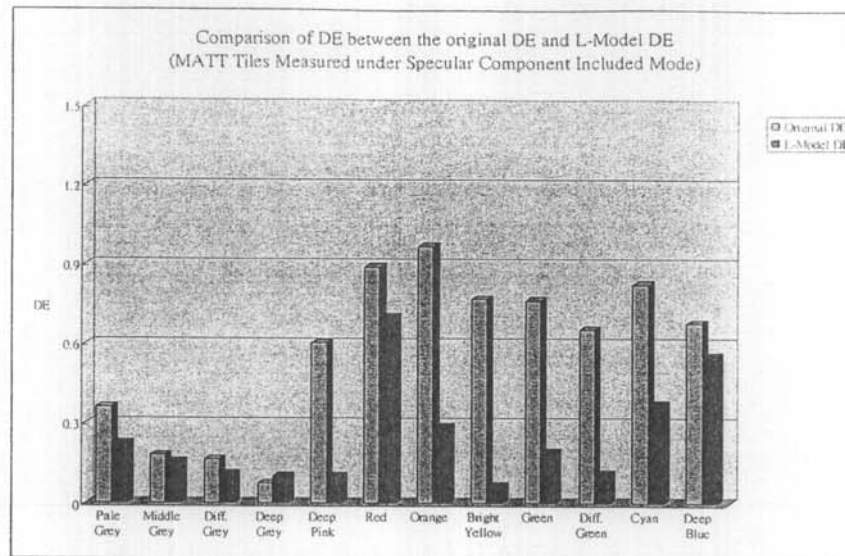
**Figure 5.1** The Comparison Of The DE Between The Original DE and L-Model For SF-600 And CE-7000A (GLOSSY Tiles Measured Using Specular Component Excluded Mode)



**Figure 5.2 The Comparison Of The DE Between The Original DE and L-Model For SF-600 And CE-7000A (GLOSSY Tiles Measured Using Specular Component Included Mode)**



**Figure 5.3 The Comparison Of The DE Between The Original DE and L-Model For SF-600 And CE-7000A (MATT Tiles Measured Using Specular Component Excluded Mode)**



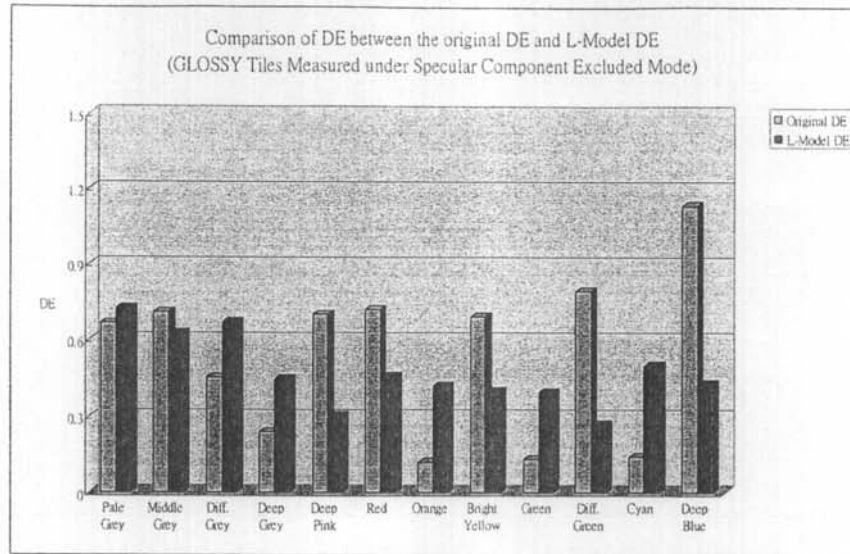
**Figure 5.4 The Comparison Of The DE Between The Original DE and L-Model For SF-600 And CE-7000A (MATT Tiles Measured Using Specular Component Included Mode)**

Figure 5.1 shows the comparison between the colour difference and L-Model for SF-600 and CE-7000A (GLOSSY tiles measured in specular component excluded mode), and it was found that the colour difference of red after modeling was higher than that of the original measurement. Red is considered to be one of the most sensitive colours compare with the others, thus the modeling result was unsatisfactory and also worse than the original result. Sensitive colour means that the colour is easily affected by the change of temperature and humidity even the change of the above factors are not significant<sup>[56,68]</sup>.

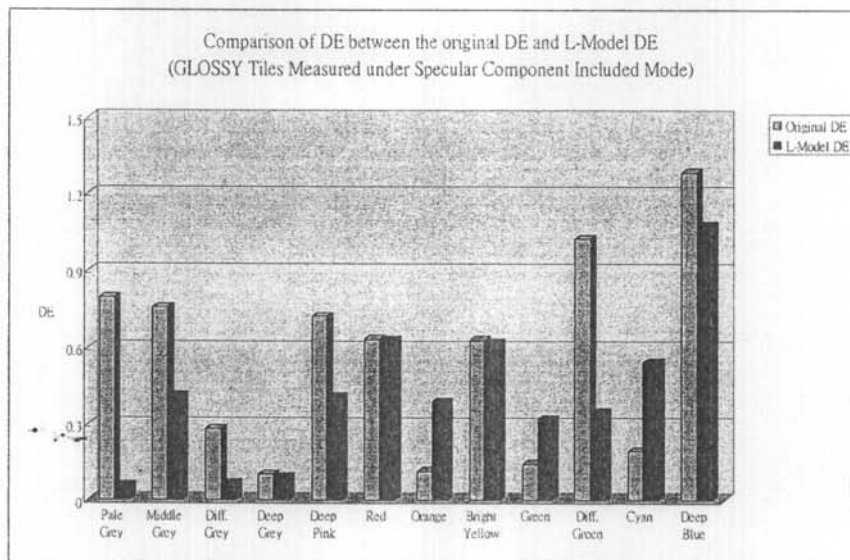


Figure 5.2 shows the comparison of the colour difference between the original colour difference and L-Model for SF-600 and CE-7000A (GLOSSY tiles measured using specular component included mode), and in Figure 5.3, which shows the comparison of the colour difference between the original colour difference and L-Model for SF-600 and CE-7000A (MATT tiles measured under specular component excluded mode), it may be seen that the entire colour difference improves after modeling. This implies that L-Model functioned well in these two combinations.

For Figure 5.4, the comparison of the colour difference between the original colour difference and L-Model for SF-600 and CE-7000A (MATT tiles measured under specular component included mode), it was found that the colour difference of deep grey after modeling was higher than that of the original measurement. This is because the signal measured by the spectrophotometer was low, thus the modeling result was unsatisfactory and also worse than the original result.



*Figure 5.5 The Comparison Of The DE Between The Original DE and L-Model For CE-2180And CE-7000A (GLOSSY Tiles Measured Using Specular Component Excluded Mode)*



*Figure 5.6 The Comparison Of The DE Between The Original DE and L-Model For CE-2180And CE-7000A (GLOSSY Tiles Measured Using Specular Component Included Mode)*

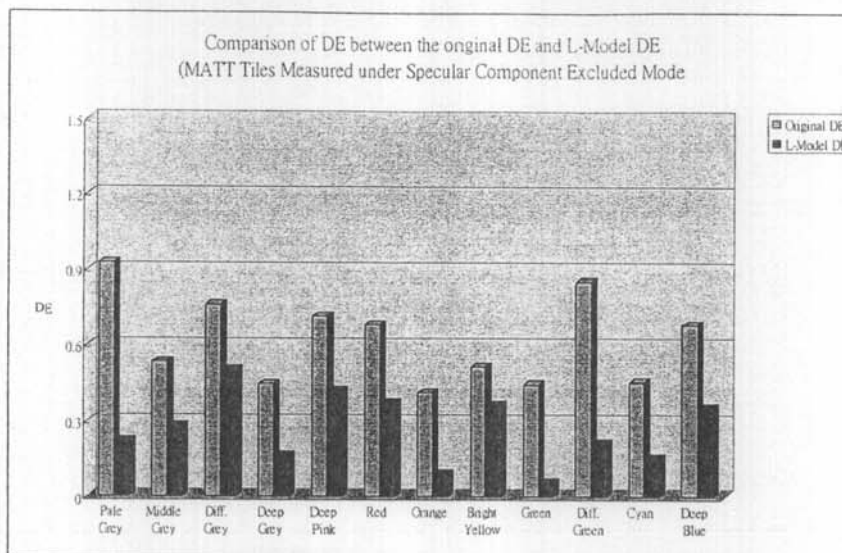


*Figure 5.7 The Comparison Of The DE Between The Original DE and L-Model For CE-2180And CE-7000A (MATT Tiles Measured Using Specular Component Excluded Mode)*

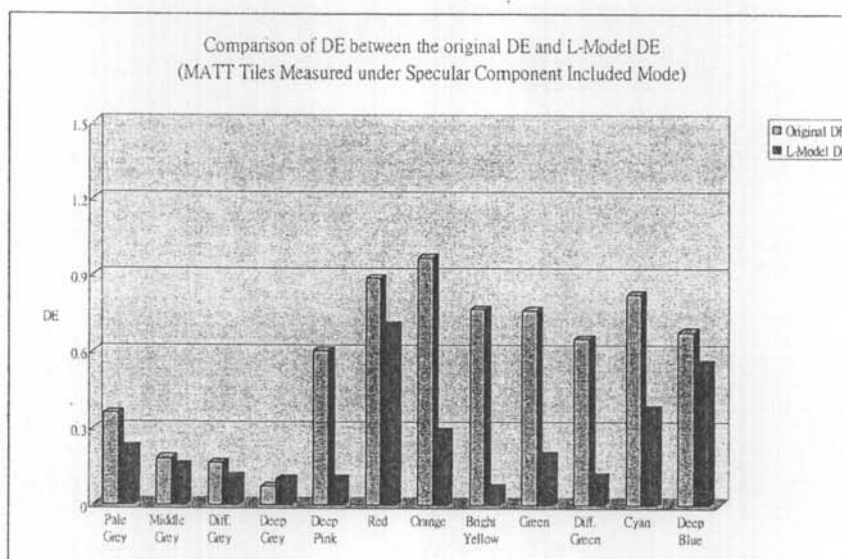


*Figure 5.8 The Comparison Of The DE Between The Original DE and L-Model For CE-2180And CE-7000A (MATT Tiles Measured Using Specular Component Included Mode)*

Figure 5.5, showing the comparison of the colour difference between the original colour difference and L-Model for CE-2180 and CE-7000A (GLOSSY tiles measured under specular component excluded mode), demonstrates that the colour difference of pale grey, different grey, deep grey, orange, green and cyan after modeling was higher than that of the original measurement. This indicated that the L-Model was not suitable for the GLOSSY tiles measured under specular component excluded conditions and further improvement is required in order to enhance the inter-instrumental agreement.

In Figure 5.6, which shows the comparison of the colour difference between the original colour difference and L-Model for CE-2180 and CE-7000A (GLOSSY tiles measured under specular component excluded mode), it may be seen that the colour difference of orange, green and cyan after modeling was higher than that of the original measurement. This shows that the L-Model was also unsuitable for the GLOSSY tiles measured under specular component included conditions especially for the sensitive colours and further improvement was required in order to enhance the inter-instrumental agreement.

For Figure 5.7, the comparison of the colour difference between the original colour difference and L-Model for CE-2180 and CE-7000A (MATT tiles measured under specular component excluded mode), all the colour differences improved after modeling. This implies that L-Model functioned well in this combination.

Figure 5.8, which show the comparison of the colour difference between the original colour difference and L-Model for SF-600 and CE-7000A (MATT tiles measured under specular component included mode), indicates that the colour difference of deep grey after modeling was higher than that of the original measurement. Since the signal for the deep colour measured by the spectrophotometer was low, the modeling result was unsatisfactory and also worse than the original result.

## **CHAPTER 6**

### **DEVELOPMENT OF THE SECOND MATHEMATICAL MODEL (R-Model)**

#### **6.1 Introduction**

#### **6.2 Development Of The Second Mathematical Model (R-Model)**

#### **6.3 The Improvement Of The Inter-Instrumental Agreement After Applying R-Model**

#### **6.1 Introduction**

The application of L-Model was found to be limited, since it was not a robust mathematical model for inter-instrumental agreement. For this reason, a powerful and robust model was developed in order to further enhance the inter-instrumental agreement between spectrophotometers.

## **6.2 Development Of The Second Mathematical Model (R-Model)**

As indicated in the inter-instrumental agreement table, the colour differences among the spectrophotometers are very high (up to 1.554 CIELAB units), implying that further correction is necessary to further enhance the inter-instrumental agreement among the spectrophotometers. Although the “L-Model” was well developed, it was not a robust mathematical model and the overall improvement of inter-instrumental agreement was insignificant. The “L-Model” was therefore ineffective in the correction of the inter-instrumental agreement.

The “R-Model”, another mathematical model, was developed to improve the inter-instrumental agreement. It was based on the correction of the reflectance value across the visual spectrum. According to the preliminary findings, the tendency of the relative reflectance difference for twelve ceramic tiles was similar. Therefore bandpass correction was deemed one of the methods for the correction of the inter-instrumental agreement<sup>[6,33, 34, 35]</sup>. The equations used in the R-Model are summarised as follows:

At 400nm

$$\text{Corrected } R_{(400)} = n \times R_{(400)} + o \times R_{(410)} + q \text{ ---- EQ.6.1}$$

At 410nm – 690nm where  $\lambda = 410, 420, \dots, 690, 700$

$$\text{Corrected } R_{(\lambda)} = m \times R_{(\lambda-10)} + n \times R_{(\lambda)} + o \times R_{(\lambda+10)} + q \text{ ---- EQ.6.2}$$

At 700nm

$$\text{Corrected } R_{(700)} = m \times R_{(690)} + n \times R_{(700)} + q \text{ ---- EQ.6.3}$$

Where m, n, o and q are wavelength dependent constant.

For the coefficients m, n, o and p, please refer to Appendix I for details.



### 6.3 The Improvement Of The Inter-Instrumental Agreement After Applying R-Model

The spectral reflectance factors of SF-600 and CE-2180 were substituted into the above equations (EQ. 6.1 to EQ. 6.3) to calculate the predicted spectral reflectance factors. The colour difference between predicted and measured reflectance values was then calculated. The inter-instrumental agreement of the CCS-II tiles is summarized in Tables 6.1 – 6.8.

**Table 6.1: Summary Of The Inter-Instrumental Agreement For The CCS-II GLOSSY Tiles Using Specular Component Excluded Mode Between SF-600 And CE-7000A After Applying The R-Model**

	<i>Original <math>\Delta E^*_{ab}</math></i>	<i>Corrected <math>\Delta E^*_{ab}</math></i>	<i>% Improvement</i>
<i>Pale Grey</i>	0.690	0.110	84.058
<i>Middle Grey</i>	0.459	0.095	79.303
<i>Diff. Grey</i>	0.495	0.175	64.646
<i>Deep Grey</i>	0.196	0.232	-18.367
<i>Deep Pink</i>	0.650	0.243	62.615
<i>Red</i>	0.650	0.773	-18.923
<i>Orange</i>	1.046	0.418	60.038
<i>Bright Yellow</i>	1.437	0.269	81.280
<i>Green</i>	1.120	0.089	92.054
<i>Diff. Green</i>	1.095	0.101	90.776
<i>Cyan</i>	1.232	0.601	51.218
<i>Deep Blue</i>	1.028	0.598	41.829
<i>Average*</i>	0.842	0.309	63.341

**Table 6.2: Summary Of The Inter-Instrumental Agreement For The CCS-II GLOSSY Tiles Using Specular Component Included Mode Between SF-600 And CE-7000A After Applying The R-Model**

	<i>Original <math>\Delta E^*_{ab}</math></i>	<i>Corrected <math>\Delta E^*_{ab}</math></i>	<i>% Improvement</i>
<i>Pale Grey</i>	0.428	0.108	74.766
<i>Middle Grey</i>	0.269	0.051	81.041
<i>Diff. Grey</i>	0.293	0.057	80.546
<i>Deep Grey</i>	0.217	0.113	47.926
<i>Deep Pink</i>	0.737	0.115	84.396
<i>Red</i>	1.263	0.216	82.898
<i>Orange</i>	1.084	0.036	96.679
<i>Bright Yellow</i>	0.930	0.347	62.688
<i>Green</i>	0.775	0.232	70.065
<i>Diff. Green</i>	0.749	0.232	69.025
<i>Cyan</i>	1.004	0.187	81.375
<i>Deep Blue</i>	0.849	0.127	85.041
<i>Average*</i>	0.717	0.152	78.821

**Table 6.3: Summary Of The Inter-Instrumental Agreement For The CCS-II MATT Tiles Using Specular Component Excluded Mode Between SF-600 And CE-7000A After Applying The R-Model**

	<i>Original <math>\Delta E^*_{ab}</math></i>	<i>Corrected <math>\Delta E^*_{ab}</math></i>	<i>% Improvement</i>
<i>Pale Grey</i>	0.590	0.096	77.570
<i>Middle Grey</i>	0.422	0.067	75.093
<i>Diff. Grey</i>	0.395	0.068	76.792
<i>Deep Grey</i>	0.183	0.071	67.281
<i>Deep Pink</i>	0.633	0.058	92.130
<i>Red</i>	0.713	0.084	93.349
<i>Orange</i>	0.874	0.033	96.956
<i>Bright Yellow</i>	0.749	0.055	94.086
<i>Green</i>	0.867	0.032	95.871
<i>Diff. Green</i>	0.788	0.062	91.722
<i>Cyan</i>	0.903	0.148	85.259
<i>Deep Blue</i>	0.890	0.055	93.522
<i>Average*</i>	0.667	0.069	90.358

**Table 6.4: Summary Of The Inter-Instrumental Agreement For The CCS-II MATT Tiles Using Specular Component Included Mode Between SF-600 And CE-7000A After Applying The R-Model**

	<i>Original <math>\Delta E^*_{ab}</math></i>	<i>Corrected <math>\Delta E^*_{ab}</math></i>	<i>% Improvement</i>
<i>Pale Grey</i>	0.361	0.066	81.717
<i>Middle Grey</i>	0.182	0.046	74.725
<i>Diff. Grey</i>	0.166	0.05	69.880
<i>Deep Grey</i>	0.074	0.061	17.568
<i>Deep Pink</i>	0.603	0.280	53.566
<i>Red</i>	0.890	0.636	28.539
<i>Orange</i>	0.968	0.069	92.872
<i>Bright Yellow</i>	0.768	0.267	65.234
<i>Green</i>	0.762	0.139	81.759
<i>Diff. Green</i>	0.652	0.031	95.245
<i>Cyan</i>	0.824	0.169	79.490
<i>Deep Blue</i>	0.677	0.208	69.276
<i>Average*</i>	0.577	0.169	70.810

**Table 6.5: Summary Of The Inter-Instrumental Agreement For The CCS-II GLOSSY Tiles Using Specular Component Excluded Mode Between CE-2180 And CE-7000A After Applying The R-Model**

	<i>Original <math>\Delta E^*_{ab}</math></i>	<i>Corrected <math>\Delta E^*_{ab}</math></i>	<i>% Improvement</i>
<i>Pale Grey</i>	0.140	0.220	-57.143
<i>Middle Grey</i>	0.130	0.111	14.615
<i>Diff. Grey</i>	0.119	0.112	5.882
<i>Deep Grey</i>	0.239	0.152	36.402
<i>Deep Pink</i>	0.700	0.459	34.429
<i>Red</i>	1.134	0.362	68.078
<i>Orange</i>	0.790	0.290	63.291
<i>Bright Yellow</i>	0.666	0.267	59.910
<i>Green</i>	0.689	0.474	31.205
<i>Diff. Green</i>	0.719	0.481	33.102
<i>Cyan</i>	0.707	0.325	54.031
<i>Deep Blue</i>	0.453	0.965	-113.024
<i>Average*</i>	0.541	0.352	34.968

**Table 6.6: Summary Of The Inter-Instrumental Agreement For The CCS-II GLOSSY Tiles Using Specular Component Included Mode Between CE-2180 And CE-7000A After Applying The R-Model**

	<i>Original <math>\Delta E^*_{ab}</math></i>	<i>Corrected <math>\Delta E^*_{ab}</math></i>	<i>% Improvement</i>
<i>Pale Grey</i>	0.195	0.478	-145.128
<i>Middle Grey</i>	0.143	0.281	-96.503
<i>Diff. Grey</i>	0.114	0.332	-191.228
<i>Deep Grey</i>	0.100	0.091	9.000
<i>Deep Pink</i>	0.723	0.369	48.963
<i>Red</i>	1.285	0.729	43.268
<i>Orange</i>	1.023	0.205	79.961
<i>Bright Yellow</i>	0.795	0.377	52.579
<i>Green</i>	0.628	0.461	26.592
<i>Diff. Green</i>	0.634	0.454	28.391
<i>Cyan</i>	0.758	0.383	49.472
<i>Deep Blue</i>	0.280	0.154	45.000
<i>Average*</i>	0.557	0.360	35.400

**Table 6.7: Summary Of The Inter-Instrumental Agreement For The CCS-II MATT Tiles Using Specular Component Excluded Mode Between CE-2180 And CE-7000A After Applying The R-Model**

	<i>Original <math>\Delta E^*_{ab}</math></i>	<i>Corrected <math>\Delta E^*_{ab}</math></i>	<i>% Improvement</i>
<i>Pale Grey</i>	0.454	0.129	71.586
<i>Middle Grey</i>	0.444	0.102	77.027
<i>Diff. Grey</i>	0.414	0.098	76.329
<i>Deep Grey</i>	0.446	0.116	73.991
<i>Deep Pink</i>	0.713	0.124	82.609
<i>Red</i>	0.679	0.042	93.814
<i>Orange</i>	0.852	0.081	90.493
<i>Bright Yellow</i>	0.928	0.039	95.797
<i>Green</i>	0.516	0.120	76.744
<i>Diff. Green</i>	0.680	0.210	69.118
<i>Cyan</i>	0.535	0.146	72.710
<i>Deep Blue</i>	0.760	0.139	81.711
<i>Average*</i>	0.618	0.112	81.862

**Table 6.8: Summary Of The Inter-Instrumental Agreement For The CCS-II MATT Tiles Using Specular Component Included Mode Between CE-2180 And CE-7000A After Applying The R-Model**

	<i>Original <math>\Delta E^*_{ab}</math></i>	<i>Corrected <math>\Delta E^*_{ab}</math></i>	<i>% Improvement</i>
<i>Pale Grey</i>	0.428	0.123	71.262
<i>Middle Grey</i>	0.500	0.099	80.200
<i>Diff. Grey</i>	0.436	0.091	79.128
<i>Deep Grey</i>	0.352	0.095	73.011
<i>Deep Pink</i>	0.718	0.095	86.769
<i>Red</i>	0.968	0.094	90.289
<i>Orange</i>	0.997	0.053	94.684
<i>Bright Yellow</i>	0.952	0.072	92.437
<i>Green</i>	0.552	0.170	69.203
<i>Diff. Green</i>	0.755	0.219	70.993
<i>Cyan</i>	0.576	0.182	68.403
<i>Deep Blue</i>	0.361	0.091	74.792
<i>Average*</i>	0.633	0.115	81.777

Note \* = (Average Original  $\Delta E^*_{ab}$  – Average Corrected  $\Delta E^*_{ab}$ ) / Average Original  $\Delta E^*_{ab}$  × 100

Tables 6.1 to 6.4 show the significant improvements in the inter-instrumental agreement between spectrophotometers, especially in the case of the MATT tiles measured using the specular component excluded mode. The average percentage improvement of the colour difference was up to 90 percent. For the other sets of data and results, the colour differences between spectrophotometers ranged from 63 to 78 percent. The results imply that the R-Model showed a good improvement of the inter-instrumental agreement between SF-600 and CE-7000A when compared with the L-Model. From tables 6.5 – 6.8, it may be seen that the percentage improvement of the inter-instrumental agreement for the “GLOSSY” tiles measured under both the specular component excluded mode and the specular component included mode was disappointing when compared with the

“MATT” tiles. This is because CE-2180 is a single-beam spectrophotometer and lacks the reference beam to overcome the glossy effect during the measurement process.

The comparison of the colour difference ( $\Delta E^*_{ab}$ ) between the two different newly developed models for SF600 vs CE-7000A is summarised in the figures below:

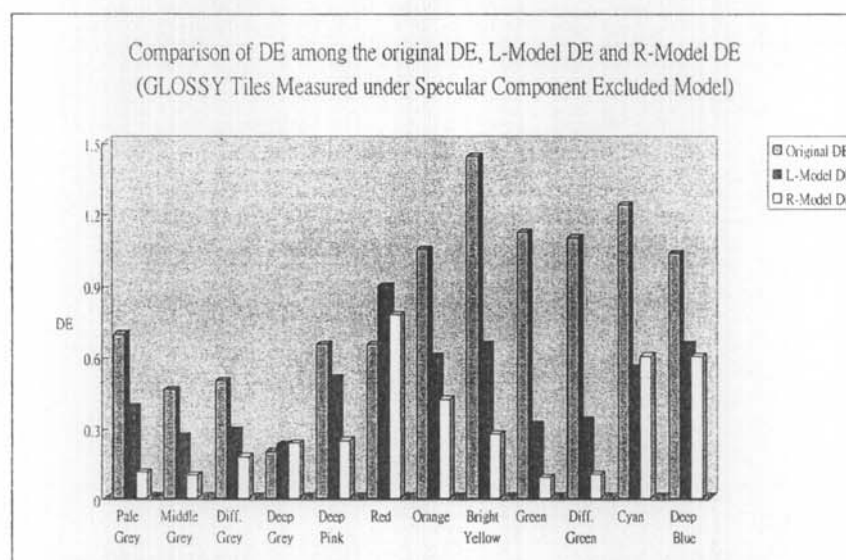


**Figure 6.1 The Comparison Of The DE Between The Two Different Developed Models (GE) For SF-600 And CE-7000A**

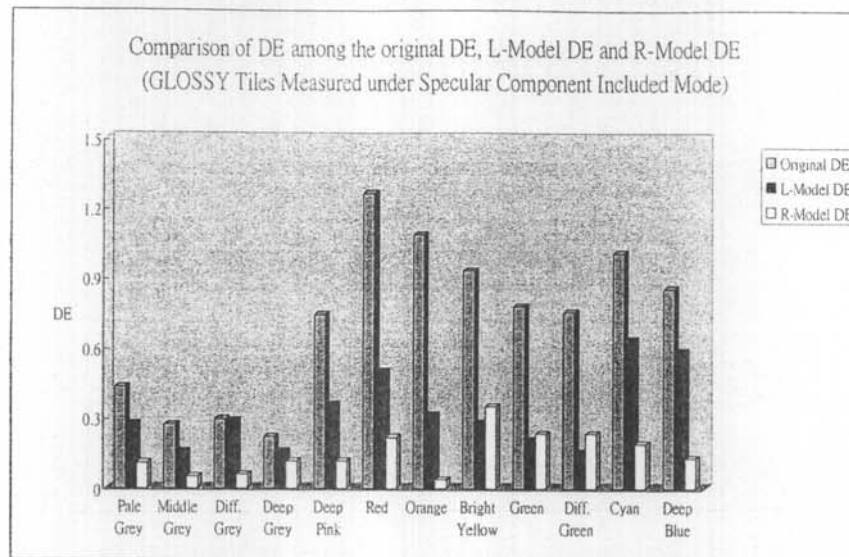


Figure 6.2 The Comparison Of The DE Between The Two Different Developed Models (GI) For SF-600 And CE-7000A

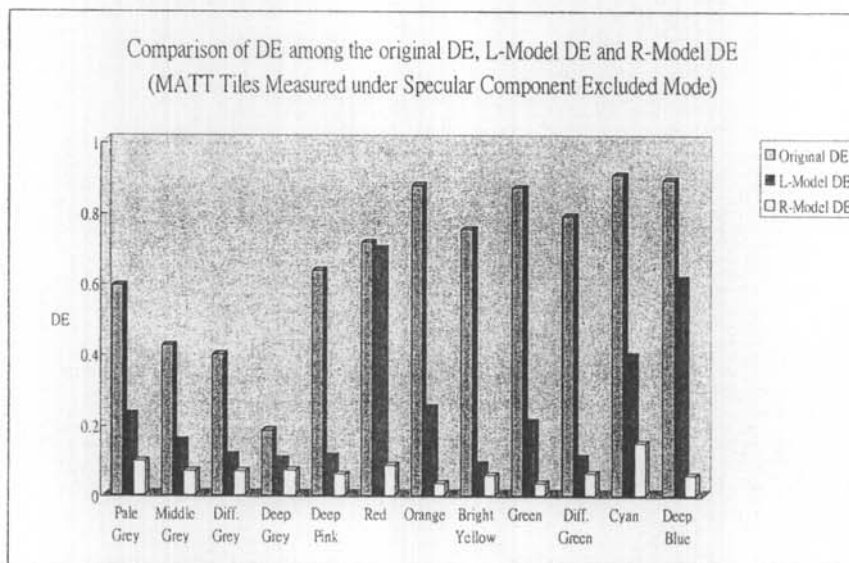
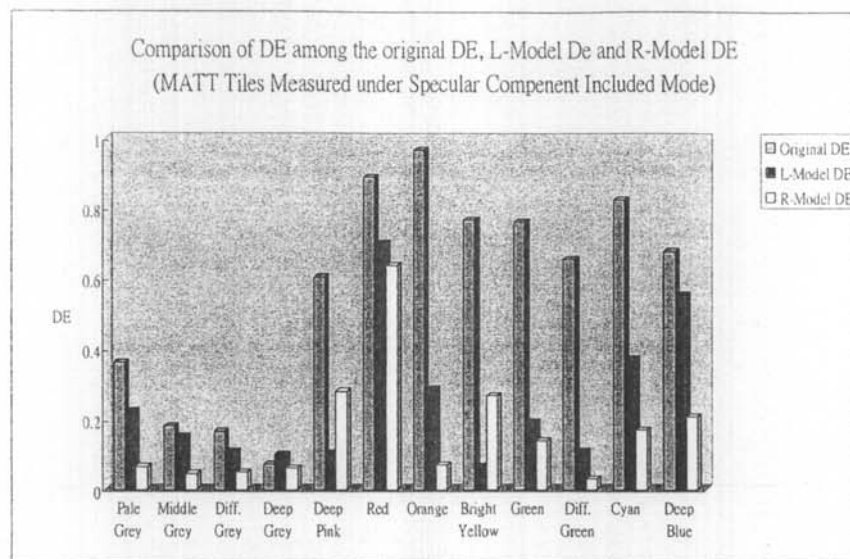


Figure 6.3 The Comparison Of The DE Between The Two Different Developed Models (ME) For SF-600 And CE-7000A



**Figure 6.4 The Comparison of the DE Between The Two Different Developed Models (MI) For SF-600 And CE-7000A**

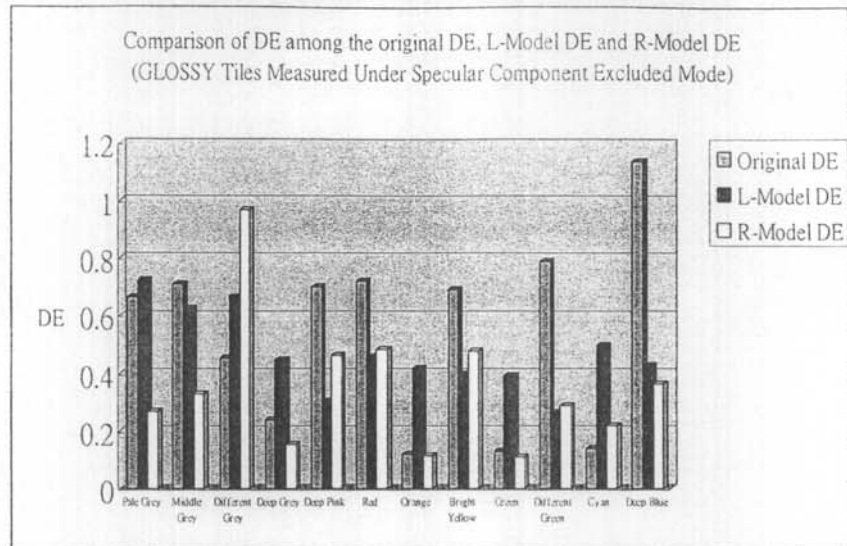
Figure 6.1, which shows results for the GLOSSY tiles measured using the specular component mode, indicates that the overall performance of “R-Model” was better than that of the “L-Model”. The average improvement of “R-Model” for the twelve tiles was 63%, while the average improvement of “L-Model” for the twelve tiles was 44%. In this figure, irrespective of whether the L-Model or R-Model is used, the inter-instrumental agreement for deep grey and red may be seen to be unsatisfactory. Red, as previously discussed, is a sensitive colour and easily affected by changes in temperature. Deep grey is also difficult to measure because the signal for the measurement is insignificant and the result for inter-instrumental agreement is poor.



Figure 6.2, which shows results for the GLOSSY tiles measured using specular component included mode, indicates that the overall performance of R-Model" is also better than that of the "L-Model" and all the colours showed improvement after applying the R-Model and L-Model. The average improvement of "R-Model" for the twelve tiles was 79%, while the average improvement of "L-Model" for the twelve tiles was 55%.

In Figure 6.3, which shows the results for the MATT tiles measured using the specular component excluded mode, it may be seen that the overall performance for the "R-Model" was better than that of the "L-Model" and all the colours showed improvement after applying both the R-Model and L-Model. The average improvement for the "R-Model" for the twelve tiles was 90%, whereas the average improvement for the "L-Model" for the twelve tiles was 62%.

In Figure 6.4, which shows the results for the MATT tiles measured using the specular component included mode, it may be seen that the overall performance for the R-Model" was also better than that of the "L-Model". The average improvement of "R-Model" for the twelve tiles was 71%, whereas the average improvement of "L-Model" for the twelve tiles was 57%.



**Figure 6.5 The Comparison Of The DE Between The Two Different Developed Models (GE) For CE-2180 And CE-7000A**

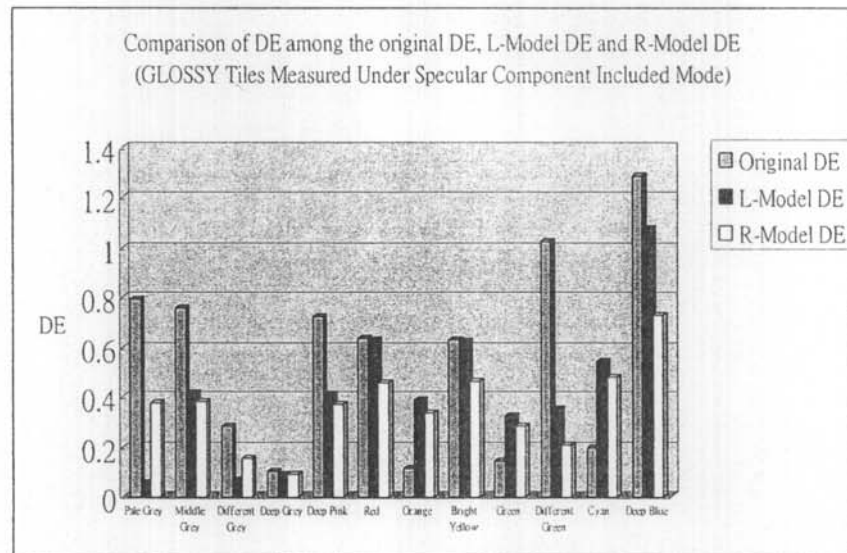


**Figure 6.6 The Comparison Of The DE Between The Two Different Developed Models (GI) For CE-2180 And CE-7000A**

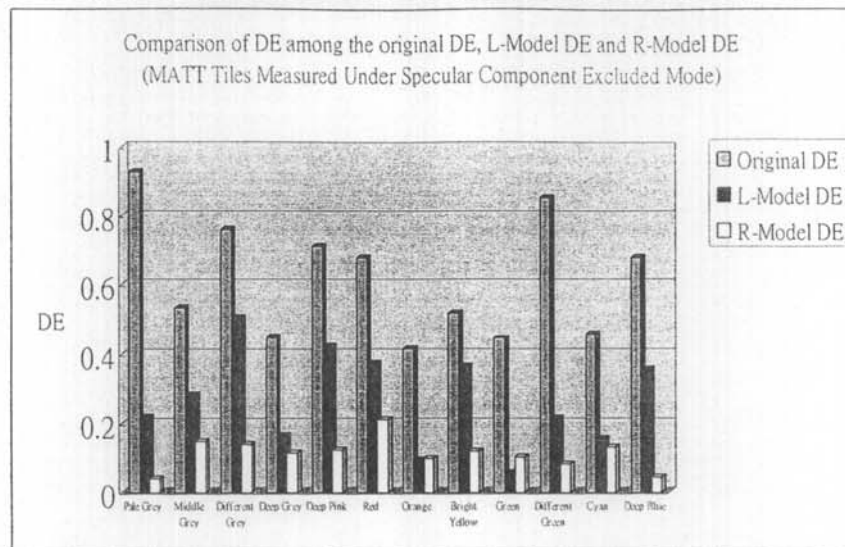


**Figure 6.7 The Comparison Of The DE Between The Two Different Developed Models (ME) For CE-2180 And CE-7000A**

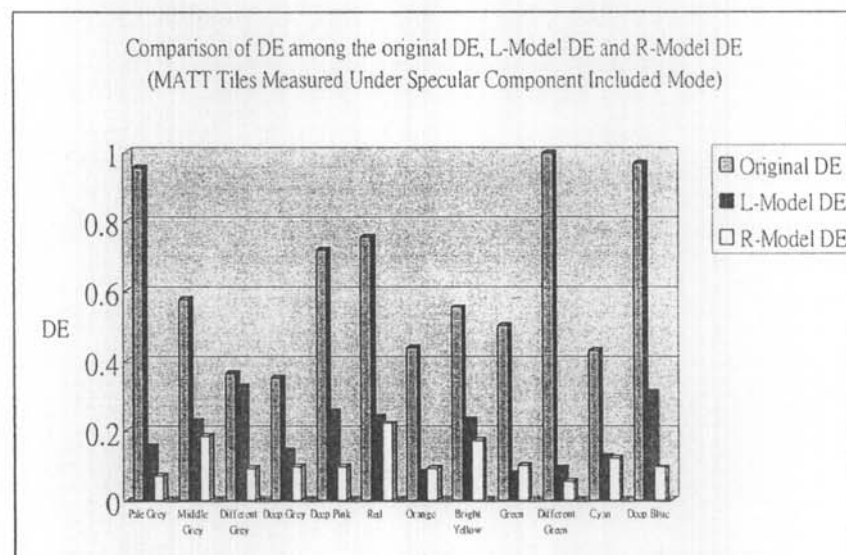


**Figure 6.8 The Comparison Of The DE Between The Two Different Developed Models (MI) For CE-2180 And CE-7000A**

In Figure 6.5, which shows the results for the GLOSSY tiles measured using the specular component excluded mode, it may be seen that the overall performance of “R-Model” was better than that of the “L-Model”. The average improvement of “R-Model” for the twelve tiles was 35%, while the average improvement of the “L-Model” for the twelve tiles was 13%. The inter-instrumental agreement for different grey and cyan was worse than the original results after applying the R-Model because the optical design for CE-2180 and CE-7000A is different.

Figure 6.6 shows the results for the GLOSSY tiles measured using the specular component included mode, and it may be seen that the overall performance for the R-Model” was also better than that of the “L-Model”. The average improvement of the “R-Model” for the twelve tiles was 36%, whereas the average improvement of the “L-Model” for the twelve tiles was 26%. After modeling it was found that the colour difference in the case of orange, green and cyan was higher than that of the original measurement, indicating that the R-Model was not suitable for application in the case of gloss-finish colours.

Figure 6.7, which shows the results for the MATT tiles measured under specular component excluded mode, indicates that the overall performance for “R-Model” was better than that of the “L-Model”. The average improvement of “R-Model” for the twelve tiles was 82%, while the average improvement of “L-Model” for the twelve tiles was 57%. All the tiles showed improvement in the inter-instrumental agreement regardless of whether they were applied to the L-Model or R-Model.

In Figure 6.8, showing the results for the MATT tiles measured under specular component included mode, it may be seen that the overall performance of the R-Model” was better than that of the “L-Model”. The average improvement of “R-Model” for the twelve tiles was 82%, while the average improvement of “L-Model” for the twelve tiles was 70%. All the tiles also showed improvement in the inter-instrumental agreement regardless of whether results were applied to the L-Model or R-Model.

Results shown in Figures 6.1 – 6.8 indicate that the “R-Model” resulted in greater improvement in the inter-instrumental agreement. Basically, the “R-Model” was developed in line with the concept of the bandpass correction and using multi linear

regression. However, the “L-Model” involved the use of linear regression only and its main purpose was to correct the colorimetric data ( $L^*$ ,  $a^*$  and  $b^*$ ).

From the above, it may be seen that the “R-Model” was a powerful, flexible and robust model when compared with the “L-Model” in the improvement of the inter-instrumental agreement. The fundamental data for this model were from the spectral reflectance factors and, once the spectral reflectance factors were corrected, the relative spectral reflectance difference errors were eliminated.

Figures 6.1 to 6.8 show that the performance of the “R-Model” was better than that of the “L-Model”. Of all the data sets, the MATT tiles measured under the specular component excluded mode showed the best improvement in inter-instrumental agreement. In addition, the MATT tiles measured under the specular component included mode also showed satisfactory improvement in inter-instrumental agreement.

The results obtained for the GLOSSY tiles, either in specular component excluded mode or in specular component included mode, were not as good as those for the MATT tiles.

In addition to the above results, the spectral reflectance factor for SF-600 and CE-2180 was calculated after applying the R-Model. The comparison of the colour difference between SF-600 and CE-2180 before and after applying the model is another important indication to test whether the newly developed mathematical models were successful or not. The comparison results are listed below:

**Table 6.9: Summary Of The Inter-Instrumental Agreement For The CCS-II GLOSSY Tiles Ussing Specular Component Excluded Mode Between CE-2180 And SF-600 Before And After Applying The R-Model**

	<i>Before Modelling <math>\Delta E^*_{ab}</math></i>	<i>After Modelling <math>\Delta E^*_{ab}</math></i>	<i>% Improvement</i>
<i>Pale Grey</i>	0.771	0.024	96.887
<i>Middle Grey</i>	0.561	0.117	79.144
<i>Diff. Grey</i>	0.500	0.125	75.000
<i>Deep Grey</i>	0.367	0.159	56.676
<i>Deep Pink</i>	0.445	0.325	26.966
<i>Red</i>	1.152	0.628	45.486
<i>Orange</i>	1.058	0.880	16.824
<i>Bright Yellow</i>	1.554	0.432	72.201
<i>Green</i>	1.134	0.380	66.490
<i>Diff. Green</i>	1.156	0.390	66.263
<i>Cyan</i>	0.887	0.234	73.619
<i>Deep Blue</i>	0.598	0.562	6.020
<i>Average*</i>	0.849	0.355	58.205

**Table 6.10: Summary Of The Inter-Instrumental Agreement For The CCS-II GLOSSY Tiles Using Specular Component Included Mode Between CE-2180 And SF-600 Before And After Applying The R-Model**

	<i>Before Modelling <math>\Delta E^*_{ab}</math></i>	<i>After Modelling <math>\Delta E^*_{ab}</math></i>	<i>% Improvement</i>
<i>Pale Grey</i>	0.582	0.260	55.326
<i>Middle Grey</i>	0.414	0.352	14.976
<i>Diff. Grey</i>	0.368	0.128	65.217
<i>Deep Grey</i>	0.261	0.079	69.732
<i>Deep Pink</i>	0.915	0.476	47.978
<i>Red</i>	0.504	0.168	66.667
<i>Orange</i>	0.904	0.142	84.292
<i>Bright Yellow</i>	1.168	0.121	89.640
<i>Green</i>	0.883	0.448	49.264
<i>Diff. Green</i>	0.846	0.464	45.154
<i>Cyan</i>	1.627	0.721	55.685
<i>Deep Blue</i>	1.718	0.814	52.619
<i>Average*</i>	0.849	0.348	58.046

**Table 6.11: Summary Of The Inter-Instrumental Agreement For The CCS-II MATT Tiles Using Specular Component Excluded Mode Between CE-2180 And SF-600 Before And After Applying The R-Model**

	<i>Before Modelling <math>\Delta E^*_{ab}</math></i>	<i>After Modelling <math>\Delta E^*_{ab}</math></i>	<i>% Improvement</i>
<i>Pale Grey</i>	0.724	0.064	91.160
<i>Middle Grey</i>	0.646	0.072	88.854
<i>Diff. Grey</i>	0.600	0.011	98.167
<i>Deep Grey</i>	0.374	0.057	84.759
<i>Deep Pink</i>	0.434	0.105	75.806
<i>Red</i>	0.297	0.125	57.912
<i>Orange</i>	0.793	0.089	88.777
<i>Bright Yellow</i>	1.106	0.239	78.391
<i>Green</i>	0.857	0.116	86.464
<i>Diff. Green</i>	1.045	0.237	77.321
<i>Cyan</i>	0.791	0.192	75.727
<i>Deep Blue</i>	0.529	0.132	75.047
<i>Average*</i>	0.683	0.120	82.443



**Table 6.12: Summary Of The Inter-Instrumental Agreement For The CCS-II MATT Tiles Using Specular Component Included Mode Between CE-2180 And SF-600 Before And After Applying The R-Model**

	Before Modelling $\Delta E^*_{ab}$	After Modelling $\Delta E^*_{ab}$	% Improvement
Pale Grey	0.970	0.462	52.371
Middle Grey	0.830	0.416	49.880
Diff. Grey	0.817	0.361	55.814
Deep Grey	0.583	0.288	50.600
Deep Pink	0.598	0.317	46.990
Red	0.412	0.265	35.680
Orange	0.891	0.264	70.370
Bright Yellow	1.167	0.050	95.716
Green	1.077	0.156	85.515
Diff. Green	1.248	0.183	85.337
Cyan	0.961	0.522	45.682
Deep Blue	0.632	0.470	25.633
Average*	0.849	0.313	63.145

Note \* = (Average Original  $\Delta E^*_{ab}$  – Average Corrected  $\Delta E^*_{ab}$ ) / Average Original  $\Delta E^*_{ab}$   $\times 100$

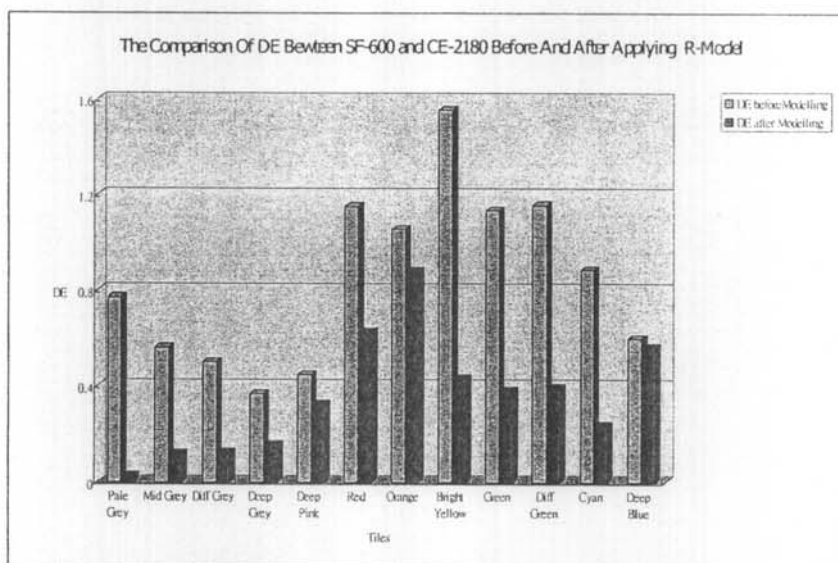


**Figure 6.9 The Comparison Of The DE Between SF-600 And CE-2180 Before After Applying R-Model (GE)**

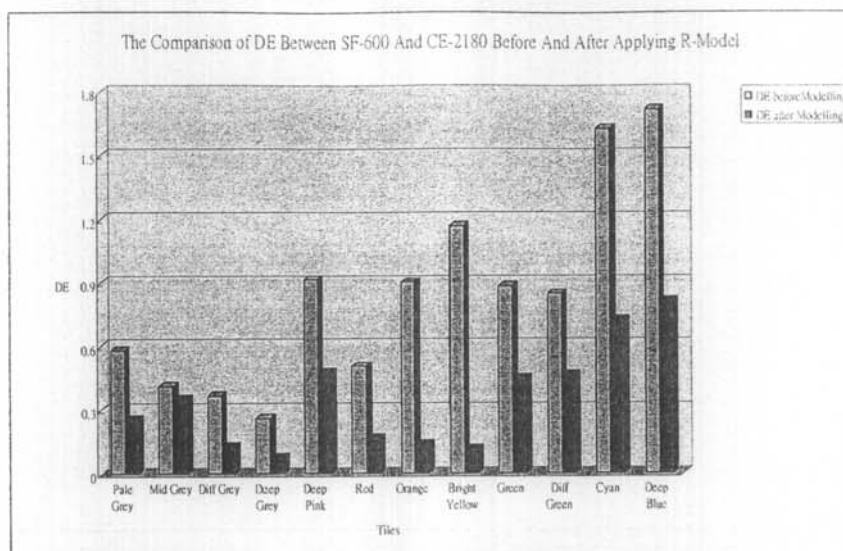


Figure 6.10 The Comparison Of The DE Between SF-600 And CE-2180 Before After Applying R-Model (GI)

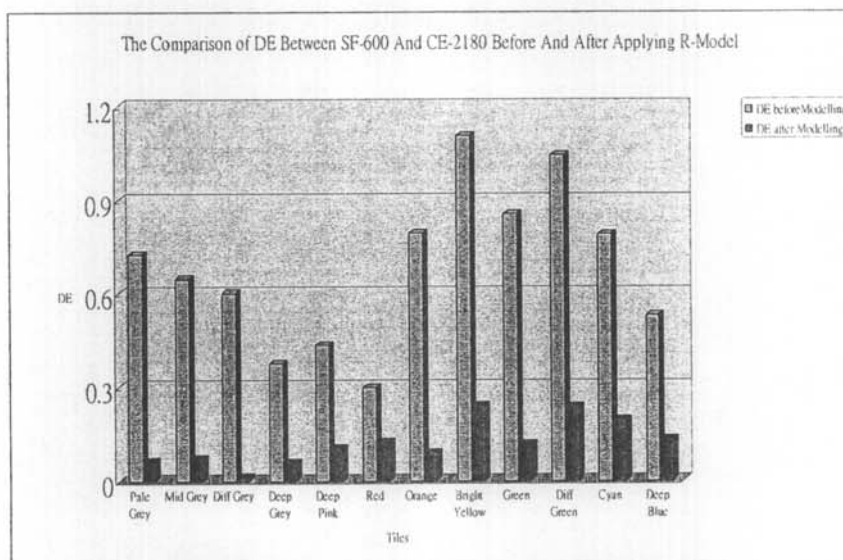
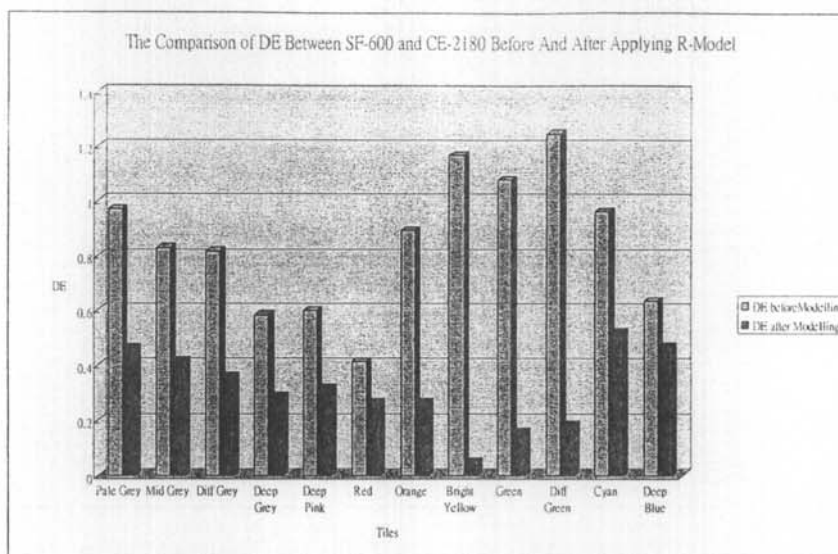


Figure 6.11 The Comparison Of The DE Between SF-600 And CE-2180 Before After Applying R-Model (ME)



*Figure 6.12 The Comparison Of The DE Between SF-600 And CE-2180 Before After Applying R-Model (MI)*

Tables 6.9 to 6.12 and Figures 6.9 to 6.12 show the improvement of the average colour difference between SF-600 and CE-2180 before and after application of the R-Model in a range from 58.1% to 82.4%. These results indicate that the application of the R-Model to the correction of the inter-instrumental agreement was successful. This also implies that the profile between CE-7000A and SF-600 and also the profile between CE-7000A and CE-2180 were successfully developed.

Lastly, the ultimate aim of this project was to develop a corrective inter-instrumental agreement model which could be applied to other colour-related products such as textiles and paper samples. Most textile products have a matt surface therefore, following on from the above results, textile samples were selected to test the "R-Model" in order to investigate the actual performance in the textile industry.

## **CHAPTER 7**

### **TESTING OF DEVELOPED MODELS**

#### **7.1 Introduction**

#### **7.2 Testing Of The R-Model Using Textile Samples**

#### **7.3 Testing Of The R-Model Using Paper Samples**

#### **7.1 Introduction**

In this chapter, results for the performance of the R-Model using textile and paper samples are summarised.

#### **7.2 Testing Of The R-Model Using Textile Samples**

As described in Chapter 3, textile samples were selected to test the performance of the newly developed mathematical model – the “R-Model”. Textile samples are generally matt in nature, and to date no results of any inter-instrumental agreement models for textile samples have been published.

129 textile samples were selected to test the performance of the “R-Model” and the results are summarised as follows:

**Table 7.1, Inter-Instrumental Agreement In Terms Of  $\Delta E$  Using GLOSSY Tiles Measured Using Specular Component Excluded Mode R-Model SF-600 Vs CE-7000A To Test The Performance Of Selected Textile Samples**

	<i>Original <math>\Delta E</math></i>	<i>Corrected <math>\Delta E</math></i>	<i>% Improvement</i>
<i>Maximum</i>	2.450	2.072	
<i>Minimum</i>	0.277	0.159	
<i>Sum</i>	134.031	78.432	41.500
<i>Average</i>	1.039	0.608	41.500

**Table 7.2, Inter-Instrumental Agreement In Terms Of  $\Delta E$  Using GLOSSY Tiles Measured Using Specular Component Included Mode R-Model SF-600 Vs CE-7000A To Test The Performance Of Selected Textile Samples**

	<i>Original <math>\Delta E</math></i>	<i>Corrected <math>\Delta E</math></i>	<i>% Improvement</i>
<i>Maximum</i>	1.901	1.402	
<i>Minimum</i>	0.269	0.152	
<i>Sum</i>	130.677	96.921	26.061
<i>Average</i>	1.013	0.749	26.061

**Table 7.3, Inter-Instrumental Agreement In Terms Of  $\Delta E$  Using MATT Tiles Measured Using Specular Component Excluded Mode R-Model SF-600 Vs CE-7000A To Test The Performance Of Selected Textile Samples**

	<i>Original <math>\Delta E</math></i>	<i>Corrected <math>\Delta E</math></i>	<i>% Improvement</i>
<i>Maximum</i>	2.450	2.506	
<i>Minimum</i>	0.277	0.067	
<i>Sum</i>	134.031	56.889	57.555
<i>Average</i>	1.039	0.441	57.555

**Table 7.4, Inter-Instrumental Agreement In Terms Of  $\Delta E$  Using MATT Tiles Measured Using Specular Component Included Mode R-Model SF-600 Vs CE-7000A To Test The Performance Of Selected Textile Samples**

	<i>Original <math>\Delta E</math></i>	<i>Corrected <math>\Delta E</math></i>	<i>% Improvement</i>
<i>Maximum</i>	1.901	1.212	
<i>Minimum</i>	0.269	0.129	
<i>Sum</i>	130.677	76.626	41.400
<i>Average</i>	1.013	0.594	41.400

Tables 7.1 to 7.4, which show the inter-instrumental agreement of the textile samples when the R-Model was applied, indicate that the colour differences between the two spectrophotometers SF-600 and CE-7000A were corrected and lowered when compared with the original values. This implies that all the four models can be applied to textile samples for inter-instrumental agreement. In the case of the MATT tiles measured using specular component included mode, the R-Model showed the best performance in the

inter-instrumental agreement. This was due to the fact that textile samples are matt in nature, thus the percentage improvement was higher and the results were better when compared with those for the other three models.

***Table 7.5, Inter-Instrumental Agreement In Terms Of  $\Delta E$  Using GLOSSY Tiles Measured Using Specular Component Excluded Mode R-Model CE-2180 Vs CE-7000A To Test The Performance Of Selected Textile Samples***

	<i>Original <math>\Delta E</math></i>	<i>Corrected <math>\Delta E</math></i>	<i>% Improvement</i>
<i>Maximum</i>	2.680	2.317	
<i>Minimum</i>	0.308	0.089	
<i>Sum</i>	111.585	98.427	11.792
<i>Average</i>	0.865	0.763	11.792

***Table 7.6, Inter-Instrumental Agreement In Terms Of  $\Delta E$  Using GLOSSY Tiles Measured Using Specular Component Included Mode R-Model CE-2180 Vs CE-7000A To Test The Performance Of Selected Textile Samples***

	<i>Original <math>\Delta E</math></i>	<i>Corrected <math>\Delta E</math></i>	<i>% Improvement</i>
<i>Maximum</i>	1.448	1.003	
<i>Minimum</i>	0.538	0.152	
<i>Sum</i>	112.746	96.621	14.302
<i>Average</i>	0.874	0.749	14.302



**Table 7.7, Inter-Instrumental Agreement In Terms Of  $\Delta E$  Using MATT Tiles Measured Using Specular Component Excluded Mode R-Model CE-2180 Vs CE-7000A To Test The Performance Of Selected Textile Samples**

	<i>Original <math>\Delta E</math></i>	<i>Corrected <math>\Delta E</math></i>	<i>% Improvement</i>
<i>Maximum</i>	2.680	2.216	
<i>Minimum</i>	0.308	0.143	
<i>Sum</i>	111.585	69.271	37.919
<i>Average</i>	0.865	0.537	37.919

**Table 7.8, Inter-Instrumental Agreement In Terms Of  $\Delta E$  Using MATT Tiles Measured Under Specular Component Included Mode R-Model CE-2180 Vs CE-7000A To Test The Performance Of Selected Textile Samples**

	<i>Original <math>\Delta E</math></i>	<i>Corrected <math>\Delta E</math></i>	<i>% Improvement</i>
<i>Maximum</i>	1.448	1.024	
<i>Minimum</i>	0.538	0.277	
<i>Sum</i>	112.746	82.173	27.117
<i>Average</i>	0.874	0.637	27.117

From the above four tables (Tables 7.5 to 7.8), showing results for the inter-instrumental agreement of the textile samples when the R-Model was applied, the colour differences between the two spectrophotometers CE-2180 and CE-7000A were also corrected and lowered when compared with the original values. This implies that all four models could be applied to the textile samples for the inter-instrumental agreement. And of the four models, the R-Model showed the best performance in the inter-instrumental agreement

for the MATT tiles measured using specular component excluded mode. Since textile samples are matt in nature, the percentage improvement was higher and the results were better when compared with the other three models.

### **7.3 Testing Of The R-Model Using Paper Samples**

As described in Chapter 3, besides textile samples, ColorCurve paper samples were also selected to test the performance of the newly developed mathematical model – the “R-Model”. ColorCurve paper samples are mainly matt in nature and, to date; no results related to inter-instrumental agreement model for correction of the measurement results of the paper samples have been published.

400 ColorCurve paper samples were selected to test the performance of the “R-Model” and the results are summarized below:

**Table 7.9, Inter-Instrumental Agreement In Terms Of  $\Delta E$  Using GLOSSY Tiles Measured Using Specular Component Excluded Mode R-Model SF-600 Vs CE-7000A To Test The Performance Of Selected ColorCurve Paper Samples**

	<i>Original <math>\Delta E</math></i>	<i>Corrected <math>\Delta E</math></i>	<i>% Improvement</i>
<i>Maximum</i>	2.026	2.211	
<i>Minimum</i>	0.290	0.041	
<i>Sum</i>	81.200	52.400	35.516
<i>Average</i>	0.203	0.131	35.516

**Table 7.10, Inter-Instrumental Agreement In Terms Of  $\Delta E$  Using GLOSSY Tiles Measured Using Specular Component Included Mode R-Model SF-600 Vs CE-7000A To Test The Performance Of Selected ColorCurve Paper Samples**

	<i>Original <math>\Delta E</math></i>	<i>Corrected <math>\Delta E</math></i>	<i>% Improvement</i>
<i>Maximum</i>	1.579	1.183	
<i>Minimum</i>	0.565	0.500	
<i>Sum</i>	385.200	332.400	13.707
<i>Average</i>	0.963	0.831	13.707

**Table 7.11, Inter-Instrumental Agreement In Terms Of  $\Delta E$  Using MATT Tiles Measured Using Specular Component Excluded Mode R-Model SF-600 Vs CE-7000A To Test The Performance Of Selected ColorCurve Paper Samples**

	<i>Original <math>\Delta E</math></i>	<i>Corrected <math>\Delta E</math></i>	<i>% Improvement</i>
<i>Maximum</i>	2.026	1.866	
<i>Minimum</i>	0.290	0.013	
<i>Sum</i>	81.200	31.600	61.084
<i>Average</i>	0.203	0.079	61.084

**Table 7.12, Inter-Instrumental Agreement In Terms Of  $\Delta E$  Using MATT Tiles Measured Using Specular Component Included Mode R-Model SF-600 Vs CE-7000A To Test The Performance Of Selected ColorCurve Paper Samples**

	<i>Original <math>\Delta E</math></i>	<i>Corrected <math>\Delta E</math></i>	<i>% Improvement</i>
<i>Maximum</i>	1.579	0.986	
<i>Minimum</i>	0.565	0.201	
<i>Sum</i>	385.200	238.400	38.103
<i>Average</i>	0.963	0.596	38.103

From the above four tables (Table 7.9 to Table 7.12), which show the results for the inter-instrumental agreement of the paper samples when applied to the R-Model, it may be seen that the colour differences between the two spectrophotometers SF-600 and CE-7000A were corrected and lowered when compared with the original values. This implies that all the four models could be applied to the ColorCurve paper samples for the inter-instrumental agreement. Of the four models, the R-Model shows the best performance in the inter-instrumental agreement for the MATT tiles measured using the specular component excluded mode. This was because the ColorCurve paper samples are matt in nature, thus the percentage improvement was better when compared with the other three models.

**Table 7.13, Inter-Instrumental Agreement In Terms Of  $\Delta E$  Using GLOSSY Tiles Measured Using Specular Component Excluded Mode R-Model CE-2180 Vs CE-7000A To Test The Performance Of Selected ColorCurve Paper Samples**

	<i>Original <math>\Delta E</math></i>	<i>Corrected <math>\Delta E</math></i>	<i>% Improvement</i>
<i>Maximum</i>	5.326	4.957	
<i>Minimum</i>	0.290	0.275	
<i>Sum</i>	239.200	173.600	27.419
<i>Average</i>	0.598	0.434	27.419

**Table 7.14, Inter-Instrumental Agreement In Terms Of  $\Delta E$  Using GLOSSY Tiles Measured Using Specular Component Included Mode R-Model CE-2180 Vs CE-7000A To Test The Performance Of Selected ColorCurve Paper Samples**

	<i>Original <math>\Delta E</math></i>	<i>Corrected <math>\Delta E</math></i>	<i>% Improvement</i>
<i>Maximum</i>	4.115	3.724	
<i>Minimum</i>	0.520	0.500	
<i>Sum</i>	272.800	180.400	33.871
<i>Average</i>	0.682	0.451	33.871

**Table 7.15, Inter-Instrumental Agreement In Terms Of  $\Delta E$  Using MATT Tiles Measured Using Specular Component Excluded Mode R-Model CE-2180 Vs CE-7000A To Test The Performance Of Selected ColorCurve Paper Samples**

	<i>Original <math>\Delta E</math></i>	<i>Corrected <math>\Delta E</math></i>	<i>% Improvement</i>
<i>Maximum</i>	5.326	4.627	
<i>Minimum</i>	0.290	0.276	
<i>Sum</i>	239.200	152.400	36.358
<i>Average</i>	0.598	0.381	36.358

**Table 7.16, Inter-Instrumental Agreement In Terms Of  $\Delta E$  Using MATT Tiles Measured Using Specular Component Included Mode R-Model CE-2180 Vs CE-7000A To Test The Performance Of Selected ColorCurve Paper Samples**

	<i>Original <math>\Delta E</math></i>	<i>Corrected <math>\Delta E</math></i>	<i>% Improvement</i>
<i>Maximum</i>	4.115	3.724	
<i>Minimum</i>	0.520	0.500	
<i>Sum</i>	272.800	179.600	34.229
<i>Average</i>	0.682	0.449	34.229

From the above four tables (Table 7.13 to Table 7.16), which show the results for the inter-instrumental agreement of the paper samples when the R-Model was applied, it may be seen that the colour differences between the two spectrophotometers CE-2180 and CE-7000A were also corrected and lowered when compared with the original values. This implies that all the four models could be applied to the ColorCurve paper samples for the inter-instrumental agreement. Of the four models, the R-Model showed best performance in the inter-instrumental agreement when the MATT tiles were measured using specular component excluded mode. Since the ColorCurve paper samples are matt in nature, the percentage improvement was correspondingly better when compared with the other three models.

**From the results of the textile samples and ColorCurve paper samples tested, it is evident that the MATT tiles measured using specular component included mode gave the best performance in the inter-instrumental agreement.**

## **CHAPTER 8**

# **COMPARISON OF THE R-MODEL WITH OTHER INTER-INSTRUMENTAL AGREEMENT MODELS**

### **8.1 Introduction**

### **8.2 Comparison Of The R-Model With Other Inter-instrumental Agreement Models Using Tiles**

### **8.3 Comparison Of The R-Model With Other Inter-instrumental Agreement Models Using Textile Samples And Paper Samples**

### **8.4 Conclusion**

### **8.1 Introduction**

In this chapter, the comparisons are drawn between the various mathematical models.

The comparisons include MATT tiles, textile and paper samples which measured using specular component excluded mode.



## **8.2 Comparison Of The R-Model With Other Inter-instrumental Agreement Models Using Tiles**

As discuss in Section 2.7, past research has yielded few inter-instrumental agreement models, and only two are commonly known, these being:

- i). Berns and Petersen's Model
- ii) Morovic's Model – Method II

The results in Chapter 6 showed that the MATT tiles measured using specular component excluded model demonstrate the best performance among the different models. The general comparison using MATT Tiles measured under specular component excluded Model among R-Model, Berns and Petersen's Model and Morovic's Model – Method II are shown as follows:

## Chapter 8 Comparison Of The R-Model With Other Inter-Instrumental Agreement Models

**Table 8.1: Inter-instrument Agreement In Terms Of  $\Delta E$  Using 12 MATT BCRA-NPL Series II Tiles Using Specular Component Excluded Mode (SF-600 vs CE-7000A)**

Tiles	Luo's Model – Method II			Berns and Petersen's Model		R Model	
	Un-corrected $\Delta E$	Corrected $\Delta E$	% Improvement	Corrected $\Delta E$	% Improvement	Corrected $\Delta E$	% Improvement
Pale Grey	0.577	0.478	17.226	1.005	-40.311	0.094	83.709
Middle Grey	0.434	0.393	9.450	0.299	31.152	0.066	84.793
Diff. Grey	0.419	0.375	10.564	0.243	41.934	0.069	83.532
Deep Grey	0.209	0.173	17.048	0.209	0.027	0.092	55.981
Deep Pink	0.649	0.056	91.373	0.068	89.510	0.086	86.749
Red	0.711	0.115	85.251	0.138	82.288	0.067	90.577
Orange	0.909	0.022	94.669	0.049	88.262	0.076	91.639
Bright Yellow	0.716	0.092	89.185	0.111	86.988	0.242	66.201
Green	0.854	0.110	74.561	0.166	61.753	0.159	81.382
Diff. Green	0.78	0.374	58.906	0.492	45.919	0.234	70.000
Cyan	0.923	0.201	65.126	0.286	50.413	0.169	81.690
Deep Blue	0.871	0.421	40.840	0.499	29.824	0.241	72.331
Average $\Delta E$	0.671	0.314	54.517	0.347	47.313	0.133	79.049

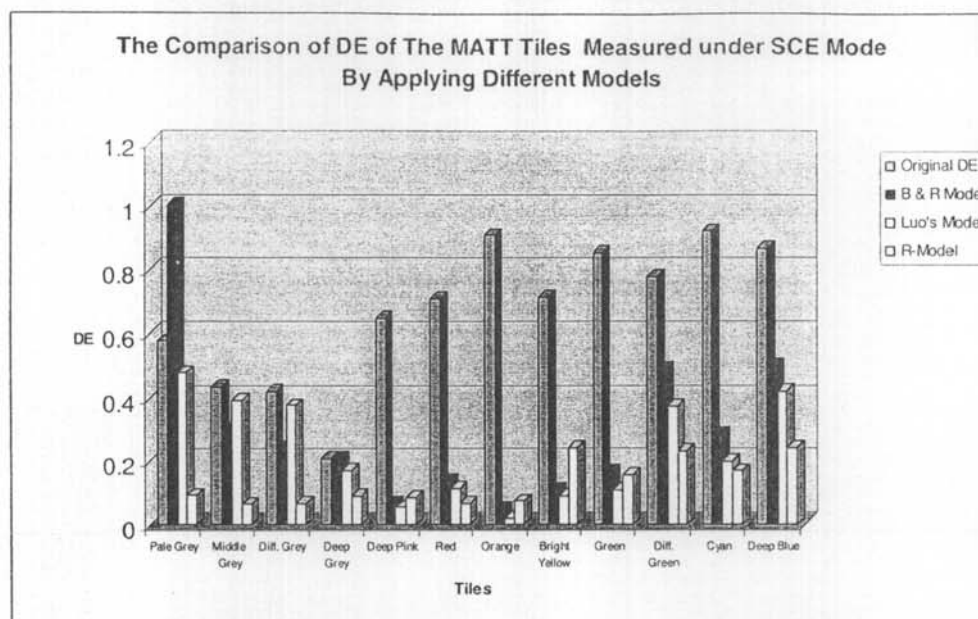


**Figure 8.2 The Comparison Of The DE For MATT Tiles Measured Using Specular Component Excluded Mode**

Based on the results in Table 8.1 and Figure 8.1, it may be concluded that after applying the different mathematical models to the MATT tiles, the colour difference is lowered than that of the original colour difference. R-Model shows the best performance among the three models. The overall improvement of R-Model is about 80% which is better than the rest two models.

### 8.3 Comparison Of The R-Model With Other Inter-Instrumental Agreement Models Using Textile Samples And Paper Samples

As discussed in section 7.2 and 7.3, the R-Model showed the best corrective performance in inter-instrumental agreement in terms of  $\Delta E$  for both the textile samples and ColorCurve paper samples for the MATT tiles measured using specular component excluded mode.

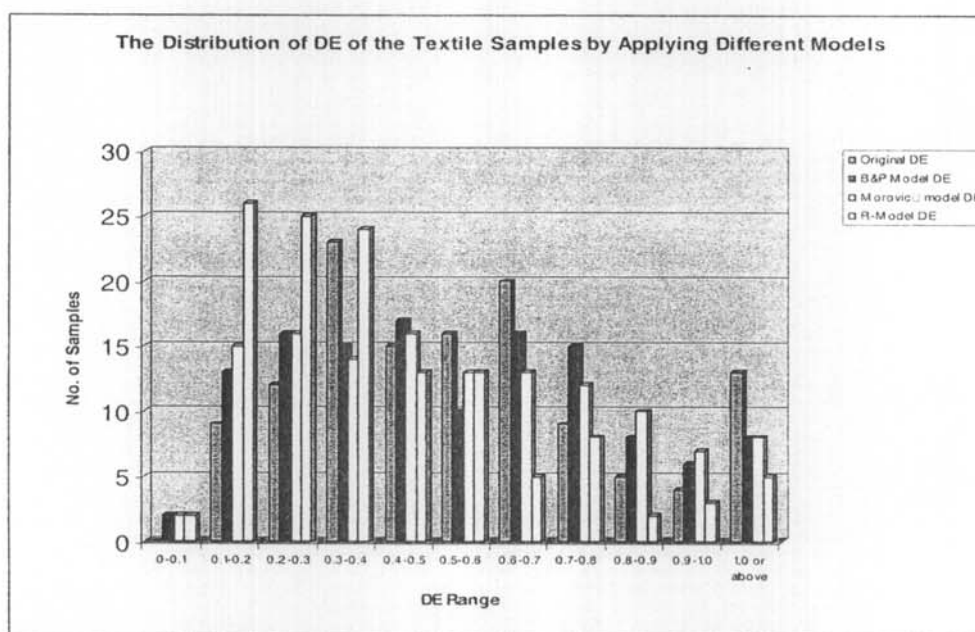


*Figure 8.2 The Distribution Of The DE For The Textile Samples By Applying To Different Models Using Matt Tiles Measured Using Specular Component Excluded Mode*

**Table 8.2 The Distribution Of The DE For The Textile Samples By Applying To Different Models Using Matt Tiles Measured Using Specular Component Excluded Mode**

$\Delta E$ Range	Original $\Delta E$	B&P Model $\Delta E$	Morovic's model $\Delta E$	R-Model $\Delta E$
0-0.1	0	2	2	2
0.1-0.2	9	13	15	26
0.2-0.3	12	16	16	25
0.3-0.4	23	15	14	24
0.4-0.5	15	17	16	13
0.5-0.6	16	10	13	13
0.6-0.7	20	16	13	5
0.7-0.8	9	15	12	8
0.8-0.9	5	8	10	2
0.9-1.0	4	6	7	3
1.0 or above	13	8	8	5

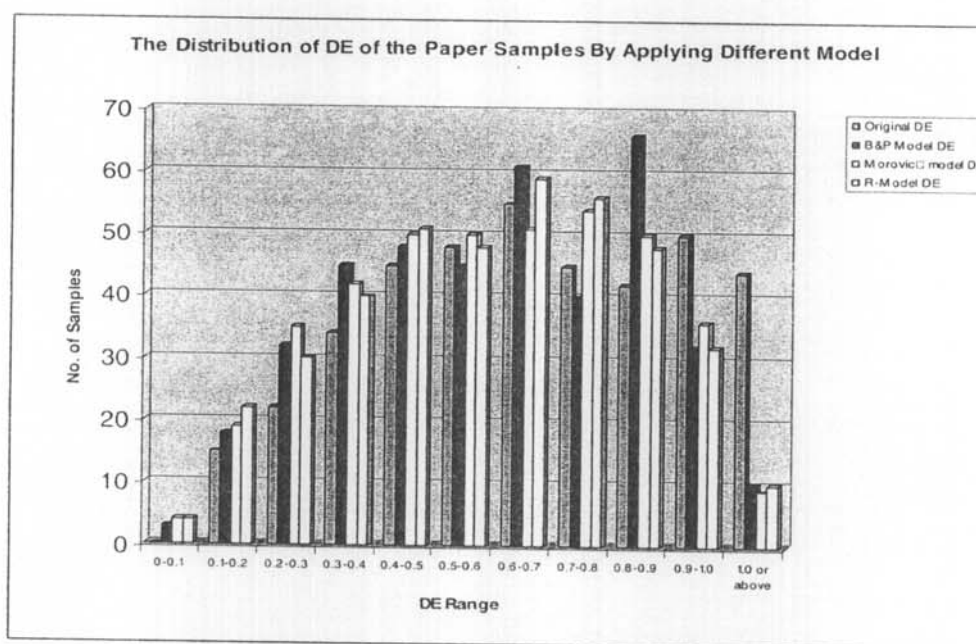


**Figure 8.3 The Distribution Of The DE For The Paper Samples By Applying To Different Models Using Matt Tiles Measured Using Specular Component Excluded Mode**

**Table 8.3 The Distribution Of The DE For The Paper Samples By Applying To Different Models Using Matt Tiles Measured Using Specular Component Excluded Mode**

<b><math>\Delta E</math> Range</b>	<b>Original <math>\Delta E</math></b>	<b>B&amp;P Model <math>\Delta E</math></b>	<b>Morovic's model <math>\Delta E</math></b>	<b>R-Model <math>\Delta E</math></b>
0-0.1	0	3	4	4
0.1-0.2	15	18	19	22
0.2-0.3	22	32	35	30
0.3-0.4	34	45	42	40
0.4-0.5	45	48	50	51
0.5-0.6	48	45	50	48
0.6-0.7	55	61	51	59
0.7-0.8	45	40	54	56
0.8-0.9	42	66	50	48
0.9-1.0	50	32	36	32
1.0 or above	44	10	9	10

From Figure 8.2 and Table 8.2, it may be seen that the colour difference value  $\Delta E$  shifted to the left hand side, i.e. the lower colour difference range, when the mathematical models were applied. When the performance of the three models was compared, it was found that the "R-Model" was better than the other two inter-instrumental mathematical models.

Figure 8.3 and Table 8.3 also indicates that the colour difference value  $\Delta E$  shifted to the left hand side, i.e., the lower colour difference range, when the mathematical models were applied. Of the three models, the "R-Model" showed the best performance in this case.

## **8.4 Conclusion**

In this chapter, the test results and the performance of the “R-Model” were described. Basically, the “R-Model” was demonstrated to be effective in the experimental work on inter-instrumental agreement across a range of samples including tiles, textile samples and Colorcurve paper samples correlations. The concept of the “R-Model” was based on bandpass error correction. In 1987, E.I. Stearns proposed the influence of spectral bandpass on the accuracy of tristimulus values. The fundamental premise of the “R-Model” is based on Stearns' concept but the coefficients of Stearns' correction model were fixed whereas the “R-Model” has flexible coefficients in order to fit different materials calculation. For this reason, the performance of the “R-Model” was better than that of the other, earlier models.

## **CHAPTER 9**

### **CONCLUSIONS AND RECOMMENDATIONS**

#### **9.1 Introduction**

#### **9.2 Conclusions Of The Research Issue**

#### **9.3 Recommendations**

#### **9.1 Introduction**

In this chapter conclusions are drawn about the significance of the research project and suggestions are made for future research and development activities.

#### **9.2 Conclusions Of The Research Issue.**

In general, spectrophotometers perform at a finite level of accuracy but as electron-mechanical-optical devices, they exhibit measurement errors relative to a theoretically error-free instrument that users must accept. If such measurement errors can be quantified and corrected, the accuracy of measurement and the inter-instrumental agreement can be further enhanced. Thus colouring by numbers can be successfully



used in digital colour communication.

At the outset of the research, it was found that the inter-instrumental agreement of the three selected spectrophotometers was unsatisfactory because the average colour difference was larger than  $0.5 \Delta E^*_{ab}$  units. The results imply that the origin of the errors and also the options for improvement should be investigated; hence the mathematical models for the inter-instrumental agreement, which should be applied in order to improve the inter-instrumental agreement. Once the inter-instrumental agreement of the spectrophotometers has been improved, the inter-instrumental agreement and non-physical sample colour communication can be further enhanced.

After the application of the “L-Model”, the colour measurement results improved but the results were not significant. Nevertheless this mathematical model gave a very good indication that mathematical correction was a good method to control the colour measurement results.

The L-Model represented a first stage in the development of the successful model for the inter-instrumental agreement. According to the concept of bandpass correction and

using the multi linear regression method, a powerful and robust mathematical model, this being termed the R-Model, was developed.

The R-Model was based on the concept of the correction of the bandpass error. When applied to the experimental results, it performed well in the inter-instrumental agreement case, the average percentage improvement having been approximately 90%, which is better than the other well developed models when tested with the CCS-II tiles.

In general, when the R-Model was used to test textile samples, the colour measurements also showed an improvement when compared with the other well known mathematical models. Such an improvement of the colour measurement in the spectral data will lead to improvements in the global colour communication between designers, coloration companies and buyers.

In the study of the inter-instrumental agreement, the variation of the colour measurements was very high, from 0.575 to 0.854 CIELAB  $\Delta E$  units when using different spectrophotometers. Because of this poor inter-instrumental agreement, different mathematical models were developed to improve the results. An empirical

model, named the “L-Model” was developed to improve the inter-instrumental agreement between spectrophotometers up to 62% based on the ceramic tile results. In addition, the “R-Model” was also developed, based on the analysis of spectral data from 400 – 700 nm and the concept of bandpass correction using the multi linear regression method. The performance of the “R-Model” was better than that of the “L-Model” and also some of the previously developed mathematical models. The improvement of the inter-instrumental agreement was found to be as high as 90% for the ceramic tiles. When the models are applied to the measurement of the coloured samples, the inter-instrumental agreement can be improved accordingly. The inter-instrumental agreement in spectral data should benefit the global colour communication between designers, coloration companies and buyers, and also improve non-physical sample communication.

### **9.3 Recommendations**

The following recommendations are made for further study.

#### **9.3.1 Calibration Sample**

Besides the CCS-II tiles, other standard materials, such as paper samples or textile samples, can be used for calibration purposes, thus the coverage of the colour range will be more than only twelve tiles.

#### **9.3.2 Quantifying Measurement Error for Hardware**

The accuracy of the measurements achieved using spectrophotometers was affected by many different factors, such as sample preparation, bandpass error, photometric error, photometric zero error etc. In this project, the instrument profile was quantified, but for other errors, further quantification is required as they are very important in colour measurement. The design of the spectrophotometers was also one of the important parameters affecting the colour measurement result. It also requires quantification in order to find out the causes of the measurement errors.

### **9.3.3 Other Mathematical Models**

In addition to the multi-linear regression method, there are many other different mathematical methods, such as simple and multi non-linear regression methods which can be used to develop new mathematical models. If a simple yet powerful mathematical method can be used, the inter-instrumental agreement for colour communication will be further enhanced in addition to the global colour communication among the designers, merchandisers and buyers.

---

**REFERENCE**

1. A. R. Robertson, The CIE 1976 Color Difference Formulae, Color Research and Application, Vol. 2, P. 7 – 11, Spring 1977
  2. A.R. Robertson, Diagnostic Performance Evaluation of Spectrophotometers, Advances in Standards and Methodology in Spectrophotometry, P.277-286, 1987
  3. Absolute Measurement of Reflectance, A New Precise Technique, Color Engineering, P. 38-39
  4. Adams, E.Q. X-Z Planes in the 1931 ICI system of Colorimetry, J. of Opt. Soc. Am. 32: P. 168-178, 1942
  5. Anni Berger-Schunn, Practical Color Measurement, John Wiley & Sons, Inc, 1994
  6. ASTM E 925 – 83 (Reapproved 1994), Standard Practice for the Periodic Calibration of Narrow Band-Pass spectrophotometers.
  7. ASTM Standards on Color and Appearance, 1996
  8. Berns R et al, An Abridged Technique to Diagnose Spectrophotometric Errors, Color Research and Application, Vol. 22, No. 1, P.51-60, Feb. 1997
  9. Berns R et al, Empirical Modelling of Systematic Spectrophotometric Errors, Color Research and Application, Vol. 13, No. 4, P.243-256, Aug. 1988
  10. Brill, M.H. Suggested Modification of CMC Formula for Acceptability, Col. Res. Appl. 17: P. 402-404, 1992
  11. British standard method for calculation of small color difference, BS 6923: 1988.
  12. Burnham, R.W. A colorimeter for research in color vision, Am.J. Physiol. 65: P. 603, 1952
  13. C. Burgess and K. D. Mielenz, Advances in Standards and Methodology in Spectrophotometry, Analytical Spectroscopy Library, 1987
  14. Ceramic Colour Standards, British Ceramic Research Association Ltd.
  15. Ceramic Colour Standards Series II, British Ceramic Research Association Ltd.
  16. Chamberlin, G.J. and Chamberlin, G.J Color, its measurement, computation and application, Heyen, London, 1980
  17. Chong T.F., Instrumental Measurement and Control of Colour, Review of Progress of Coloration, Vol. 18, P. 47-55, 1988
  18. CIE Publication No 15,2 (TC-1.3), Colorimetry, Official Recommendation, International Commission on Illumination, Wien 3. Bezirk, Kegelgass 27/1, Austria, 1986, 2<sup>nd</sup> ed.
  19. Clarke, F.J.J., MacDonald, R. and Rigg, B. (1984). Modification to the JPC79 Formula, J. Soc. Dyers Col. 100: P. 128-132, 1978
-

20. Colour at the Centre of Everything, International Dyer, P. 9-14, Jan 1997
21. Connolly C et al, Colour Measurement by Video Camera, Journal of the Society of Dyers and Colourists, Vol. 111, P. 373-375, Dec. 1995
22. Connolly C et al, The Use of Video Camera for Remote Colour Measurement, Journal of the Society of Dyers and Colourists, Vol. 112, P. 40-43, Feb. 1996
23. D. C. Rich et al, Evaluation of the Long -Term Repeatability of Reflectance Spectrophotometers, Spectrophotometry, Luminescence and Colour, P.137-153, 1995
24. D. C. Rich, Colorimetric Repeatability and Reproducibility of CHROMA-SENSOR Spectrocolorimeters, Die Farbe 37, P.247-261, 1990
25. D. C. Rich, The Chroma Sensor CS-5: A Tradition of Improved Performance, Color Research and Application, Vol. 16, No. 5, P.322-336, Oct 1991
26. D. Scott Reininger, Recent Developments in Portable Color Measurement Instruments and Applications in the Textile Industry, AATCC 1994 International Conference and Exhibition Book of Papers, P. 273 – 280
27. D. Scott Reininger, Textile Application for Hand-Held Color Measuring Instruments, Textile Chemists and Colorists, Vol. 29, No. 2, P. 13 – 17, February 1997
28. Dan Randall, Instruments for the Measurement of Color, Textile Chemist and Colorist, Vol. 30, No. 2, P. 20 – 26, February 1998
29. Datacolor International, Spectraflash® 600 PLUS Operators Manual, April 1997
30. Development of Standards for Inter-instrument Calibration of spectrophotometer in Computer Colour Systems, Colourage, P. 29 – 34, December 1995
31. Donaldson, R. A colorimeter with six matching stimuli, Proc. Phys. Soc. (London) 59: P. 554, 1947
32. Donaldson, R. A trichromatic colorimeter, Proc. Phys. Soc. (London) 47: P.1068, 1927
33. E. I. Stearns and R. E. Stearns, An Example of a Method for Correcting Radiance Data for Bandpass Error, Vol. 13, No. 4, P. 257 – 259, August 1988
34. E. I. Stearns, Influence of spectrophotometer Slits on Tristimulus Calculation, Color Research and Application, Vol. 6, No. 2, P. 78 – 84, Summer 1981
35. E. I. Stearns, The Influence of Spectral Bandpass on Accuracy of Tristimulus Data, Color Research and Application, Vol. 12, No. 5, P. 282 – 284, October, 1997
36. Ellen C. Carter et al, Material Standards and Their Use in Color Measurement, Color Research and Application, Vol. 4, No. 2, P.97-100, Summer 1979
37. F. J. J. Clarke and P.S. Samways, The Spectrophotometric Properties of a Selection of Ceramic Tiles, National Physical Laboratory Report MC2, August

1968

38. F. J. J. Clarke et al, Development of a New Series of Ceramic Colour Standards, *Journal of the Society of Dyers and Colourists*, Vol. 97, P.503-504, Dec. 1981
39. F. J. J. Clarke, Problem of Spectrofluorimetric Standards for Reflection and Colorimetric Use, National Physical Laboratory Report MOM 12, August 1968
40. F. W. Billmeyer, Jr et al, Assessment of Color-Measuring Instruments, *Color Research and Application*, Vol. 6, No. 4, Winter 1981
41. F. W. Billmeyer, Jr et al, Instrumentation for Colour Measurement and its Performance, Golden Jubilee of Colour in the CIE, The Society of Dyers and Colourists, Bradford, England, 1981, P.98-112
42. F. W. Billmeyer, Jr. and H. Hemmendinger, Instrumentation for Color Measurement and its Performance, Golden Jubilee of Colour in the CIE, P. 98 – 112, 1981
43. Fairchild, M.D. and Pirrota, E. Predicting the Lightness of Chromatic Object Colors using CIELAB, *Col. Res. Appl.* 16: P. 385-392, 1991
44. Fenn R et al, The Use of Non-physical Standards in Colour Communication and Matching, *Journal of the Society of Dyers and Colourists*, Vol. 113, P.56-58, Feb. 1997
45. Fred W. Billmeyer, Jr. and Assessment of Color-Measuring Instruments, *Colour Research and application*, Vol. 6, No. 4, P. 195 – 202, Winter 1981
46. Fred W. Billmeyer, Jr., An Objective Approach to Coloring, *Color Engineering*, P. 10 – 13, September, 1963
47. Fred W. Billmeyer, Jr., The Precision of Spectrophotometry As Practiced in Industry, *Color Engineering*, Vol. 3 No. 4, P. 16 – 20, July – august, 1965
48. Fred W. Billmeyer, Jr., The Present and Future of Industrial Color Measurement, *Color Engineering*, Vol. 4, No. 4,P. 14 – 18, July – August 1996
49. Guild J. A trichromatic colorimeter suitable for standardization work, *Trans. Opt. Soc. (London)* 27: P. 106, 1925
50. H. P. Lee et al, Calibrating Spectrophotometers Using Neural Networks, *SPIE* Vol. 3300, P. 274-282, 1998
51. H. S. Shan and R. S. Gandhi, Instrumental Colour Measurement and Computer Aided Colour Matching for Textiles, Mahajan BookDistributors, 1990
52. Henry Hemmendinger, Colorimetric Information and Colorimetric Errors, *Color Technology in the Textile Industry*. P. 2 – 23
53. Hugh R. Davidson and Henry Hemmendinger, Specification and Control of Color, *Color Engineering*, P. 15 – 28, April, 1963
54. Hugh S. Fairman and Henry Hemmendinger, Stability of Ceramic Color Reflectance standards, *Color Research and Application*, Vol. 23, No. 6, P. 408 –



- 415, December 1998
55. Isadore Nimeroff, The Variability of Color Measurement, Color Engineering, P. 24 –44, March – April, 1967
56. J. Anne Compton, The Thermochromic Properties of the Ceramic Colour Standards, Color Research and Application, Vol. 9, No. 1, P.15-22, Spring 1984
57. James R. Vasconcellos, Supply Chain Management of Color and appearance: Evolution vs. Revolution, AATCC Review P. 14 – 37, June, 2001
58. James Rodgers et al, A Comparative Study of Color Measurement Instrumentation, Color Research and Application, Vol. 19, No. 5, Oct 1994
59. James T. DeGroff, Developments In Color Instrument Design Utilizing LED Technology For Textile Applications, AATCC 1995 International Conference and Exhibition Book of Papers, P. 477 – 481
60. Joanne C. Zwinkels, Colour-measuring Instruments and Their Calibration, Display, Vol, 16, No. 4, P. 163 – 171, 1996
61. Joanne C. Zwinkels, Errors in Colorimetry Caused by the Measuring Instrument, Textile chemist and Colorist, Vol. 21, No. 2, P. 23 – 29, February 1989
62. Konrad Hoffmann, Chromatic Integrating-Sphere Error In Tristimulus Colorimeters, Journal of Color & Appearance, Vol. 1, No.2, P. 16 – 41, September/ October 1971
63. L. Reniff, Transferring the 45/0 Spectral Reflectance Factor Scale, Color Research and Application, Vol. 19, No. 5, P.332-340, Oct 1994
64. Lee, R.L. Jr., Col. Res. Appl., 13: P. 180-186, 1988
65. Lovibond, J.W. The tintometer, a new instrument ...measurement of color, J. Soc. Dyers Col. III (2) 26 Dec, 1887
66. Lueo, M.R. and Rigg, B. Uniform color space based on the CMC (l:c) color-difference formula, J. Soc. Dyers Col. 102: 164-171, 1996
67. Luo, M.R. and Rigg, B. BFD (l:c) Color Difference Formula, Part 1.J.Soc. Dyer Col., 103: P. 86-94, 1987
68. M. D. Fairchild et al, Thermochromism of Ceramic Reference Tiles, Applied Optics, Vol. 24, No. 21, P.3432-3433, Nov. 1985
69. MacAdam, D.L. Loci of constant hue and brightness determined with various surrounding colors, J. Opt. Soc. Am. 40: P. 589, 1950
70. Macbeth® COLOR-EYE® 2180 Spectrophotometer Operation Manual, February 1996
71. Macbeth® COLOR-EYE® 7000A Spectrophotometer Operation Manual, October 1996
72. MacDonal, R. Industrial pass/fail Color Matching Part II., J. Soc. Dyers. Col. 96: P. 418-433, 1980

## Reference

---

73. MacDonald, R. and Smith, K.J. CIE94-a new color difference formula, J. Soc. Dyer Col., 111: P. 376-379, 1995
74. MacDonald, R. Industrial Pass/ Fail Color Matching Part I., J. Soc. Dyers. Col. 96: P. 372-376, 1980
75. Malkin F. et al, The BCRA-NPL Ceramic Colour Standards, Series II – Master Spectral Reflectance and Thermochromism Data, Journal of the Society of Dyers and Colourists, Vol. 113, P.84-94, Mar. 1997
76. McDonald, R. Industrial pass/fail color matching, part III. Development of a pass/fail formula for use with instrumental measurement of color difference, J.Soc.Dyers.Col., 96: P. 486-46, 1980
77. McLaren, K. In: "AIC Color 77", Bristol: Adam-Hilger, 503 pp.
78. Nayatani, Y., Umemura, Y., Sobagachi, H., Takahama, K. and Hashimoto, K. Lightness Perception of Chromatic Object Colors, Col. Res. Appl. 16: P. 16-25, 1991
79. Norusis M. J., SPSS Advanced Statistics™ 6.1, SPSS Inc. – Chicago, 1994
80. Norusis M. J., SPSS® for Windows™ Base system User's Guide Release 6.0, SPSS Inc. – Chicago, 1993
81. Norusis M. J., The SPSS Guide to Data Analysis for SPSS / PC+™, Second Edition, SPSS Inc. – Chicago, 1991
82. NPL (National Physical Laboratory), Optical Radiation Measurement Newsletter, issue 1. Spring, 1996
83. Oglesby, S. The effectiveness of CIE94- compared with CMC equation, J. Soc. Dyer Col., 111: P. 380-382, 1995
84. P. Morovic, H. Xu and M. R. Luo, Inter-Comparison of Colour Measuring Instruments
85. Patrick T. F. Chong, Colorimetry for Textile Applications, Modern Textile Characterisation Methods, P. 355 391, 1996
86. Patrick T. F. Chong, Reproducibility of Color Difference Measurements On Textile Samples, AATCC 1993 International Conference and Exhibition Book of Papers, P. 323 – 332
87. Proceedings of the Eighth Session (Cambridge, English, 1931), International Commission on Illumination, Wien 3. Bezirk, Kegelgass 27/1, Austria
88. R. Seve, New Formula for the computation of CIE 1976 Hue Difference, Colour Research and Application, Vol. 16, P. 217 – 218, June, 1991
89. R. W. G. Hunt, Measuring Colour (2<sup>nd</sup> Edition), Ellis Horwood Limited, 1991
90. Randall D, Instruments for the Measuring of Color, Textile Chemist and Colorist, Vol. 30, No. 2, P.20-26, Feb. 1998
91. Reining D.S., Textile Applicatins fr Hand-Held Colour Measuring Instruments,

## Reference

---

- Textile Chemist and Colorist, Vol. 29, No.2, P. 13-17, Feb. 1997
92. Robert T. Marcus and Fred W. Billmeyer, Jr., Statistical Study of Color-Measurement Instrumentation, Applied Optics, Vol. 13, No.6, P. 1519 – 1531, June 1974
  93. Robert T. Marcus, Long-Term Repeatability of Color-Measuring Instrumentation: Storing Numerical Standards, Color Research and Application, Vol. 3, No. 1, spring 1978
  94. Robert Willis, Instrumentation for Color Measurement, AATCC Workshop, Color Measurement Principles and the Textile Industry, 1988
  95. Roderick McDonald, Color Communication in the 90s, AATCC 1991 International Conference and Exhibition Book of Papers, P. 148 – 152
  96. Roderick McDonald, Colour Physics for Industry (2<sup>nd</sup> Edition), Society of Dyers and Colourists, 1997
  97. Roderick McDonald, Colour Physics for Industry, Society of Dyers and Colourists, 1987
  98. Roland Derby, Studies of Illuminating and Viewing Conditions in Colorimetry of Reflecting Materials, Color Engineering, P. 14 – 23
  99. Ruth Johnston, Analysis and Description of Color With Spectrophotometry, Color Engineering, Vol. 3, No. 3, P. 12-18, May – June 1965
  100. Ruth M. Johnston and Robert P. Ericson, Control of Color Standards, Color Engineering, Vol. 2, No. 11 – 12, P. 10 – 23, November – December 1964
  101. Ruth M. Johnston, and et. al., Preparation and Use of Stable Secondary Standards for Colorimetry, Color Engineering, Vol. 6 No. 2, P. 34 – 38, March – April, 1968
  102. Ruth M. Johnston, Color Measuring Instruments: A Guide To Their Selection, Journal of Color and Appearance, Vol. 1 No. 2, P. 27 – 38, September/ October, 1971
  103. Seve, R. New Formula for Computation of CIE 1976 Hue Difference, Col. Res. Appl. 16: P. 217-218, 1991
  104. Stroke, M. and Brill, M.H. Col. Res. Appl. 17: P. 410-411, 1992
  105. Verill, JF and et al., New Methods of Disgosing Errors in Colour Measuring Instruments, Die Fabre, Vol. 39, P. 285 – 295, 1993
  106. Verrill F. J. et al, European Project on Intercomparison of Colour Measurement, EUR14982EN, 1993
  107. Verrill F. J. et al, Intercomparison of Colour Measurements, NPL Spectrophotometry and Colorimetry Club, NPL Report QU 113, 1995
  108. Witt, K. Col. Res. Appl., 19: (1994), P. 273, 1994
  109. Wright, W.D. A trichromatic colorimeter with spectral stimuli, Trans. Opt. Soc. (London) 29: P. 225, 1927

#### Reference

---

110. Wyszecki, G Matching color differences, J. Opt. Soc. Am. 55: P. 1319-1324, 1965
111. Wyszecki, G Reanalysis of the NRC field trial of color-matching functions, J. Opt. Soc. Am. 54: P. 710-714, 1964

**APPENDIX I:**  
**The Coefficient  $m$ ,  $n$ ,  $o$  and  $q$  used in R-Model.**

Appendix I

**Table 1: The coefficient  $m$ ,  $n$ ,  $o$ , and  $q$  for the EQ. 6.1, 6.2 and 6.3 of the CCS-II GLOSSY Tiles under the condition of Specular Component Excluded SF-600 vs CE-7000A**

Wavelength	$m$	$n$	$o$	$q$
400	0.000	1.117	-0.951	-0.097
410	-0.058	1.198	-0.111	-0.064
420	0.000	1.125	-0.095	-0.098
430	0.000	1.164	-0.136	-0.046
440	0.000	1.145	-0.118	-0.041
450	0.000	1.131	-0.106	-0.033
460	0.000	1.121	-0.097	-0.023
470	0.000	1.127	-0.105	-0.008
480	0.000	0.944	0.080	-0.040
490	0.086	1.017	-0.079	-0.041
500	0.089	1.000	-0.065	0.035
510	0.052	1.043	-0.070	-0.043
520	0.067	1.008	-0.053	-0.029
530	0.068	0.990	-0.037	-0.027
540	0.097	0.954	-0.033	-0.016
550	0.106	0.951	-0.040	-0.011
560	0.000	0.913	0.106	-0.034
570	0.000	0.937	0.081	-0.018
580	0.000	1.141	-0.126	0.057
590	0.047	1.044	-0.075	0.030
600	0.000	1.187	-0.017	0.069
610	0.198	0.819	0.000	0.036
620	0.146	0.872	0.000	0.028
630	0.014	0.877	0.000	0.013
640	0.136	0.880	0.000	0.006
650	0.116	0.910	0.000	0.022
660	0.093	0.925	0.000	-0.001
670	0.000	1.016	0.000	-0.047
680	0.000	1.014	0.000	-0.046
690	0.263	0.747	0.000	0.046
700	0.483	0.000	0.520	0.244

**Table 2: The coefficient  $m$ ,  $n$ ,  $o$ , and  $q$  for the EQ. 6.1, 6.2 and 6.3 of the CCS-II GLOSSY Tiles under the condition of Specular Component Included SF-600 vs CE-7000A**

Wavelength	$m$	$n$	$o$	$q$
400	0.000	1.072	-0.060	-0.028
410	-0.081	1.224	-0.125	-0.040
420	0.569	0.000	0.453	-0.039
430	0.575	0.000	0.448	-0.075
440	0.576	0.000	0.445	-0.142
450	0.598	0.000	0.424	-0.221
460	-0.016	1.143	-0.112	-0.030
470	0.000	1.122	-0.107	-0.031
480	-0.060	1.076	0.000	-0.060
490	0.086	1.013	-0.083	-0.074
500	0.092	0.993	-0.068	-0.096
510	0.049	1.043	-0.077	-0.078
520	0.069	1.001	-0.055	-0.071
530	0.064	0.994	-0.046	-0.074
540	0.090	0.960	-0.038	-0.064
550	0.106	0.949	-0.043	-0.067
560	0.000	0.111	0.901	-0.071
570	0.055	1.006	-0.051	-0.052
580	0.058	1.023	-0.069	-0.040
590	0.067	0.999	-0.057	-0.014
600	0.000	1.176	-0.167	-0.029
610	0.201	0.810	0.000	-0.032
620	0.149	0.862	0.000	-0.024
630	0.143	0.867	0.000	-0.024
640	0.143	0.866	0.000	-0.035
650	0.119	0.891	0.000	-0.024
660	0.091	0.919	0.000	-0.041
670	0.000	1.009	0.000	-0.067
680	0.000	1.007	0.000	-0.073
690	0.241	0.763	0.000	0.009
700	0.050	0.500	0.000	0.249

**Table 3: The coefficient  $m$ ,  $n$ ,  $o$ , and  $q$  for the EQ. 6.1, 6.2 and 6.3 of the CCS-II MATT Tiles under the condition of Specular Component Excluded SF-600 vs CE-7000A**

Wavelength	$m$	$n$	$o$	$q$
400	0.000	1.132	-0.111	-0.210
410	0.000	1.108	-0.080	-0.207
420	0.000	1.124	-0.097	-0.195
430	0.157	0.870	0.000	-0.164
440	0.142	0.883	0.000	-0.146
450	0.140	0.883	0.000	-0.161
460	0.124	0.899	0.000	-0.155
470	0.144	0.878	0.000	-0.154
480	0.071	0.095	0.000	-0.158
490	0.065	1.046	-0.091	-0.119
500	0.069	1.037	-0.085	-0.141
510	0.041	1.064	-0.085	-0.129
520	0.070	1.010	-0.060	-0.126
530	0.076	0.987	-0.044	-0.124
540	0.092	0.970	-0.046	-0.088
550	0.168	0.847	0.000	-0.124
560	0.113	0.902	0.000	-0.084
570	0.107	0.907	0.000	-0.069
580	0.125	0.888	0.000	-0.060
590	0.140	0.874	0.000	-0.053
600	0.188	0.825	0.000	-0.028
610	0.143	0.869	0.000	0.018
620	0.130	0.882	0.000	0.017
630	0.109	0.903	0.000	-0.006
640	0.094	0.917	0.000	-0.009
650	0.091	0.920	0.000	-0.004
660	0.000	1.095	-0.083	-0.004
670	0.000	1.011	0.000	-0.045
680	0.000	1.009	0.000	-0.009
690	0.000	1.007	0.000	-0.183
700	0.510	0.499	0.000	0.340



**Table 4: The coefficient  $m$ ,  $n$ ,  $o$ , and  $q$  for the EQ. 6.1, 6.2 and 6.3 of the CCS-II MATT Tiles under the condition of Specular Component Included SF-600 vs CE-7000A**

Wavelength	$m$	$n$	$o$	$q$
400	0.000	1.116	-0.105	-0.136
410	0.000	1.090	-0.073	-0.164
420	0.000	1.124	-0.106	-0.183
430	0.159	0.858	0.000	-0.162
440	0.145	0.871	0.000	-0.160
450	0.136	0.877	0.000	-0.161
460	0.116	0.896	0.000	-0.136
470	0.151	0.863	0.000	-0.167
480	0.085	0.931	0.000	-0.167
490	0.100	0.975	-0.063	-0.145
500	0.093	0.984	-0.063	-0.151
510	0.057	1.206	-0.071	-0.129
520	0.000	0.895	0.119	-0.125
530	0.107	0.904	0.000	-0.164
540	0.072	0.991	-0.054	-0.126
550	0.063	1.028	-0.083	-0.097
560	0.000	1.126	0.118	-0.078
570	0.104	0.905	0.000	-0.122
580	0.083	0.983	-0.056	-0.100
590	0.075	0.990	0.057	-0.058
600	0.139	0.911	-0.043	-0.049
610	0.016	0.850	0.000	-0.041
620	0.000	0.864	0.145	-0.060
630	0.000	0.885	0.121	-0.037
640	0.121	0.884	0.000	-0.046
650	0.107	0.899	0.000	-0.036
660	0.085	0.920	0.000	-0.040
670	0.060	0.940	0.000	-0.057
680	0.000	1.004	0.000	-0.044
690	0.241	0.760	0.000	0.040
700	0.482	0.512	0.000	0.304

**Table 5: The coefficient  $m$ ,  $n$ ,  $o$ , and  $q$  for the EQ. 6.1, 6.2 and 6.3 of the CCS-II GLOSSY Tiles under the condition of Specular Component Excluded CE-2180 vs CE-7000A**

Wavelength	$m$	$n$	$o$	$q$
400	0.000	0.907	0.0862	-0.0108
410	0.000	0.920	0.07505	-0.104
420	0.000	0.913	0.0886	-0.0614
430	0.000	0.906	0.09773	-0.120
440	-0.102	1.104	0.000	-0.0825
450	-0.0918	1.094	0.000	-0.0601
460	-0.100	1.104	0.000	-0.0422
470	-0.117	1.122	0.000	-0.0418
480	-0.0968	1.102	0.000	-0.0488
490	-0.127	1.135	0.000	-0.0293
500	-0.110	1.111	0.000	-0.0374
510	-0.0979	1.101	0.000	-0.0214
520	-0.087	1.090	0.000	-0.0822
530	-0.0486	1.057	0.000	-0.0651
540	-0.0557	1.064	0.000	-0.0952
550	-0.0695	1.075	0.000	-0.0809
560	0.000	0.997	0.02991	-0.136
570	0.000	0.973	0.03471	-0.105
580	0.000	0.945	0.06327	-0.167
590	-0.074	1.081	0.000	-0.155
600	-0.116	1.122	0.000	-0.0733
610	-0.0723	1.080	0.000	-0.146
620	-0.0685	1.077	0.000	-0.134
630	-0.107	1.114	0.000	-0.118
640	-0.131	1.140	0.000	-0.246
650	-0.144	1.155	0.000	-0.0609
660	-0.128	1.140	0.000	-0.279
670	0.000	0.786	0.227	-0.268
680	0.000	0.769	0.247	-0.335
690	-0.359	1.380	0.000	-0.410
700	0.000	1.023	0.000	-0.321

**Table 6: The coefficient  $m$ ,  $n$ ,  $o$ , and  $q$  for the EQ. 6.1, 6.2 and 6.3 of the CCS-II GLOSSY Tiles under the condition of Specular Component Included CE-2180 vs CE-7000A**

Wavelength	$m$	$n$	$o$	$q$
400	0.000	0.957	0.0484	-0.111
410	-0.0558	1.065	0.000	-0.116
420	-0.0779	1.078	0.000	-0.0527
430	-0.0988	1.107	0.000	-0.0833
440	-0.101	1.107	0.000	-0.0922
450	-0.0828	1.091	0.000	-0.0684
460	-0.104	1.107	0.000	-0.0441
470	0.000	0.917	0.08891	-0.133
480	-0.105	1.109	0.000	-0.0408
490	-0.144	1.147	0.000	-0.0133
500	-0.131	1.143	0.000	-0.135
510	-0.116	1.126	0.000	-0.160
520	-0.0981	1.107	0.000	-0.155
530	-0.0546	1.059	0.000	-0.0285
540	-0.0675	1.075	0.000	-0.121
550	-0.0987	1.109	0.000	-0.058
560	-0.0566	1.069	0.000	-0.221
570	0.000	0.933	0.07939	-0.234
580	-0.0707	1.083	0.000	-0.209
590	-0.102	1.112	0.000	-0.165
600	-0.139	1.151	0.000	-0.195
610	0.000	0.901	0.111	-0.205
620	-0.102	1.112	0.000	-0.173
630	-0.135	1.143	0.000	-0.121
640	0.000	0.828	0.186	-0.245
650	-0.165	1.175	0.000	-0.179
660	-0.161	1.176	0.000	-0.303
670	-0.225	1.240	0.000	-0.286
680	-0.221	1.237	0.000	-0.304
690	-0.274	1.283	0.000	-0.337
700	0.000	1.021	0.000	-0.141

**Table 7: The coefficient  $m$ ,  $n$ ,  $o$ , and  $q$  for the EQ. 6.1, 6.2 and 6.3 of the CCS-II MATT Tiles under the condition of Specular Component Excluded CE-2180 vs CE-7000A**

Wavelength	$m$	$n$	$o$	$q$
400	0.000	0.933	0.07099	0.187
410	-0.0913	1.095	0.000	0.01656
420	-0.0855	1.093	0.000	0.104
430	-0.104	1.115	0.000	0.03505
440	-0.112	1.122	0.000	0.04694
450	-0.109	1.116	0.000	0.169
460	-0.118	1.128	0.000	0.137
470	-0.120	1.131	0.000	0.128
480	-0.0888	1.102	0.000	0.134
490	-0.130	1.144	0.000	0.138
500	-0.119	1.129	0.000	0.141
510	-0.104	1.115	0.000	0.199
520	-0.0849	1.096	0.000	0.118
530	-0.0583	1.075	0.000	0.140
540	-0.0654	1.082	0.000	0.09268
550	-0.0678	1.082	0.000	0.03527
560	-0.0488	1.063	0.000	0.04185
570	-0.043	1.058	0.000	0.0393
580	-0.0604	1.075	0.000	0.009935
590	-0.0691	1.084	0.000	0.002368
600	-0.112	1.127	0.000	0.0972
610	-0.0556	1.069	0.000	0.159
620	0.000	0.975	0.04183	0.05131
630	0.000	0.947	0.06727	0.101
640	0.000	0.910	0.107	0.01904
650	0.000	0.882	0.134	0.131
660	0.000	1.020	0.000	-0.0042
670	0.000	1.020	0.000	-0.0565
680	0.000	1.022	0.000	-0.00453
690	0.000	0.828	0.197	-0.217
700	-0.311	1.341	0.000	-0.437

**Table 8: The coefficient  $m$ ,  $n$ ,  $o$ , and  $q$  for the EQ. 6.1, 6.2 and 6.3 of the CCS-II MATT Tiles under the condition of Specular Component Included CE-2180 vs CE-7000A**

Wavelength	$m$	$n$	$o$	$q$
400	0.000	0.943	0.06714	0.0027
410	-0.0898	1.101	0.000	0.05033
420	-0.0801	1.084	0.000	0.133
430	-0.089	1.102	0.000	0.04999
440	-0.0989	1.109	0.000	0.05568
450	-0.0902	1.104	0.000	0.09046
460	-0.0997	1.110	0.000	0.09568
470	-0.132	1.144	0.000	0.105
480	-0.104	1.111	0.000	0.187
490	-0.130	1.136	0.000	0.194
500	-0.123	1.141	0.000	0.07708
510	-0.112	1.130	0.000	0.04547
520	-0.0992	1.114	0.000	0.05354
530	-0.0596	1.068	0.000	0.115
540	-0.0625	1.075	0.000	0.110
550	0.000	0.953	0.06575	0.02639
560	-0.0647	1.081	0.000	-0.0126
570	-0.0573	1.073	0.000	0.01328
580	-0.0733	1.091	0.000	0.0145
590	-0.101	1.116	0.000	0.02241
600	-0.148	1.163	0.000	-0.0459
610	-0.101	1.117	0.000	-0.0445
620	0.000	0.917	0.0992	-0.0332
630	0.000	0.878	0.137	0.002278
640	-0.109	1.128	0.000	-0.0624
650	-0.147	1.163	0.000	-0.0142
660	-0.118	1.138	0.000	-0.154
670	0.000	0.864	0.158	-0.241
680	0.000	1.023	0.000	-0.128
690	0.000	0.811	0.211	-0.362
700	-0.273	1.300	0.000	-0.420

**APPENDIX II:**  
**Summary For The Repeatability in terms of  $\Delta L^*$ ,  $\Delta a^*$ ,  $\Delta b^*$ ,  $\Delta C^*$ ,  $\Delta H^*$  and  $\Delta E^*_{ab}$  of the CCS-II Tiles Measured By Different Spectrophotometers**

Appendix II

**Table 1: Summary For The Repeatability Of The CCS-II GLOSSY Tiles Measured By Gretag Macbeth CE-2180 With Specular Component Excluded Mode**

<i>Tile</i>	$\Delta L^*$	$\Delta a^*$	$\Delta b^*$	$\Delta C^*$	$\Delta H^*$	$\Delta E^*_{ab}$
<i>Pale Grey</i>						
<i>Sample avge</i>	-0.020	0.032	0.112	0.063	0.098	0.118
<i>Mid Grey</i>						
<i>Sample avge</i>	0.022	-0.053	0.120	0.099	0.086	0.133
<i>Diff Grey</i>						
<i>Sample avge</i>	-0.002	-0.027	0.066	0.066	0.027	0.071
<i>Deep Grey</i>						
<i>Sample avge</i>	-0.028	-0.159	0.301	0.322	0.110	0.342
<i>Deep Pink</i>						
<i>Sample avge</i>	0.017	-0.006	0.271	0.036	0.269	0.272
<i>Red</i>						
<i>Sample avge</i>	0.103	-0.141	0.783	0.374	0.702	0.802
<i>Orange</i>						
<i>Sample avge</i>	0.014	-0.071	0.259	0.174	0.205	0.269
<i>Bright Yellow</i>						
<i>Sample avge</i>	0.001	-0.018	0.186	0.186	0.018	0.187
<i>Green</i>						
<i>Sample avge</i>	-0.013	-0.156	0.108	0.188	0.026	0.190
<i>Diff Green</i>						
<i>Sample avge</i>	-0.019	-0.222	0.113	0.249	0.007	0.250
<i>Cyan</i>						
<i>Sample avge</i>	0.016	-0.019	0.125	-0.095	0.083	0.127
<i>Deep Blue</i>						
<i>Sample avge</i>	0.140	-0.678	0.412	-0.709	0.356	0.806
<b><i>Average <math>\Delta E^*_{ab}</math></i></b>						<b><i>0.297</i></b>

Appendix II

**Table 2: Summary For The Repeatability Of The CCS-II GLOSSY Tiles Measured By Gretag Macbeth CE-2180 With Specular Component Included Mode**

<i>Tile</i>	$\Delta L^*$	$\Delta a^*$	$\Delta b^*$	$\Delta C^*$	$\Delta H^*$	$\Delta E^*_{ab}$
<i>Pale Grey</i>						
<i>Sample avge</i>	0.073	-0.076	0.065	0.100	0.001	0.124
<i>Mid Grey</i>						
<i>Sample avge</i>	0.015	-0.047	-0.028	0.033	0.044	0.057
<i>Diff Grey</i>						
<i>Sample avge</i>	0.048	-0.047	-0.029	0.010	0.054	0.073
<i>Deep Grey</i>						
<i>Sample avge</i>	-0.037	-0.017	-0.134	-0.133	0.024	0.140
<i>Deep Pink</i>						
<i>Sample avge</i>	0.015	0.091	0.029	0.095	0.010	0.097
<i>Red</i>						
<i>Sample avge</i>	0.033	0.192	0.026	0.181	0.069	0.197
<i>Orange</i>						
<i>Sample avge</i>	0.105	-0.016	0.250	0.188	0.166	0.272
<i>Bright Yellow</i>						
<i>Sample avge</i>	0.096	-0.098	0.074	0.072	0.099	0.156
<i>Green</i>						
<i>Sample avge</i>	0.064	-0.123	0.045	0.129	0.023	0.146
<i>Diff Green</i>						
<i>Sample avge</i>	0.074	-0.102	-0.051	0.061	0.096	0.136
<i>Cyan</i>						
<i>Sample avge</i>	0.036	-0.095	-0.041	0.084	0.060	0.110
<i>Deep Blue</i>						
<i>Sample avge</i>	-0.025	0.060	-0.135	0.148	0.000	0.150
<b>Average <math>\Delta E^*_{ab}</math></b>						<b>0.140</b>



Appendix II

**Table 3: Summary For The Repeatability Of The CCS-II MATT Tiles Measured By Gretag Macbeth CE-2180 With Specular Component Excluded Mode**

<i>Tile</i>	$\Delta L^*$	$\Delta a^*$	$\Delta b^*$	$\Delta C^*$	$\Delta H^*$	$\Delta E^*_{ab}$
<i>Pale Grey</i>						
<i>Sample avge</i>	0.042	0.054	0.099	0.063	0.094	0.120
<i>Mid Grey</i>						
<i>Sample avge</i>	0.094	0.016	0.144	0.019	0.144	0.173
<i>Diff Grey</i>						
<i>Sample avge</i>	0.135	0.040	0.191	0.100	0.168	0.237
<i>Deep Grey</i>						
<i>Sample avge</i>	0.257	0.047	0.252	-0.256	0.013	0.363
<i>Deep Pink</i>						
<i>Sample avge</i>	0.219	-0.081	0.241	-0.057	0.248	0.336
<i>Red</i>						
<i>Sample avge</i>	0.256	-0.107	0.235	0.000	0.258	0.364
<i>Orange</i>						
<i>Sample avge</i>	0.140	-0.114	0.152	0.040	0.186	0.236
<i>Bright Yellow</i>						
<i>Sample avge</i>	0.079	-0.063	-0.005	-0.006	0.063	0.101
<i>Green</i>						
<i>Sample avge</i>	0.133	0.101	0.081	-0.058	0.116	0.186
<i>Diff Green</i>						
<i>Sample avge</i>	0.114	-0.005	0.099	0.055	0.082	0.151
<i>Cyan</i>						
<i>Sample avge</i>	0.156	0.103	0.196	-0.221	0.014	0.271
<i>Deep Blue</i>						
<i>Sample avge</i>	0.332	-0.099	0.468	-0.474	0.064	0.582
<b>Average <math>\Delta E^*_{ab}</math></b>						<b>0.260</b>

**Table 4: Summary For The Repeatability Of The CCS-II MATT Tiles Measured By Gretag Macbeth CE-2180 With Specular Component Included Mode**

<i>Tile</i>	$\Delta L^*$	$\Delta a^*$	$\Delta b^*$	$\Delta C^*$	$\Delta H^*$	$\Delta E^*_{ab}$
<i>Pale Grey</i>						
<i>Sample avge</i>	0.047	-0.087	0.073	0.113	0.011	0.123
<i>Mid Grey</i>						
<i>Sample avge</i>	0.072	-0.052	0.028	0.047	0.036	0.093
<i>Diff Grey</i>						
<i>Sample avge</i>	0.069	-0.053	0.061	0.079	0.017	0.106
<i>Deep Grey</i>						
<i>Sample avge</i>	-0.008	-0.069	0.022	-0.014	0.071	0.073
<i>Deep Pink</i>						
<i>Sample avge</i>	0.020	-0.039	0.070	-0.032	0.073	0.083
<i>Red</i>						
<i>Sample avge</i>	0.068	0.071	0.035	0.080	0.000	0.104
<i>Orange</i>						
<i>Sample avge</i>	0.125	-0.024	0.189	0.126	0.143	0.228
<i>Bright Yellow</i>						
<i>Sample avge</i>	0.052	-0.104	-0.007	-0.010	0.104	0.116
<i>Green</i>						
<i>Sample avge</i>	0.057	-0.070	0.004	0.065	0.026	0.090
<i>Diff Green</i>						
<i>Sample avge</i>	0.040	-0.134	-0.019	0.105	0.085	0.141
<i>Cyan</i>						
<i>Sample avge</i>	0.058	-0.151	0.068	0.019	0.165	0.175
<i>Deep Blue</i>						
<i>Sample avge</i>	0.003	-0.080	-0.015	-0.015	0.080	0.081
<i>Average <math>\Delta E^*_{ab}</math></i>						<i>0.118</i>

Appendix II

**Table 5: Summary For The Repeatability Of The CCS-II GLOSSY Tiles Measured By DataColor SF-600 With Specular Component Excluded Mode**

<i>Tile</i>	$\Delta L^*$	$\Delta a^*$	$\Delta b^*$	$\Delta C^*$	$\Delta H^*$	$\Delta E^*_{ab}$
<i>Pale Grey</i>						
<i>Sample avge</i>	0.011	0.009	-0.029	-0.019	0.031	0.038
<i>Mid Grey</i>						
<i>Sample avge</i>	0.022	0.013	-0.037	-0.018	0.037	0.047
<i>Diff Grey</i>						
<i>Sample avge</i>	0.012	0.018	-0.047	-0.045	0.025	0.053
<i>Deep Grey</i>						
<i>Sample avge</i>	0.055	0.018	-0.071	-0.073	0.041	0.100
<i>Deep Pink</i>						
<i>Sample avge</i>	0.030	-0.008	-0.072	-0.017	0.075	0.083
<i>Red</i>						
<i>Sample avge</i>	0.050	-0.030	-0.239	-0.170	0.182	0.254
<i>Orange</i>						
<i>Sample avge</i>	0.015	-0.016	-0.104	-0.095	0.065	0.116
<i>Bright Yellow</i>						
<i>Sample avge</i>	0.010	-0.014	-0.118	-0.118	0.040	0.125
<i>Green</i>						
<i>Sample avge</i>	0.017	0.009	-0.029	-0.021	0.042	0.050
<i>Diff Green</i>						
<i>Sample avge</i>	0.028	0.001	-0.029	-0.016	0.049	0.059
<i>Cyan</i>						
<i>Sample avge</i>	0.026	0.020	-0.014	0.001	0.033	0.042
<i>Deep Blue</i>						
<i>Sample avge</i>	0.188	-0.116	0.095	-0.142	0.084	0.250
<b>Average <math>\Delta E^*_{ab}</math></b>						<b>0.101</b>

Appendix II

**Table 6: Summary For The Repeatability Of The CCS-II GLOSSY Tiles Measured By DataColor SF-600 With Specular Component Included Mode**

<i>Tile</i>	$\Delta L^*$	$\Delta a^*$	$\Delta b^*$	$\Delta C^*$	$\Delta H^*$	$\Delta E^*_{ab}$
<i>Pale Grey</i>						
<i>Sample avge</i>	0.012	0.003	-0.027	-0.012	0.031	0.035
<i>Mid Grey</i>						
<i>Sample avge</i>	0.011	0.005	-0.029	-0.005	0.033	0.035
<i>Diff Grey</i>						
<i>Sample avge</i>	0.012	0.000	-0.039	-0.028	0.032	0.044
<i>Deep Grey</i>						
<i>Sample avge</i>	0.027	-0.006	-0.027	-0.027	0.020	0.043
<i>Deep Pink</i>						
<i>Sample avge</i>	0.005	0.018	-0.027	0.014	0.038	0.041
<i>Red</i>						
<i>Sample avge</i>	0.031	0.022	0.005	0.022	0.035	0.052
<i>Orange</i>						
<i>Sample avge</i>	0.019	-0.034	-0.018	-0.035	0.045	0.060
<i>Bright Yellow</i>						
<i>Sample avge</i>	0.011	-0.029	-0.062	-0.062	0.041	0.075
<i>Green</i>						
<i>Sample avge</i>	0.022	-0.023	-0.020	0.012	0.041	0.048
<i>Diff Green</i>						
<i>Sample avge</i>	0.027	-0.013	-0.023	0.000	0.040	0.048
<i>Cyan</i>						
<i>Sample avge</i>	0.021	-0.002	-0.013	0.012	0.022	0.033
<i>Deep Blue</i>						
<i>Sample avge</i>	0.021	0.013	-0.033	0.035	0.025	0.048
<b><i>Average <math>\Delta E^*_{ab}</math></i></b>						<b><i>0.047</i></b>

Appendix II

**Table 7: Summary For The Repeatability Of The CCS-II MATT Tiles Measured By DataColor SF-600 With Specular Component Excluded Mode**

<i>Tile</i>	$\Delta L^*$	$\Delta a^*$	$\Delta b^*$	$\Delta C^*$	$\Delta H^*$	$\Delta E^*_{ab}$
<i>Pale Grey</i>						
<i>Sample avge</i>	-0.006	0.019	-0.032	-0.034	0.018	0.039
<i>Mid Grey</i>						
<i>Sample avge</i>	0.010	0.006	-0.035	0.014	0.035	0.039
<i>Diff Grey</i>						
<i>Sample avge</i>	0.007	0.014	-0.029	-0.029	0.018	0.035
<i>Deep Grey</i>						
<i>Sample avge</i>	0.025	0.009	-0.033	0.031	0.030	0.050
<i>Deep Pink</i>						
<i>Sample avge</i>	0.033	0.001	-0.050	-0.004	0.054	0.063
<i>Red</i>						
<i>Sample avge</i>	0.018	-0.001	-0.041	-0.017	0.051	0.057
<i>Orange</i>						
<i>Sample avge</i>	0.010	-0.034	-0.058	-0.066	0.046	0.081
<i>Bright Yellow</i>						
<i>Sample avge</i>	0.005	-0.019	-0.019	-0.020	0.056	0.060
<i>Green</i>						
<i>Sample avge</i>	0.023	0.009	-0.042	-0.026	0.045	0.057
<i>Diff Green</i>						
<i>Sample avge</i>	0.002	0.002	-0.030	-0.017	0.038	0.042
<i>Cyan</i>						
<i>Sample avge</i>	0.038	0.012	0.010	-0.015	0.019	0.045
<i>Deep Blue</i>						
<i>Sample avge</i>	0.025	0.018	-0.033	0.038	0.025	0.052
<b><i>Average <math>\Delta E^*_{ab}</math></i></b>						<b><i>0.052</i></b>

**Table 8: Summary For The Repeatability Of The CCS-II MATT Tiles Measured By DataColor SF-600 With Specular Component Included Mode**

<i>Tile</i>	$\Delta L^*$	$\Delta a^*$	$\Delta b^*$	$\Delta C^*$	$\Delta H^*$	$\Delta E^*_{ab}$
<i>Pale Grey</i>						
<i>Sample avge</i>	-0.005	0.002	-0.014	-0.010	0.021	0.024
<i>Mid Grey</i>						
<i>Sample avge</i>	0.005	0.001	-0.024	0.009	0.026	0.028
<i>Diff Grey</i>						
<i>Sample avge</i>	0.003	0.013	-0.035	-0.032	0.022	0.039
<i>Deep Grey</i>						
<i>Sample avge</i>	0.012	0.018	-0.032	0.029	0.026	0.041
<i>Deep Pink</i>						
<i>Sample avge</i>	0.022	0.021	-0.041	0.017	0.046	0.054
<i>Red</i>						
<i>Sample avge</i>	0.021	0.035	-0.003	0.031	0.035	0.051
<i>Orange</i>						
<i>Sample avge</i>	0.028	-0.034	-0.018	-0.035	0.040	0.060
<i>Bright Yellow</i>						
<i>Sample avge</i>	-0.007	-0.040	-0.034	-0.035	0.056	0.066
<i>Green</i>						
<i>Sample avge</i>	0.024	-0.001	-0.038	-0.015	0.045	0.053
<i>Diff Green</i>						
<i>Sample avge</i>	0.013	-0.031	-0.004	0.025	0.040	0.049
<i>Cyan</i>						
<i>Sample avge</i>	0.021	-0.006	0.007	-0.002	0.024	0.032
<i>Deep Blue</i>						
<i>Sample avge</i>	0.012	0.031	-0.035	0.044	0.020	0.050
<b><i>Average <math>\Delta E^*_{ab}</math></i></b>						<b><i>0.046</i></b>

**Table 9: Summary For The Repeatability Of The CCS-II GLOSSY Tiles Measured By Gretag Macbeth CE-7000A With Specular Component Excluded Mode**

<i>Tile</i>	$\Delta L^*$	$\Delta a^*$	$\Delta b^*$	$\Delta C^*$	$\Delta H^*$	$\Delta E^*_{ab}$
<i>Pale Grey</i>						
<i>Sample avge</i>	-0.015	-0.002	0.000	0.001	0.019	0.024
<i>Mid Grey</i>						
<i>Sample avge</i>	0.004	0.007	-0.006	-0.009	0.017	0.020
<i>Diff Grey</i>						
<i>Sample avge</i>	0.000	0.003	-0.003	-0.005	0.019	0.020
<i>Deep Grey</i>						
<i>Sample avge</i>	0.062	0.025	-0.029	-0.035	0.043	0.083
<i>Deep Pink</i>						
<i>Sample avge</i>	0.020	-0.012	-0.029	-0.017	0.038	0.046
<i>Red</i>						
<i>Sample avge</i>	0.050	-0.061	-0.320	-0.246	0.217	0.332
<i>Orange</i>						
<i>Sample avge</i>	0.002	-0.054	-0.096	-0.110	0.048	0.120
<i>Bright Yellow</i>						
<i>Sample avge</i>	-0.031	-0.025	-0.144	-0.144	0.048	0.155
<i>Green</i>						
<i>Sample avge</i>	0.006	0.021	-0.008	-0.023	0.041	0.047
<i>Diff Green</i>						
<i>Sample avge</i>	-0.005	0.019	-0.027	-0.030	0.045	0.054
<i>Cyan</i>						
<i>Sample avge</i>	-0.002	0.022	0.027	-0.035	0.041	0.054
<i>Deep Blue</i>						
<i>Sample avge</i>	0.181	-0.254	0.228	-0.328	0.105	0.389
<i>Average <math>\Delta E^*_{ab}</math></i>						<i>0.098</i>

**Table 10: Summary For The Repeatability Of The CCS-II GLOSSY Tiles Measured By Gretag Macbeth CE-7000A With Specular Component Included Mode**

<i>Tile</i>	$\Delta L^*$	$\Delta a^*$	$\Delta b^*$	$\Delta C^*$	$\Delta H^*$	$\Delta E^*_{ab}$
<i>Pale Grey</i>						
<i>Sample avge</i>	-0.008	-0.003	0.004	0.005	0.015	0.018
<i>Mid Grey</i>						
<i>Sample avge</i>	0.006	-0.002	-0.004	0.000	0.017	0.018
<i>Diff Grey</i>						
<i>Sample avge</i>	0.002	-0.001	-0.006	-0.004	0.021	0.021
<i>Deep Grey</i>						
<i>Sample avge</i>	0.027	-0.010	-0.010	-0.005	0.026	0.038
<i>Deep Pink</i>						
<i>Sample avge</i>	0.000	-0.005	-0.005	-0.005	0.030	0.030
<i>Red</i>						
<i>Sample avge</i>	0.018	-0.018	-0.014	-0.023	0.034	0.045
<i>Orange</i>						
<i>Sample avge</i>	-0.001	-0.054	-0.043	-0.067	0.044	0.080
<i>Bright Yellow</i>						
<i>Sample avge</i>	-0.021	-0.020	-0.091	-0.091	0.041	0.102
<i>Green</i>						
<i>Sample avge</i>	0.014	0.002	-0.011	-0.007	0.029	0.033
<i>Diff Green</i>						
<i>Sample avge</i>	0.018	-0.004	-0.004	0.002	0.030	0.035
<i>Cyan</i>						
<i>Sample avge</i>	0.019	-0.001	0.021	-0.018	0.034	0.043
<i>Deep Blue</i>						
<i>Sample avge</i>	0.067	-0.036	0.059	-0.068	0.030	0.100
<b>Average <math>\Delta E^*_{ab}</math></b>						<b>0.047</b>



**Table II: Summary For The Repeatability Of The CCS-II MATT Tiles Measured By Gretag Macbeth CE-7000A With Specular Component Excluded Mode**

<i>Tile</i>	$\Delta L^*$	$\Delta a^*$	$\Delta b^*$	$\Delta C^*$	$\Delta H^*$	$\Delta E^*_{ab}$
<i>Pale Grey</i>						
<i>Sample avge</i>	-0.015	-0.002	0.000	0.001	0.019	0.024
<i>Mid Grey</i>						
<i>Sample avge</i>	0.011	-0.002	-0.006	0.001	0.020	0.023
<i>Diff Grey</i>						
<i>Sample avge</i>	0.024	-0.006	-0.005	0.002	0.020	0.031
<i>Deep Grey</i>						
<i>Sample avge</i>	0.039	-0.002	0.003	-0.002	0.022	0.045
<i>Deep Pink</i>						
<i>Sample avge</i>	0.035	-0.020	-0.013	-0.021	0.023	0.047
<i>Red</i>						
<i>Sample avge</i>	0.045	-0.002	-0.012	-0.007	0.033	0.056
<i>Orange</i>						
<i>Sample avge</i>	-0.006	-0.033	-0.098	-0.096	0.051	0.109
<i>Bright Yellow</i>						
<i>Sample avge</i>	0.008	-0.023	-0.026	-0.027	0.044	0.052
<i>Green</i>						
<i>Sample avge</i>	0.019	0.025	-0.020	-0.031	0.030	0.047
<i>Diff Green</i>						
<i>Sample avge</i>	0.003	-0.015	-0.016	0.005	0.036	0.036
<i>Cyan</i>						
<i>Sample avge</i>	0.018	-0.006	0.031	-0.024	0.040	0.050
<i>Deep Blue</i>						
<i>Sample avge</i>	0.057	-0.015	0.021	-0.025	0.027	0.068
<b><i>Average <math>\Delta E^*_{ab}</math></i></b>						<b><i>0.049</i></b>

Appendix II

**Table 12: Summary For The Repeatability Of The CCS-II MATT Tiles Measured By Gretag Macbeth CE-7000A With Specular Component Included Mode**

<i>Tile</i>	$\Delta L^*$	$\Delta a^*$	$\Delta b^*$	$\Delta C^*$	$\Delta H^*$	$\Delta E^*_{ab}$
<i>Pale Grey</i>						
<i>Sample avge*</i>	-0.020	-0.004	0.018	0.017	0.015	0.030
<i>Mid Grey</i>						
<i>Sample avge</i>	-0.007	-0.006	0.003	0.007	0.016	0.019
<i>Diff Grey</i>						
<i>Sample avge</i>	-0.002	0.002	0.020	0.011	0.022	0.025
<i>Deep Grey</i>						
<i>Sample avge</i>	0.030	0.006	-0.005	0.004	0.018	0.035
<i>Deep Pink</i>						
<i>Sample avge</i>	0.025	-0.006	-0.016	-0.008	0.026	0.037
<i>Red</i>						
<i>Sample avge</i>	0.038	-0.023	-0.039	-0.037	0.043	0.068
<i>Orange</i>						
<i>Sample avge</i>	0.037	-0.025	-0.013	-0.026	0.049	0.067
<i>Bright Yellow</i>						
<i>Sample avge</i>	0.031	-0.017	-0.009	-0.009	0.045	0.055
<i>Green</i>						
<i>Sample avge</i>	0.030	0.021	-0.023	-0.029	0.034	0.054
<i>Diff Green</i>						
<i>Sample avge</i>	0.017	-0.002	-0.010	-0.004	0.033	0.037
<i>Cyan</i>						
<i>Sample avge</i>	0.026	0.003	0.016	-0.015	0.036	0.047
<i>Deep Blue</i>						
<i>Sample avge</i>	0.050	-0.001	0.016	-0.015	0.023	0.057
<b>Average <math>\Delta E^*_{ab}</math></b>						<b>0.044</b>

**APPENDIX III:**  
**Summary For The Inter-Instrumental Agreement in terms of  $\Delta L^*$ ,  $\Delta a^*$ ,  $\Delta b^*$ ,  $\Delta C^*$ ,  $\Delta H^*$  and  $\Delta E^*_{ab}$  of the CCS-II Tiles Measured By Different Spectrophotometers**

Appendix III

**Table 1: Summary For The Inter-Instrumental Agreement Of The CCS-II GLOSSY Tiles Measured Under The Condition Of Specular Component Excluded Mode Between SF-600 And CE-7000A**

<i>Tile</i>	$\Delta L^*$	$\Delta a^*$	$\Delta b^*$	$\Delta C^*$	$\Delta H^*$	$\Delta E^*_{ab}$
<i>Pale Grey</i>						
<i>Sample avge</i>	-0.641	0.009	0.253	0.134	0.217	0.690
<i>Mid Grey</i>						
<i>Sample avge</i>	-0.448	0.012	0.099	0.014	0.099	0.459
<i>Diff Grey</i>						
<i>Sample avge</i>	-0.483	-0.031	0.101	0.094	0.054	0.495
<i>Deep Grey</i>						
<i>Sample avge</i>	-0.177	-0.037	0.067	0.075	0.038	0.196
<i>Deep Pink</i>						
<i>Sample avge</i>	-0.065	-0.027	0.752	0.087	0.748	0.756
<i>Red</i>						
<i>Sample avge</i>	0.622	0.088	0.144	0.158	0.103	0.650
<i>Orange</i>						
<i>Sample avge</i>	0.049	-0.991	0.327	-0.288	1.009	1.050
<i>Bright Yellow</i>						
<i>Sample avge</i>	-0.342	-0.551	-1.282	-1.289	0.535	1.437
<i>Green</i>						
<i>Sample avge</i>	-0.581	0.277	-0.916	-0.655	0.698	1.120
<i>Diff Green</i>						
<i>Sample avge</i>	-0.535	-0.226	-0.928	-0.666	0.685	1.095
<i>Cyan</i>						
<i>Sample avge</i>	-0.782	0.922	-0.233	-0.288	0.907	1.232
<i>Deep Blue</i>						
<i>Sample avge</i>	-0.196	-0.531	0.853	-1.005	0.091	1.028
<i>Average <math>\Delta E^*_{ab}</math></i>						<b>0.851</b>

Appendix III

**Table 2: Summary For The Inter-Instrumental Agreement Of The CCS-II GLOSSY Tiles Measured Under The Condition Of Specular Component Included Mode Between SF-600 And CE-7000A**

<i>Tile</i>	$\Delta L^*$	$\Delta a^*$	$\Delta b^*$	$\Delta C^*$	$\Delta H^*$	$\Delta E^*_{ab}$
<i>Pale Grey</i>						
<i>Sample avge</i>	-0.389	0.052	0.171	0.040	0.174	0.428
<i>Mid Grey</i>						
<i>Sample avge</i>	-0.242	-0.004	0.117	0.025	0.115	0.269
<i>Diff Grey</i>						
<i>Sample avge</i>	-0.263	-0.049	0.119	0.119	0.050	0.293
<i>Deep Grey</i>						
<i>Sample avge</i>	-0.051	-0.102	0.183	0.192	0.087	0.217
<i>Deep Pink</i>						
<i>Sample avge</i>	0.060	0.072	0.730	0.175	0.713	0.737
<i>Red</i>						
<i>Sample avge</i>	0.387	0.671	0.998	1.059	0.569	1.263
<i>Orange</i>						
<i>Sample avge</i>	0.223	-0.865	0.612	-0.045	1.060	1.084
<i>Bright Yellow</i>						
<i>Sample avge</i>	-0.108	-0.579	-0.719	-0.727	0.570	0.930
<i>Green</i>						
<i>Sample avge</i>	-0.362	0.162	-0.666	-0.437	0.528	0.775
<i>Diff Green</i>						
<i>Sample avge</i>	-0.330	0.119	-0.661	-0.434	0.514	0.749
<i>Cyan</i>						
<i>Sample avge</i>	-0.547	0.806	-0.243	-0.199	0.818	1.004
<i>Deep Blue</i>						
<i>Sample avge</i>	-0.068	-0.374	0.759	-0.845	0.046	0.849
<b>Average <math>\Delta E^*_{ab}</math></b>						<b>0.717</b>

Appendix III

**Table 3: Summary For The Inter-Instrumental Agreement Of The CCS-II MATT Tiles Measured Under The Condition Of Specular Component Excluded Mode Between SF-600 And CE-7000A**

<i>Tile</i>	$\Delta L^*$	$\Delta a^*$	$\Delta b^*$	$\Delta C^*$	$\Delta H^*$	$\Delta E^*_{ab}$
<i>Pale Grey</i>						
<i>Sample avge</i>	-0.534	0.019	0.251	0.176	0.179	0.590
<i>Mid Grey</i>						
<i>Sample avge</i>	-0.382	-0.031	0.175	0.018	0.178	0.422
<i>Diff Grey</i>						
<i>Sample avge</i>	-0.383	0.005	0.093	0.057	0.078	0.395
<i>Deep Grey</i>						
<i>Sample avge</i>	-0.129	-0.058	0.114	-0.099	0.084	0.183
<i>Deep Pink</i>						
<i>Sample avge</i>	-0.036	0.009	0.632	0.073	0.628	0.633
<i>Red</i>						
<i>Sample avge</i>	0.204	0.422	0.536	0.605	0.317	0.713
<i>Orange</i>						
<i>Sample avge</i>	0.149	-0.703	0.496	-0.087	0.857	0.874
<i>Bright Yellow</i>						
<i>Sample avge</i>	-0.151	-0.498	-0.538	-0.547	0.489	0.749
<i>Green</i>						
<i>Sample avge</i>	-0.476	0.303	-0.658	-0.551	0.471	0.867
<i>Diff Green</i>						
<i>Sample avge</i>	-0.452	0.169	-0.623	-0.458	0.455	0.788
<i>Cyan</i>						
<i>Sample avge</i>	-0.551	0.705	-0.118	-0.259	0.667	0.903
<i>Deep Blue</i>						
<i>Sample avge</i>	-0.074	-0.410	0.786	-0.880	0.111	0.890
<b><i>Average <math>\Delta E^*_{ab}</math></i></b>						<b><i>0.667</i></b>

**Table 4: Summary For The Inter-Instrumental Agreement Of The CCS-II MATT Tiles Measured Under The Condition Of Specular Component Included Mode Between SF-600 And CE-7000A**

<i>Tile</i>	$\Delta L^*$	$\Delta a^*$	$\Delta b^*$	$\Delta C^*$	$\Delta H^*$	$\Delta E^*_{ab}$
<i>Pale Grey</i>						
<i>Sample avge</i>	-0.326	0.057	0.145	0.069	0.139	0.361
<i>Mid Grey</i>						
<i>Sample avge</i>	-0.157	-0.015	0.090	0.002	0.092	0.182
<i>Diff Grey</i>						
<i>Sample avge</i>	-0.164	0.024	0.008	-0.013	0.022	0.166
<i>Deep Grey</i>						
<i>Sample avge</i>	-0.019	-0.046	0.052	-0.042	0.058	0.074
<i>Deep Pink</i>						
<i>Sample avge</i>	0.134	0.119	0.575	0.176	0.561	0.603
<i>Red</i>						
<i>Sample avge</i>	0.353	0.578	0.577	0.763	0.292	0.890
<i>Orange</i>						
<i>Sample avge</i>	0.353	-0.676	0.595	0.005	0.901	0.968
<i>Bright Yellow</i>						
<i>Sample avge</i>	0.045	-0.566	-0.516	-0.527	0.557	0.768
<i>Green</i>						
<i>Sample avge</i>	-0.258	0.201	-0.687	-0.470	0.541	0.762
<i>Diff Green</i>						
<i>Sample avge</i>	-0.228	0.049	-0.609	-0.346	0.503	0.652
<i>Cyan</i>						
<i>Sample avge</i>	-0.359	0.685	-0.283	-0.105	0.734	0.824
<i>Deep Blue</i>						
<i>Sample avge</i>	-0.021	-0.329	0.592	-0.669	0.102	0.677
<b>Average <math>\Delta E^*_{ab}</math></b>						<b>0.577</b>

## Appendix III

**Table 5: Summary For The Inter-Instrumental Agreement Of The CCS-II GLOSSY Tiles Measured Under The Condition Of Specular Component Excluded Mode Between CE-2180 And CE-7000A**

<i>Tile</i>	$\Delta L^*$	$\Delta a^*$	$\Delta b^*$	$\Delta C^*$	$\Delta H^*$	$\Delta E^*_{ab}$
<i>Pale Grey</i>						
<i>Sample avge</i>	-0.399	0.475	-0.243	-0.236	-0.478	0.666
<i>Mid Grey</i>						
<i>Sample avge</i>	0.224	-0.299	0.6	-0.355	-0.569	0.707
<i>Diff Grey</i>						
<i>Sample avge</i>	0.436	0.051	-0.114	0.124	-0.018	0.453
<i>Deep Grey</i>						
<i>Sample avge</i>	0.126	0.173	-0.106	-0.139	-0.148	0.239
<i>Deep Pink</i>						
<i>Sample avge</i>	-0.105	-0.345	-0.600	-0.434	-0.539	0.700
<i>Red</i>						
<i>Sample avge</i>	-0.035	0.631	0.341	-0.371	-0.614	0.719
<i>Orange</i>						
<i>Sample avge</i>	-0.011	0.104	-0.058	-0.114	-0.034	0.119
<i>Bright Yellow</i>						
<i>Sample avge</i>	-0.038	0.550	0.412	-0.311	-0.613	0.689
<i>Green</i>						
<i>Sample avge</i>	-0.101	0.073	-0.038	-0.082	0.010	0.130
<i>Diff Green</i>						
<i>Sample avge</i>	-0.267	-0.048	-0.742	-0.642	-0.376	0.790
<i>Cyan</i>						
<i>Sample avge</i>	-0.110	0.067	-0.056	-0.087	-0.006	0.140
<i>Deep Blue</i>						
<i>Sample avge</i>	-0.374	-0.496	-0.949	-0.976	-0.440	1.134
<b>Average <math>\Delta E^*_{ab}</math></b>						<b>0.541</b>



**Table 6: Summary For The Inter-Instrumental Agreement Of The CCS-II GLOSSY Tiles Measured Under The Condition Of Specular Component Included Mode Between CE-2180 And CE-7000A**

<i>Tile</i>	$\Delta L^*$	$\Delta a^*$	$\Delta b^*$	$\Delta C^*$	$\Delta H^*$	$\Delta E^*_{ab}$
<i>Pale Grey</i>						
<i>Sample avge</i>	-0.492	0.493	-0.384	-0.377	-0.498	0.795
<i>Mid Grey</i>						
<i>Sample avge</i>	0.190	-0.331	0.655	-0.399	-0.615	0.758
<i>Diff Grey</i>						
<i>Sample avge</i>	0.277	0.023	0.037	-0.024	0.036	0.280
<i>Deep Grey</i>						
<i>Sample avge</i>	0.051	0.054	0.066	0.060	-0.061	0.100
<i>Deep Pink</i>						
<i>Sample avge</i>	-0.187	-0.477	-0.511	-0.547	-0.434	0.723
<i>Red</i>						
<i>Sample avge</i>	-0.086	0.529	0.339	-0.288	-0.558	0.634
<i>Orange</i>						
<i>Sample avge</i>	-0.075	0.085	0.010	-0.051	-0.069	0.114
<i>Bright Yellow</i>						
<i>Sample avge</i>	-0.085	0.523	0.336	-0.323	-0.531	0.628
<i>Green</i>						
<i>Sample avge</i>	-0.138	0.027	0.026	-0.016	-0.034	0.143
<i>Diff Green</i>						
<i>Sample avge</i>	-0.448	-0.023	-0.919	-0.744	-0.541	1.023
<i>Cyan</i>						
<i>Sample avge</i>	-0.188	-0.005	-0.052	-0.027	0.045	0.195
<i>Deep Blue</i>						
<i>Sample avge</i>	-0.244	-1.057	-0.689	-1.257	-0.110	1.285
<b>Average <math>\Delta E^*_{ab}</math></b>						<b>0.557</b>

**Table 7: Summary For The Inter-Instrumental Agreement Of The CCS-II MATT Tiles Measured Under The Condition Of Specular Component Excluded Mode Between CE-2180 And CE-7000A**

<i>Tile</i>	$\Delta L^*$	$\Delta a^*$	$\Delta b^*$	$\Delta C^*$	$\Delta H^*$	$\Delta E^*_{ab}$
<i>Pale Grey</i>						
<i>Sample avge</i>	-0.719	0.528	-0.257	-0.246	-0.533	0.928
<i>Mid Grey</i>						
<i>Sample avge</i>	-0.237	-0.255	0.407	-0.222	-0.426	0.535
<i>Diff Grey</i>						
<i>Sample avge</i>	-0.449	0.260	-0.555	0.611	0.049	0.760
<i>Deep Grey</i>						
<i>Sample avge</i>	-0.410	0.022	-0.174	0.164	0.061	0.446
<i>Deep Pink</i>						
<i>Sample avge</i>	-0.486	-0.181	-0.490	-0.231	-0.468	0.713
<i>Red</i>						
<i>Sample avge</i>	-0.543	0.389	0.125	-0.275	-0.302	0.680
<i>Orange</i>						
<i>Sample avge</i>	-0.407	0.048	-0.062	-0.077	0.015	0.414
<i>Bright Yellow</i>						
<i>Sample avge</i>	-0.355	0.266	0.263	-0.132	-0.350	0.516
<i>Green</i>						
<i>Sample avge</i>	-0.433	0.011	-0.101	-0.024	0.099	0.444
<i>Diff Green</i>						
<i>Sample avge</i>	-0.695	-0.032	-0.492	-0.393	-0.296	0.852
<i>Cyan</i>						
<i>Sample avge</i>	-0.437	0.056	-0.110	-0.122	0.013	0.454
<i>Deep Blue</i>						
<i>Sample avge</i>	-0.494	-0.331	-0.327	-0.437	-0.162	0.679
<b>Average <math>\Delta E^*_{ab}</math></b>						<b>0.618</b>

**Table 8: Summary For The Inter-Instrumental Agreement Of The CCS-II MATT Tiles Measured Under The Condition Of Specular Component Included Mode Between CE-2180 And CE-7000A**

<i>Tile</i>	$\Delta L^*$	$\Delta a^*$	$\Delta b^*$	$\Delta C^*$	$\Delta H^*$	$\Delta E^*_{ab}$
<i>Pale Grey</i>						
<i>Sample avge</i>	-0.717	0.522	-0.347	-0.336	-0.529	0.952
<i>Mid Grey</i>						
<i>Sample avge</i>	-0.199	-0.190	0.506	-0.341	-0.419	0.576
<i>Diff Grey</i>						
<i>Sample avge</i>	-0.234	0.225	-0.157	0.226	0.156	0.361
<i>Deep Grey</i>						
<i>Sample avge</i>	-0.316	0.132	-0.083	0.061	0.144	0.352
<i>Deep Pink</i>						
<i>Sample avge</i>	-0.479	-0.300	-0.443	-0.344	-0.409	0.718
<i>Red</i>						
<i>Sample avge</i>	-0.523	0.516	0.173	-0.362	-0.407	0.755
<i>Orange</i>						
<i>Sample avge</i>	-0.428	0.086	-0.006	-0.069	-0.052	0.436
<i>Bright Yellow</i>						
<i>Sample avge</i>	-0.303	0.336	0.317	-0.173	-0.428	0.552
<i>Green</i>						
<i>Sample avge</i>	-0.494	0.062	-0.053	-0.057	0.059	0.500
<i>Diff Green</i>						
<i>Sample avge</i>	-0.739	-0.016	-0.668	-0.516	-0.424	0.997
<i>Cyan</i>						
<i>Sample avge</i>	-0.417	-0.014	-0.095	-0.065	0.071	0.428
<i>Deep Blue</i>						
<i>Sample avge</i>	-0.542	-0.671	-0.439	-0.792	-0.124	0.968
<i>Average <math>\Delta E^*_{ab}</math></i>						<i>0.633</i>

**APPENDIX IV:**  
**The Repeatability of CCS-II Tiles Measured Among The Spectrophotometers Over 60 Weeks**

**Table 1: The Repeatability of GLOSSY Tiles Measured Under Specular Component Excluded Mode By CE-2180 Over 60 Weeks**

Week	Pale Grey	Middel Grey	Diff. Grey	Deep Grey	Deep Pink	Red	Orange	Bright Yellow	Green	Diff. Green	Cyan	Deep Blue
1	0.051	0.039	0.045	0.207	0.174	0.735	0.269	0.183	0.042	0.179	0.049	0.734
2	0.151	0.080	0.026	0.113	0.213	1.290	0.764	0.244	0.125	0.272	0.124	0.850
3	0.073	0.075	0.072	0.169	0.081	0.506	0.123	0.144	0.069	0.239	0.093	0.316
4	0.071	0.059	0.059	0.341	0.130	0.588	0.099	0.134	0.190	0.109	0.036	0.624
5	0.119	0.133	0.071	0.280	0.272	0.802	0.269	0.187	0.213	0.250	0.127	0.805
6	0.067	0.080	0.090	1.033	0.157	0.990	0.189	0.202	0.720	0.368	0.137	0.665
7	0.041	0.258	0.220	0.099	0.735	0.368	0.560	1.481	0.147	0.923	0.421	0.805
8	0.043	0.412	0.039	1.517	0.152	0.513	0.282	0.209	1.131	1.273	0.096	0.414
9	0.115	0.082	0.415	0.119	0.169	0.077	1.198	1.687	0.560	0.138	0.732	0.409
10	0.036	0.012	0.115	0.204	0.113	0.491	0.082	0.094	0.058	0.184	0.074	0.376
11	0.074	0.061	0.054	0.308	0.071	0.402	0.104	0.116	0.137	0.283	0.116	0.241
12	0.093	0.085	0.065	0.283	0.159	1.003	0.171	0.273	0.153	0.236	0.085	1.501
13	0.144	0.200	0.219	0.579	0.193	0.793	0.269	0.199	0.366	0.551	0.305	0.852
14	0.074	0.117	0.110	0.359	0.200	1.446	0.388	0.388	0.248	0.347	0.143	0.699
15	0.018	0.039	0.030	0.161	0.131	0.771	0.202	0.043	0.113	0.157	0.025	0.785
16	0.105	0.097	0.081	0.386	0.063	0.619	0.132	0.116	0.242	0.360	0.188	1.613
17	0.012	0.087	0.063	0.280	0.137	1.005	0.284	0.452	0.323	0.412	0.119	0.382
18	0.030	0.054	0.079	0.060	0.264	1.469	0.386	0.059	0.080	0.110	0.092	0.122
19	0.054	0.132	0.042	0.142	0.055	0.226	0.050	0.238	0.077	0.165	0.115	0.142

Appendix IV

20	0.039	0.021	0.021	0.021	0.200	0.226	0.836	0.315	0.209	0.170	0.211	0.095	0.376
21	0.018	0.101	0.039	0.180	0.195	0.632	0.262	0.039	0.132	0.239	0.065	0.376	
22	0.107	0.074	0.063	0.107	0.109	0.542	0.191	0.119	0.091	0.164	0.127	0.624	
23	0.073	0.075	0.072	0.119	0.098	0.342	0.113	0.134	0.720	0.272	0.124	0.805	
24	0.071	0.059	0.059	0.204	0.200	0.588	0.269	0.187	0.147	0.239	0.093	0.665	
25	0.119	0.133	0.071	0.308	0.131	0.802	0.368	0.202	1.131	0.109	0.036	0.805	
26	0.067	0.080	0.090	0.283	0.063	0.990	0.123	1.481	0.077	0.250	0.127	0.414	
27	0.041	0.258	0.220	0.579	0.098	0.668	0.099	0.209	0.058	0.368	0.137	0.409	
28	0.043	0.412	0.039	0.359	0.264	0.513	0.269	1.687	0.137	0.923	0.421	0.376	
29	0.115	0.082	0.415	0.161	0.055	0.137	0.189	0.094	0.153	1.273	0.096	0.241	
30	0.036	0.012	0.115	0.386	0.226	0.491	0.368	0.116	0.366	0.138	0.732	1.501	
31	0.074	0.061	0.054	0.280	0.195	0.402	0.123	0.273	0.248	0.184	0.074	0.852	
32	0.093	0.085	0.065	0.060	0.109	1.003	0.099	0.199	0.113	0.283	0.116	0.699	
33	0.144	0.039	0.219	0.142	0.098	0.793	0.269	0.388	0.242	0.236	0.085	0.785	
34	0.030	0.080	0.110	0.200	0.174	1.446	0.189	0.043	0.323	0.283	0.093	1.613	
35	0.054	0.075	0.030	0.180	0.213	0.226	0.560	0.116	0.080	0.236	0.036	0.376	
36	0.039	0.059	0.081	0.107	0.081	0.836	0.282	0.183	0.042	0.551	0.127	0.241	
37	0.018	0.133	0.045	0.119	0.130	0.632	1.168	0.244	0.125	0.347	0.137	1.501	
38	0.107	0.080	0.026	0.204	0.272	0.542	0.082	0.144	0.069	0.157	0.421	0.852	
39	0.073	0.258	0.072	0.308	0.157	0.342	0.202	0.134	0.190	0.360	0.096	0.699	
40	0.071	0.412	0.059	0.283	0.735	0.588	0.132	0.187	0.213	0.412	0.732	0.785	

Appendix IV

41	0.119	0.200	0.071	0.207	0.152	0.802	0.284	0.202	0.720	0.110	0.074	1.613
42	0.067	0.117	0.090	0.113	0.169	0.990	0.386	0.199	0.147	0.165	0.732	0.382
43	0.051	0.039	0.063	0.169	0.113	0.159	0.050	0.388	1.131	0.211	0.074	0.122
44	0.151	0.097	0.079	0.341	0.071	0.513	0.315	0.043	0.077	0.239	0.116	0.142
45	0.073	0.087	0.042	0.280	0.169	0.513	0.262	0.116	0.058	0.164	0.085	0.376
46	0.071	0.054	0.021	1.033	0.193	0.674	0.191	0.452	0.137	0.368	0.305	0.376
47	0.119	0.132	0.045	0.359	0.137	0.491	0.113	0.059	0.153	0.923	0.143	0.414
48	0.067	0.021	0.026	0.161	0.264	0.402	0.123	0.238	0.366	1.273	0.025	0.409
49	0.041	0.054	0.072	0.386	0.055	1.003	0.099	0.209	0.137	0.138	0.188	0.376
50	0.043	0.132	0.059	0.280	0.226	0.793	0.269	0.039	0.153	0.184	0.119	0.241
51	0.071	0.021	0.071	0.060	0.195	1.446	0.189	0.119	0.366	0.283	0.092	1.501
52	0.119	0.101	0.090	0.142	0.109	0.226	0.560	0.134	0.248	0.236	0.115	0.852
53	0.067	0.074	0.220	0.200	0.098	0.836	0.282	0.187	0.113	0.283	0.095	0.699
54	0.041	0.075	0.039	0.180	0.174	0.632	1.927	0.202	0.242	0.236	0.065	0.785
55	0.043	0.059	0.415	0.107	0.213	0.764	0.082	1.481	0.323	0.551	0.127	1.613
56	0.115	0.133	0.115	0.180	0.081	1.290	0.202	0.209	0.080	0.347	0.124	0.376
57	0.036	0.080	0.065	0.107	0.130	0.506	0.132	1.687	0.042	0.157	0.093	0.241
58	0.074	0.258	0.219	0.119	0.272	0.588	0.284	0.094	0.125	0.360	0.305	0.699
59	0.093	0.412	0.110	0.204	0.159	0.802	0.386	0.116	0.069	0.368	0.143	0.785
60	0.144	0.412	0.030	0.308	0.193	0.990	0.099	0.273	0.190	0.923	0.025	1.613

**Table 2: The Repeatability of GLOS Y Tiles Measured Under Specular Component Included Mode By CE-2180 Over 60 Weeks**

Week	Pale Grey	Middel Grey	Diff. Grey	Deep Grey	Deep Pink	Red	Orange	Bright Yellow	Green	Diff. Green	Cyan	Deep Blue
1	0.055	0.039	0.078	0.131	0.147	0.240	0.294	0.214	0.104	0.136	0.107	0.176
2	0.124	0.080	0.351	1.029	0.995	1.783	1.663	0.133	0.989	0.972	0.679	0.150
3	0.102	0.075	0.051	0.129	0.141	0.244	0.305	0.155	0.193	0.191	0.160	0.333
4	0.064	0.059	0.067	0.144	0.057	0.196	0.147	0.461	0.113	0.075	0.082	0.148
5	0.060	0.133	0.073	0.140	0.097	0.598	0.271	0.230	0.145	0.136	0.109	0.150
6	0.084	0.080	0.232	0.584	0.462	0.279	0.478	0.175	0.141	0.384	0.439	1.053
7	0.066	0.258	0.070	0.195	0.195	0.204	0.292	0.090	0.172	0.124	0.135	0.469
8	0.074	0.412	0.056	0.146	0.182	0.033	0.237	0.161	0.115	0.134	0.058	0.287
9	0.036	0.082	0.023	0.124	0.098	0.176	0.114	0.189	0.162	0.045	0.067	0.119
10	0.098	0.012	0.074	0.053	0.131	0.141	0.235	0.258	0.116	0.137	0.089	0.239
11	0.123	0.061	0.061	0.149	0.128	0.277	0.292	0.184	0.186	0.027	0.041	0.164
12	0.021	0.085	0.082	0.207	0.224	0.213	0.220	0.083	0.128	0.153	0.116	0.443
13	0.040	0.200	0.042	0.053	0.123	0.132	0.064	0.124	0.089	0.079	0.078	0.216
14	0.060	0.117	0.116	0.208	0.130	0.119	0.149	0.122	0.096	0.100	0.082	0.231
15	0.084	0.039	0.034	0.095	0.120	0.243	0.252	0.395	0.142	0.053	0.110	0.267
16	0.066	0.097	0.044	0.135	0.190	0.183	0.158	0.099	0.088	0.049	0.051	0.263
17	0.074	0.087	0.033	0.112	0.194	0.488	0.416	0.174	0.302	0.307	0.084	0.237
18	0.036	0.054	0.162	0.402	0.324	0.098	0.172	0.205	0.110	0.043	0.315	0.865
19	0.049	0.132	0.033	0.101	0.090	0.149	0.201	0.534	0.099	0.085	0.081	0.138



Appendix IV

20	0.065	0.021	0.050	0.133	0.106	0.263	0.231	0.161	0.106	0.105	0.049	0.267
21	0.066	0.101	0.047	0.184	0.185	0.587	0.520	0.133	0.357	0.333	0.040	0.264
22	0.074	0.074	0.107	0.067	0.322	0.076	0.305	0.155	0.126	0.112	0.240	0.666
23	0.098	0.133	0.056	0.195	0.100	0.196	0.147	0.461	0.145	0.191	0.073	0.175
24	0.123	0.080	0.351	0.146	0.141	0.598	0.271	0.230	0.141	0.075	0.058	0.176
25	0.021	0.258	0.051	0.124	0.057	0.279	0.478	0.175	0.172	0.136	0.067	0.666
26	0.066	0.412	0.067	0.053	0.097	0.204	0.292	0.090	0.115	0.384	0.089	0.333
27	0.074	0.082	0.073	0.149	0.462	0.033	0.237	0.161	0.162	0.124	0.041	0.148
28	0.036	0.012	0.232	0.207	0.195	0.176	0.114	0.189	0.116	0.134	0.116	0.150
29	0.098	0.061	0.070	0.053	0.182	0.141	0.235	0.258	0.186	0.045	0.078	1.053
30	0.123	0.085	0.056	0.208	0.098	0.277	0.220	0.184	0.128	0.136	0.082	0.469
31	0.021	0.054	0.023	0.095	0.131	0.240	0.064	0.258	0.104	0.972	0.110	0.287
32	0.040	0.132	0.074	0.135	0.128	1.687	0.149	0.184	0.989	0.191	0.051	0.119
33	0.074	0.021	0.061	0.112	0.224	0.244	0.252	0.083	0.193	0.075	0.084	0.239
34	0.036	0.101	0.082	0.144	0.123	0.196	0.158	0.124	0.113	0.136	0.315	0.164
35	0.049	0.074	0.042	0.140	0.120	0.598	0.416	0.122	0.145	0.384	0.082	0.443
36	0.065	0.133	0.116	0.584	0.190	0.279	0.271	0.395	0.141	0.124	0.110	0.216
37	0.066	0.012	0.074	0.195	0.194	0.204	0.478	0.099	0.142	0.137	0.051	0.231
38	0.021	0.061	0.061	0.146	0.324	0.183	0.292	0.155	0.088	0.027	0.084	0.267
39	0.081	0.085	0.082	0.124	0.090	0.488	0.237	0.461	0.302	0.153	0.315	0.263
40	0.055	0.200	0.042	0.053	0.190	0.098	0.114	0.230	0.110	0.079	0.081	0.237

Appendix IV

41	0.124	0.117	0.116	0.149	0.194	0.149	0.235	0.133	0.099	0.100	0.049	0.865
42	0.102	0.039	0.034	0.207	0.324	0.207	0.292	0.155	0.106	0.053	0.040	0.138
43	0.064	0.097	0.044	0.124	0.090	0.124	0.220	0.461	0.357	0.049	0.240	0.267
44	0.040	0.087	0.033	0.053	0.106	0.053	0.064	0.230	0.126	0.307	0.073	0.264
45	0.060	0.039	0.162	0.149	0.185	0.149	0.149	0.175	0.145	0.045	0.058	0.666
46	0.084	0.080	0.033	0.207	0.322	0.207	0.252	0.090	0.172	0.136	0.067	0.175
47	0.066	0.075	0.050	0.053	0.100	0.053	0.158	0.161	0.115	0.972	0.089	0.267
48	0.074	0.059	0.047	0.208	0.141	0.208	0.416	0.189	0.162	0.191	0.041	0.263
49	0.098	0.133	0.107	0.095	0.147	0.095	0.271	0.083	0.116	0.075	0.107	0.237
50	0.123	0.080	0.056	0.135	0.995	0.135	0.478	0.124	0.186	0.136	0.679	0.865
51	0.021	0.012	0.078	0.112	0.141	0.112	0.292	0.122	0.128	0.384	0.160	0.138
52	0.025	0.061	0.351	0.402	0.057	0.402	0.235	0.395	0.141	0.124	0.082	0.267
53	0.036	0.085	0.051	0.101	0.097	0.101	0.220	0.099	0.142	0.137	0.109	0.264
54	0.049	0.200	0.067	0.124	0.462	0.124	0.064	0.174	0.088	0.027	0.439	0.666
55	0.065	0.117	0.073	0.053	0.195	0.053	0.149	0.099	0.302	0.136	0.135	0.175
56	0.080	0.054	0.232	0.149	0.182	0.149	0.252	0.155	0.110	0.972	0.058	0.176
57	0.046	0.132	0.070	0.207	0.098	0.207	0.158	0.461	0.099	0.191	0.067	0.237
58	0.036	0.021	0.056	0.053	0.131	0.053	0.416	0.090	0.106	0.075	0.110	0.333
59	0.084	0.101	0.023	0.208	0.141	0.208	0.252	0.161	0.357	0.136	0.051	0.148
60	0.021	0.074	0.074	0.095	0.057	0.095	0.158	0.189	0.126	0.384	0.084	0.150

**Table 3: The Repeatability of MATT Tiles Measured Under Specular Component Excluded Mode By CE-2180 Over 60 Weeks**

Week	Pale Grey	Middel Grey	Diff. Grey	Deep Grey	Deep Pink	Red	Orange	Bright Yellow	Green	Diff. Green	Cyan	Deep Blue
1	0.076	0.050	0.165	0.362	0.247	0.261	0.318	0.158	0.165	0.120	0.221	0.560
2	0.120	0.046	0.222	0.247	0.204	0.169	0.602	0.167	0.157	0.062	0.123	0.431
3	0.121	0.173	0.119	0.230	0.163	0.132	0.135	0.059	0.125	0.125	0.145	0.129
4	0.103	0.106	0.164	0.245	0.083	0.075	0.195	0.102	0.082	0.141	0.271	0.376
5	0.133	0.100	0.173	0.448	0.336	0.364	0.151	0.155	0.186	0.087	0.168	0.583
6	0.136	0.102	0.087	0.275	0.181	0.211	0.238	0.144	0.107	0.087	0.170	0.449
7	0.170	0.050	0.179	0.117	0.254	0.283	0.242	0.165	0.146	0.062	0.104	0.493
8	0.081	0.046	0.170	0.253	0.235	0.439	0.253	0.490	0.101	0.124	0.233	0.310
9	0.085	0.173	0.192	0.360	0.386	0.179	0.237	0.152	0.346	0.126	0.194	0.474
10	0.087	0.106	0.164	0.271	0.180	0.221	0.262	0.130	0.219	0.127	0.196	0.439
11	0.089	0.100	0.180	0.260	0.189	0.234	0.505	0.110	0.216	0.063	0.186	0.420
12	0.105	0.102	0.151	0.247	0.229	0.195	0.192	0.106	0.169	0.152	0.142	0.544
13	0.118	0.245	0.257	0.240	0.225	0.046	0.297	0.158	0.043	0.100	0.047	0.493
14	0.076	0.101	0.071	0.194	0.108	0.191	0.192	0.167	0.203	0.120	0.158	0.310
15	0.120	0.152	0.075	0.049	0.272	0.216	0.068	0.059	0.208	0.062	0.168	0.474
16	0.121	0.076	0.237	0.362	0.245	0.203	0.236	0.102	0.185	0.125	0.171	0.439
17	0.103	0.059	0.174	0.247	0.244	0.242	0.109	0.155	0.186	0.141	0.191	0.420
18	0.133	0.128	0.165	0.230	0.237	0.151	0.196	0.144	0.154	0.087	0.132	0.256
19	0.136	0.093	0.222	0.245	0.173	0.230	0.068	0.165	0.202	0.087	0.320	0.494

Appendix IV

20	0.170	0.108	0.119	0.448	0.400	0.169	0.236	0.490	0.091	0.109	0.140	0.425
21	0.081	0.153	0.164	0.275	0.198	0.100	0.109	0.152	0.149	0.118	0.094	0.368
22	0.085	0.096	0.173	0.302	0.158	0.256	0.297	0.130	0.208	0.149	0.154	0.376
23	0.087	0.205	0.087	0.342	0.245	0.216	0.192	0.110	0.203	0.161	0.123	0.583
24	0.089	0.069	0.046	0.256	0.244	0.203	0.068	0.106	0.208	0.098	0.145	0.449
25	0.086	0.073	0.179	0.117	0.237	0.242	0.236	0.106	0.185	0.151	0.271	0.493
26	0.091	0.137	0.170	0.253	0.235	0.151	0.109	0.177	0.186	0.114	0.168	0.310
27	0.098	0.096	0.192	0.360	0.386	0.230	0.196	0.147	0.154	0.107	0.170	0.474
28	0.142	0.205	0.164	0.271	0.180	0.211	0.318	0.175	0.186	0.109	0.104	0.439
29	0.187	0.106	0.180	0.260	0.189	0.283	0.602	0.256	0.107	0.161	0.233	0.420
30	0.064	0.100	0.233	0.211	0.229	0.439	0.135	0.143	0.146	0.063	0.194	0.544
31	0.016	0.102	0.177	0.314	0.225	0.179	0.195	0.119	0.101	0.152	0.047	0.415
32	0.045	0.245	0.115	0.136	0.108	0.221	0.151	0.078	0.346	0.100	0.158	0.172
33	0.086	0.101	0.149	0.205	0.386	0.234	0.238	0.094	0.219	0.120	0.168	0.411
34	0.091	0.152	0.192	0.285	0.180	0.195	0.175	0.152	0.216	0.062	0.171	0.483
35	0.098	0.076	0.164	0.205	0.189	0.046	0.176	0.130	0.154	0.125	0.191	0.379
36	0.142	0.059	0.180	0.285	0.189	0.191	0.242	0.110	0.202	0.141	0.132	0.310
37	0.187	0.128	0.151	0.117	0.229	0.283	0.253	0.106	0.082	0.087	0.233	0.474
38	0.064	0.093	0.257	0.253	0.225	0.439	0.237	0.106	0.186	0.087	0.194	0.439
39	0.016	0.108	0.071	0.360	0.108	0.179	0.262	0.177	0.107	0.109	0.196	0.420
40	0.118	0.050	0.071	0.271	0.247	0.221	0.505	0.130	0.146	0.118	0.186	0.256

Appendix IV

41	0.076	0.046	0.075	0.260	0.204	0.234	0.192	0.110	0.101	0.125	0.142	0.494
42	0.120	0.173	0.174	0.211	0.163	0.261	0.124	0.106	0.346	0.141	0.047	0.310
43	0.121	0.106	0.165	0.285	0.083	0.169	0.192	0.158	0.219	0.087	0.158	0.474
44	0.103	0.100	0.222	0.117	0.336	0.132	0.192	0.167	0.216	0.087	0.168	0.439
45	0.133	0.102	0.119	0.253	0.235	0.075	0.068	0.059	0.169	0.062	0.171	0.420
46	0.136	0.050	0.164	0.360	0.386	0.364	0.236	0.102	0.186	0.124	0.191	0.544
47	0.170	0.046	0.173	0.271	0.180	0.211	0.109	0.155	0.107	0.126	0.132	0.415
48	0.170	0.069	0.164	0.260	0.189	0.283	0.196	0.144	0.146	0.127	0.320	0.172
49	0.081	0.073	0.180	0.211	0.229	0.439	0.068	0.152	0.101	0.063	0.158	0.411
50	0.085	0.137	0.151	0.314	0.225	0.179	0.236	0.130	0.346	0.152	0.168	0.483
51	0.087	0.096	0.257	0.230	0.108	0.221	0.109	0.110	0.219	0.100	0.171	0.474
52	0.089	0.205	0.071	0.245	0.272	0.221	0.297	0.106	0.216	0.120	0.191	0.439
53	0.086	0.106	0.075	0.448	0.245	0.234	0.192	0.106	0.169	0.062	0.132	0.420
54	0.091	0.100	0.237	0.275	0.244	0.242	0.068	0.177	0.154	0.125	0.320	0.256
55	0.098	0.102	0.174	0.302	0.237	0.151	0.236	0.165	0.202	0.141	0.140	0.494
56	0.142	0.245	0.149	0.342	0.173	0.230	0.109	0.490	0.082	0.087	0.094	0.310
57	0.187	0.050	0.192	0.256	0.400	0.211	0.196	0.152	0.101	0.087	0.154	0.560
58	0.064	0.046	0.164	0.117	0.247	0.283	0.318	0.130	0.346	0.109	0.123	0.431
59	0.016	0.173	0.180	0.253	0.204	0.283	0.602	0.110	0.219	0.118	0.145	0.129
60	0.045	0.106	0.222	0.360	0.163	0.439	0.192	0.106	0.216	0.149	0.271	0.376

**Table 4: The Repeatability of MATT Tiles Measured Under Specular Component Included Mode By CE-2180 Over 60 Weeks**

Week	Pale Grey	Middel Grey	Diff. Grey	Deep Grey	Deep Pink	Red	Orange	Bright Yellow	Green	Diff. Green	Cyan	Deep Blue
1	0.037	0.054	0.074	0.066	0.024	0.165	0.281	0.127	0.207	0.073	0.196	0.171
2	0.077	0.084	0.086	0.070	0.085	0.180	0.290	0.141	0.130	0.140	0.186	0.137
3	0.123	0.078	0.104	0.065	0.046	0.299	0.055	0.182	0.085	0.327	0.142	0.063
4	0.048	0.084	0.054	0.094	0.088	0.040	0.227	0.063	0.232	0.200	0.047	0.081
5	0.028	0.082	0.059	0.090	0.067	0.087	0.345	0.206	0.068	0.087	0.158	0.540
6	0.035	0.096	0.042	0.238	0.090	0.036	0.329	0.149	0.141	0.247	0.168	0.038
7	0.045	0.040	0.054	0.104	0.036	0.167	0.246	0.170	0.036	0.116	0.171	0.399
8	0.077	0.101	0.119	0.078	0.038	0.069	0.468	0.087	0.089	0.082	0.191	0.117
9	0.075	0.093	0.054	0.143	0.083	0.039	0.199	0.168	0.088	0.066	0.132	0.171
10	0.061	0.090	0.106	0.076	0.204	0.135	0.243	0.123	0.086	0.140	0.320	0.137
11	0.123	0.076	0.093	0.073	0.143	0.110	0.140	0.079	0.090	0.187	0.140	0.063
12	0.048	0.096	0.095	0.312	0.036	0.135	0.279	0.085	0.207	0.092	0.170	0.081
13	0.028	0.040	0.043	0.189	0.227	0.158	0.129	0.063	0.130	0.142	0.104	0.540
14	0.035	0.101	0.035	0.022	0.046	0.105	0.166	0.206	0.085	0.194	0.233	0.038
15	0.045	0.093	0.106	0.238	0.059	0.249	0.196	0.149	0.232	0.073	0.194	0.399
16	0.077	0.090	0.093	0.104	0.079	0.165	0.262	0.170	0.068	0.140	0.196	0.117
17	0.075	0.076	0.045	0.066	0.062	0.180	0.254	0.087	0.141	0.327	0.186	0.065
18	0.061	0.054	0.064	0.129	0.114	0.299	0.233	0.168	0.089	0.200	0.142	0.082
19	0.089	0.084	0.086	0.066	0.057	0.040	0.198	0.123	0.088	0.087	0.047	0.089

## Appendix IV

20	0.167	0.078	0.074	0.070	0.057	0.087	0.259	0.079	0.086	0.247	0.158	0.107
21	0.084	0.084	0.086	0.065	0.024	0.036	0.152	0.085	0.090	0.116	0.196	0.061
22	0.034	0.082	0.104	0.094	0.085	0.167	0.141	0.140	0.207	0.143	0.186	0.081
23	0.088	0.114	0.054	0.090	0.046	0.069	0.468	0.127	0.130	0.097	0.142	0.061
24	0.051	0.033	0.059	0.121	0.088	0.039	0.199	0.141	0.085	0.109	0.047	0.076
25	0.077	0.073	0.042	0.101	0.067	0.089	0.243	0.182	0.232	0.082	0.158	0.120
26	0.027	0.065	0.054	0.093	0.087	0.088	0.140	0.063	0.068	0.066	0.123	0.053
27	0.037	0.075	0.119	0.101	0.075	0.129	0.279	0.169	0.141	0.140	0.145	0.164
28	0.061	0.031	0.054	0.101	0.143	0.095	0.129	0.054	0.036	0.187	0.123	0.105
29	0.089	0.030	0.055	0.073	0.036	0.091	0.166	0.116	0.061	0.167	0.145	0.055
30	0.167	0.076	0.045	0.022	0.227	0.166	0.196	0.335	0.105	0.095	0.271	0.540
31	0.084	0.096	0.034	0.238	0.046	0.022	0.262	0.230	0.052	0.144	0.168	0.038
32	0.034	0.040	0.062	0.104	0.059	0.072	0.281	0.075	0.068	0.116	0.170	0.399
33	0.088	0.101	0.063	0.066	0.088	0.039	0.290	0.366	0.090	0.107	0.104	0.117
34	0.051	0.093	0.086	0.129	0.067	0.089	0.055	0.075	0.088	0.110	0.123	0.065
35	0.077	0.090	0.104	0.066	0.090	0.088	0.227	0.366	0.059	0.109	0.145	0.082
36	0.045	0.076	0.054	0.070	0.036	0.129	0.345	0.102	0.061	0.082	0.271	0.089
37	0.077	0.082	0.059	0.065	0.038	0.095	0.329	0.140	0.044	0.066	0.168	0.107
38	0.075	0.114	0.042	0.094	0.083	0.158	0.246	0.127	0.029	0.140	0.221	0.061
39	0.061	0.033	0.054	0.090	0.204	0.105	0.468	0.141	0.009	0.247	0.123	0.081
40	0.123	0.073	0.119	0.121	0.143	0.249	0.199	0.169	0.085	0.116	0.145	0.061

Appendix IV

41	0.048	0.065	0.054	0.104	0.036	0.165	0.243	0.054	0.232	0.082	0.271	0.076
42	0.028	0.075	0.055	0.078	0.227	0.180	0.259	0.116	0.068	0.066	0.168	0.107
43	0.035	0.031	0.045	0.143	0.046	0.299	0.152	0.335	0.105	0.140	0.170	0.061
44	0.045	0.030	0.119	0.076	0.059	0.040	0.141	0.230	0.052	0.116	0.104	0.081
45	0.077	0.096	0.054	0.073	0.083	0.087	0.468	0.075	0.068	0.082	0.233	0.061
46	0.075	0.040	0.055	0.312	0.204	0.036	0.199	0.366	0.036	0.066	0.194	0.076
47	0.061	0.101	0.045	0.189	0.143	0.087	0.243	0.102	0.061	0.140	0.196	0.120
48	0.123	0.093	0.034	0.066	0.036	0.036	0.140	0.140	0.105	0.187	0.186	0.053
49	0.048	0.090	0.062	0.070	0.227	0.167	0.279	0.127	0.052	0.092	0.142	0.164
50	0.028	0.076	0.063	0.065	0.046	0.069	0.129	0.141	0.068	0.142	0.047	0.105
51	0.035	0.096	0.054	0.094	0.059	0.039	0.166	0.182	0.141	0.194	0.158	0.055
52	0.167	0.040	0.059	0.090	0.079	0.089	0.196	0.063	0.036	0.073	0.168	0.540
53	0.084	0.101	0.042	0.238	0.062	0.039	0.262	0.206	0.061	0.140	0.171	0.038
54	0.034	0.054	0.054	0.104	0.114	0.135	0.281	0.149	0.105	0.327	0.191	0.399
55	0.088	0.084	0.119	0.078	0.057	0.110	0.290	0.170	0.052	0.200	0.132	0.540
56	0.051	0.078	0.054	0.143	0.057	0.135	0.055	0.087	0.068	0.087	0.320	0.038
57	0.077	0.084	0.106	0.076	0.088	0.158	0.227	0.168	0.090	0.082	0.140	0.399
58	0.075	0.082	0.093	0.073	0.067	0.105	0.345	0.123	0.088	0.066	0.094	0.117
59	0.061	0.076	0.095	0.022	0.087	0.249	0.345	0.079	0.059	0.140	0.154	0.171
60	0.123	0.082	0.119	0.238	0.075	0.165	0.329	0.085	0.061	0.187	0.158	0.137



**Table 5: The Repeatability of GLOSSY Tiles Measured Under Specular Component Excluded Mode By SF-600 Over 60 Weeks**

Week	Pale Grey	Middle Grey	Diff. Grey	Deep Grey	Deep Pink	Red	Orange	Bright Yellow	Green	Diff. Green	Cyan	Deep Blue
1	0.102	0.454	0.063	0.309	0.185	0.042	0.217	0.155	0.158	0.177	0.915	0.245
2	0.038	0.456	0.079	0.142	0.099	0.201	0.173	0.013	0.053	0.081	0.920	0.286
3	0.056	0.478	0.042	0.063	0.108	0.460	0.099	0.183	0.062	0.068	0.828	0.286
4	0.020	0.495	0.021	0.071	0.038	0.096	0.106	0.060	0.037	0.044	0.914	0.076
5	0.039	0.482	0.039	0.080	0.082	0.339	0.101	0.114	0.067	0.085	0.867	0.314
6	0.014	0.450	0.063	0.101	0.043	0.177	0.106	0.090	0.045	0.059	1.086	0.115
7	0.022	0.431	0.045	0.051	0.042	0.118	0.131	0.130	0.005	0.034	0.971	0.183
8	0.042	0.460	0.026	0.151	0.105	0.135	0.049	0.147	0.071	0.077	0.848	0.200
9	0.023	0.457	0.072	0.096	0.090	0.233	0.058	0.189	0.048	0.023	0.862	0.160
10	0.055	0.447	0.059	0.077	0.085	0.262	0.115	0.090	0.006	0.054	0.920	0.335
11	0.014	0.460	0.071	0.079	0.065	0.375	0.202	0.130	0.054	0.033	0.828	0.294
12	0.020	0.450	0.090	0.134	0.106	0.105	0.090	0.147	0.070	0.062	0.914	0.150
13	0.051	0.478	0.220	0.062	0.099	0.163	0.112	0.189	0.068	0.079	0.867	0.379
14	0.033	0.445	0.039	0.125	0.084	0.274	0.126	0.125	0.074	0.067	1.086	0.283
15	0.015	0.454	0.415	0.096	0.073	0.042	0.071	0.186	0.032	0.065	0.971	0.230
16	0.023	0.462	0.115	0.062	0.064	0.201	0.108	0.086	0.038	0.028	0.848	0.130
17	0.029	0.450	0.054	0.076	0.082	0.460	0.033	0.136	0.034	0.040	0.862	0.222
18	0.031	0.450	0.065	0.046	0.039	0.096	0.082	0.083	0.040	0.047	0.896	0.183
19	0.040	0.459	0.219	0.068	0.070	0.339	0.230	0.155	0.049	0.033	0.898	0.167

Appendix IV

20	0.096	0.449	0.110	0.104	0.074	0.177	0.074	0.377	0.022	0.016	0.840	0.335
21	0.036	0.463	0.030	0.067	0.051	0.118	0.129	0.148	0.038	0.059	0.906	0.343
22	0.043	0.466	0.081	0.063	0.120	0.215	0.200	0.060	0.060	0.081	0.857	0.222
23	0.038	0.431	0.063	0.071	0.042	0.065	0.202	0.114	0.067	0.068	0.868	0.286
24	0.020	0.460	0.079	0.080	0.105	0.233	0.090	0.090	0.045	0.044	0.864	0.286
25	0.039	0.457	0.042	0.101	0.090	0.071	0.112	0.130	0.005	0.085	0.784	0.076
26	0.014	0.447	0.021	0.051	0.085	0.310	0.126	0.147	0.071	0.059	0.875	0.314
27	0.022	0.460	0.039	0.151	0.065	0.305	0.071	0.189	0.068	0.034	0.860	0.115
28	0.042	0.450	0.054	0.096	0.106	0.135	0.108	0.125	0.074	0.077	0.953	0.183
29	0.023	0.478	0.065	0.077	0.099	0.233	0.033	0.072	0.032	0.023	0.914	0.200
30	0.055	0.445	0.219	0.079	0.084	0.262	0.082	0.083	0.038	0.551	0.867	0.160
31	0.014	0.454	0.110	0.134	0.073	0.375	0.230	0.045	0.034	0.347	1.086	0.200
32	0.020	0.462	0.030	0.062	0.064	0.105	0.074	0.101	0.040	0.157	0.971	0.160
33	0.051	0.450	0.081	0.125	0.082	0.163	0.992	0.186	0.049	0.360	0.848	0.335
34	0.033	0.450	0.063	0.187	0.084	0.274	0.173	0.086	0.022	0.412	0.862	0.294
35	0.015	0.459	0.079	0.266	0.073	0.042	0.099	0.136	0.038	0.110	0.896	0.150
36	0.102	0.449	0.042	0.210	0.064	0.201	0.106	0.083	0.060	0.165	0.898	0.343
37	0.038	0.463	0.021	0.194	0.082	0.042	0.101	0.155	0.067	0.360	0.840	0.222
38	0.056	0.466	0.039	0.201	0.039	0.201	0.106	0.377	0.045	0.412	0.848	0.286
39	0.020	0.431	0.063	0.175	0.070	0.460	0.131	0.148	0.005	0.110	0.862	0.286
40	0.039	0.454	0.039	0.194	0.074	0.096	0.049	0.136	0.071	0.165	0.896	0.076

## Appendix IV

41	0.014	0.456	0.415	0.062	0.051	0.339	0.058	0.083	0.062	0.211	0.898	0.314
42	0.022	0.478	0.115	0.076	0.120	0.177	0.115	0.155	0.037	0.239	0.840	0.115
43	0.042	0.495	0.054	0.046	0.074	0.118	0.202	0.013	0.067	0.164	0.906	0.183
44	0.055	0.482	0.065	0.068	0.051	0.215	0.090	0.183	0.045	0.283	0.857	0.200
45	0.014	0.450	0.063	0.104	0.120	0.065	0.202	0.060	0.005	0.236	0.868	0.160
46	0.020	0.431	0.079	0.067	0.042	0.305	0.090	0.114	0.071	0.551	0.864	0.245
47	0.051	0.460	0.042	0.063	0.105	0.135	0.112	0.090	0.048	0.412	0.920	0.286
48	0.033	0.457	0.021	0.071	0.185	0.233	0.126	0.130	0.006	0.110	0.828	0.286
49	0.015	0.447	0.039	0.080	0.099	0.262	0.071	0.147	0.054	0.165	0.914	0.076
50	0.023	0.450	0.063	0.101	0.108	0.375	0.108	0.189	0.070	0.360	0.867	0.314
51	0.029	0.450	0.045	0.051	0.038	0.177	0.033	0.125	0.067	0.412	1.086	0.115
52	0.031	0.459	0.026	0.191	0.082	0.118	0.082	0.072	0.045	0.110	0.971	0.183
53	0.022	0.449	0.072	0.182	0.043	0.215	0.230	0.083	0.005	0.165	0.848	0.200
54	0.042	0.463	0.039	0.188	0.042	0.065	0.106	0.045	0.071	0.109	0.862	0.160
55	0.023	0.466	0.415	0.193	0.105	0.233	0.101	0.101	0.062	0.250	0.896	0.335
56	0.055	0.431	0.115	0.189	0.090	0.071	0.106	0.186	0.037	0.368	0.898	0.294
57	0.014	0.454	0.054	0.190	0.085	0.310	0.131	0.086	0.067	0.923	0.840	0.150
58	0.020	0.456	0.065	0.191	0.065	0.305	0.049	0.095	0.045	1.273	0.906	0.379
59	0.051	0.478	0.063	0.178	0.106	0.135	0.058	0.128	0.005	0.360	0.857	0.283
60	0.033	0.495	0.079	0.187	0.099	0.233	0.115	0.086	0.071	0.412	0.868	0.321

**Table 6: The Repeatability of GLOSSY Tiles Measured Under Specular Component Included Mode By SF-600 Over 60 Weeks**

Week	Pale Grey	Middel Grey	Diff. Grey	Deep Grey	Deep Pink	Red	Orange	Bright Yellow	Green	Diff. Green	Cyan	Deep Blue
1	0.054	0.066	0.071	0.045	0.056	0.027	0.094	0.019	0.073	0.020	0.045	0.081
2	0.051	0.030	0.048	0.033	0.045	0.057	0.052	0.106	0.053	0.060	0.033	0.036
3	0.025	0.045	0.062	0.028	0.052	0.062	0.070	0.043	0.061	0.022	0.049	0.077
4	0.036	0.011	0.018	0.062	0.048	0.033	0.045	0.094	0.017	0.047	0.014	0.023
5	0.016	0.046	0.064	0.020	0.030	0.073	0.081	0.088	0.068	0.052	0.039	0.058
6	0.025	0.010	0.015	0.039	0.006	0.024	0.051	0.011	0.037	0.072	0.023	0.011
7	0.048	0.015	0.019	0.034	0.059	0.054	0.042	0.084	0.040	0.054	0.036	0.027
8	0.022	0.041	0.049	0.031	0.030	0.133	0.098	0.130	0.089	0.059	0.041	0.051
9	0.051	0.060	0.020	0.059	0.045	0.052	0.037	0.092	0.056	0.026	0.025	0.030
10	0.014	0.020	0.060	0.045	0.017	0.043	0.045	0.072	0.038	0.069	0.048	0.064
11	0.024	0.012	0.030	0.028	0.012	0.039	0.047	0.020	0.022	0.027	0.018	0.039
12	0.036	0.042	0.022	0.043	0.029	0.026	0.029	0.128	0.078	0.037	0.028	0.030
13	0.039	0.053	0.057	0.045	0.059	0.077	0.089	0.019	0.071	0.084	0.039	0.030
14	0.022	0.020	0.057	0.035	0.019	0.065	0.072	0.011	0.026	0.039	0.034	0.073
15	0.031	0.027	0.030	0.066	0.049	0.030	0.030	0.084	0.047	0.039	0.022	0.042
16	0.043	0.032	0.042	0.044	0.056	0.067	0.080	0.106	0.031	0.033	0.022	0.060
17	0.030	0.017	0.049	0.020	0.029	0.047	0.056	0.049	0.054	0.020	0.030	0.064
18	0.027	0.024	0.031	0.039	0.036	0.073	0.069	0.088	0.032	0.060	0.027	0.065
19	0.060	0.091	0.044	0.081	0.089	0.058	0.042	0.103	0.074	0.022	0.026	0.068

Appendix IV

20	0.039	0.043	0.091	0.051	0.058	0.104	0.060	0.048	0.047	0.054	0.044
21	0.036	0.026	0.053	0.041	0.044	0.057	0.066	0.031	0.052	0.032	0.054
22	0.043	0.046	0.039	0.063	0.024	0.029	0.127	0.031	0.052	0.032	0.068
23	0.051	0.010	0.052	0.028	0.033	0.055	0.107	0.040	0.032	0.035	0.023
24	0.014	0.015	0.049	0.062	0.133	0.081	0.045	0.089	0.091	0.014	0.058
25	0.024	0.041	0.020	0.020	0.052	0.051	0.051	0.056	0.051	0.039	0.011
26	0.036	0.060	0.060	0.039	0.043	0.042	0.092	0.038	0.036	0.023	0.027
27	0.039	0.020	0.030	0.034	0.039	0.098	0.130	0.022	0.037	0.036	0.051
28	0.022	0.060	0.022	0.031	0.026	0.037	0.092	0.078	0.054	0.041	0.030
29	0.031	0.020	0.057	0.059	0.077	0.045	0.072	0.071	0.059	0.025	0.064
30	0.036	0.012	0.057	0.045	0.065	0.047	0.020	0.026	0.026	0.048	0.039
31	0.016	0.042	0.030	0.028	0.027	0.029	0.128	0.053	0.069	0.018	0.030
32	0.025	0.053	0.042	0.043	0.057	0.089	0.019	0.061	0.027	0.028	0.030
33	0.048	0.020	0.064	0.045	0.062	0.072	0.106	0.017	0.037	0.039	0.051
34	0.022	0.027	0.015	0.035	0.033	0.051	0.043	0.068	0.084	0.034	0.030
35	0.051	0.032	0.019	0.066	0.073	0.042	0.094	0.037	0.039	0.022	0.064
36	0.014	0.017	0.049	0.045	0.024	0.098	0.088	0.040	0.047	0.045	0.039
37	0.054	0.066	0.020	0.033	0.054	0.037	0.011	0.089	0.052	0.033	0.030
38	0.051	0.030	0.060	0.028	0.133	0.045	0.084	0.056	0.052	0.049	0.030
39	0.025	0.045	0.030	0.062	0.052	0.047	0.106	0.038	0.032	0.014	0.073
40	0.036	0.011	0.022	0.020	0.043	0.029	0.049	0.022	0.091	0.039	0.042

Appendix IV

41	0.016	0.046	0.057	0.028	0.059	0.030	0.089	0.088	0.073	0.051	0.023	0.060
42	0.025	0.010	0.057	0.043	0.019	0.067	0.072	0.103	0.053	0.036	0.036	0.064
43	0.036	0.024	0.030	0.045	0.049	0.047	0.030	0.060	0.061	0.037	0.041	0.065
44	0.039	0.091	0.042	0.035	0.056	0.073	0.080	0.066	0.017	0.069	0.025	0.068
45	0.022	0.043	0.057	0.066	0.029	0.058	0.056	0.127	0.068	0.027	0.048	0.044
46	0.031	0.026	0.057	0.044	0.036	0.058	0.069	0.107	0.037	0.037	0.018	0.060
47	0.043	0.046	0.030	0.020	0.089	0.044	0.042	0.045	0.040	0.084	0.048	0.064
48	0.030	0.010	0.042	0.039	0.051	0.024	0.104	0.051	0.089	0.039	0.018	0.065
49	0.027	0.015	0.049	0.081	0.029	0.033	0.057	0.127	0.026	0.039	0.028	0.068
50	0.060	0.041	0.031	0.051	0.056	0.133	0.094	0.107	0.047	0.033	0.039	0.044
51	0.039	0.060	0.044	0.034	0.045	0.052	0.052	0.045	0.031	0.020	0.034	0.054
52	0.036	0.020	0.091	0.031	0.052	0.043	0.070	0.051	0.054	0.060	0.022	0.068
53	0.043	0.060	0.053	0.059	0.048	0.057	0.045	0.092	0.032	0.022	0.022	0.023
54	0.051	0.020	0.039	0.045	0.030	0.062	0.081	0.130	0.074	0.047	0.030	0.058
55	0.014	0.027	0.052	0.028	0.006	0.033	0.051	0.092	0.048	0.052	0.027	0.011
56	0.024	0.032	0.049	0.043	0.059	0.073	0.042	0.072	0.031	0.052	0.026	0.027
57	0.036	0.017	0.020	0.045	0.029	0.024	0.047	0.020	0.031	0.032	0.054	0.051
58	0.039	0.066	0.060	0.035	0.059	0.054	0.029	0.128	0.040	0.020	0.018	0.030
59	0.022	0.030	0.044	0.028	0.019	0.133	0.089	0.019	0.089	0.060	0.028	0.060
60	0.036	0.045	0.091	0.043	0.049	0.052	0.072	0.106	0.056	0.022	0.039	0.064

**Table 7: The Repeatability of MATT Tiles Measured Under Specular Component Excluded Mode By SF-600 Over 60 Weeks**

Week	Pale Grey	Middel Grey	Diff. Grey	Deep Grey	Deep Pink	Red	Orange	Bright Yellow	Green	Diff. Green	Cyan	Deep Blue
1	0.093	0.046	0.094	0.184	0.026	0.169	0.154	0.055	0.039	0.142	0.061	0.154
2	0.042	0.012	0.040	0.097	0.074	0.064	0.063	0.024	0.064	0.039	0.046	0.085
3	0.042	0.020	0.050	0.058	0.033	0.050	0.052	0.082	0.038	0.046	0.063	0.067
4	0.009	0.022	0.013	0.042	0.036	0.056	0.086	0.044	0.037	0.044	0.038	0.009
5	0.039	0.061	0.032	0.033	0.085	0.037	0.037	0.025	0.083	0.060	0.056	0.033
6	0.014	0.019	0.012	0.040	0.079	0.032	0.080	0.044	0.053	0.014	0.040	0.018
7	0.044	0.058	0.021	0.053	0.022	0.063	0.164	0.077	0.065	0.044	0.040	0.021
8	0.019	0.016	0.044	0.029	0.048	0.027	0.096	0.148	0.063	0.061	0.051	0.072
9	0.054	0.046	0.018	0.060	0.090	0.034	0.079	0.032	0.010	0.030	0.035	0.065
10	0.030	0.107	0.050	0.020	0.019	0.021	0.079	0.024	0.078	0.043	0.048	0.020
11	0.026	0.054	0.005	0.026	0.053	0.055	0.013	0.082	0.038	0.020	0.030	0.032
12	0.047	0.046	0.024	0.056	0.040	0.067	0.039	0.044	0.041	0.059	0.036	0.090
13	0.042	0.012	0.043	0.056	0.043	0.070	0.089	0.025	0.070	0.085	0.038	0.097
14	0.024	0.020	0.014	0.020	0.054	0.040	0.154	0.044	0.021	0.052	0.052	0.035
15	0.028	0.022	0.023	0.054	0.090	0.046	0.063	0.077	0.077	0.027	0.032	0.045
16	0.020	0.061	0.033	0.030	0.019	0.067	0.052	0.148	0.033	0.013	0.048	0.031
17	0.040	0.019	0.030	0.010	0.053	0.026	0.086	0.032	0.035	0.020	0.044	0.026
18	0.037	0.058	0.026	0.023	0.040	0.054	0.037	0.024	0.096	0.006	0.035	0.039
19	0.098	0.016	0.073	0.029	0.043	0.061	0.080	0.018	0.029	0.044	0.042	0.044

Appendix IV

20	0.054	0.014	0.043	0.060	0.054	0.068	0.164	0.069	0.039	0.034	0.064	0.055
21	0.051	0.052	0.052	0.020	0.026	0.081	0.096	0.022	0.064	0.054	0.042	0.079
22	0.038	0.042	0.033	0.026	0.074	0.055	0.072	0.108	0.038	0.023	0.060	0.030
23	0.044	0.020	0.021	0.056	0.033	0.050	0.093	0.037	0.037	0.046	0.041	0.018
24	0.019	0.032	0.044	0.056	0.036	0.056	0.087	0.057	0.083	0.044	0.056	0.021
25	0.054	0.025	0.018	0.020	0.085	0.037	0.044	0.012	0.053	0.060	0.040	0.072
26	0.030	0.024	0.050	0.184	0.079	0.032	0.042	0.025	0.065	0.014	0.040	0.065
27	0.026	0.032	0.005	0.084	0.022	0.063	0.096	0.044	0.047	0.044	0.051	0.020
28	0.047	0.062	0.024	0.050	0.048	0.067	0.021	0.077	0.065	0.061	0.035	0.032
29	0.042	0.040	0.043	0.054	0.073	0.026	0.079	0.148	0.063	0.030	0.048	0.090
30	0.024	0.050	0.014	0.040	0.044	0.054	0.013	0.032	0.010	0.043	0.030	0.097
31	0.028	0.035	0.023	0.058	0.050	0.061	0.039	0.024	0.078	0.020	0.036	0.035
32	0.020	0.061	0.033	0.042	0.082	0.034	0.110	0.082	0.038	0.059	0.038	0.045
33	0.040	0.019	0.030	0.033	0.069	0.021	0.040	0.044	0.041	0.085	0.052	0.031
34	0.037	0.058	0.030	0.040	0.090	0.055	0.087	0.025	0.070	0.052	0.032	0.026
35	0.024	0.016	0.026	0.053	0.033	0.067	0.044	0.044	0.021	0.142	0.061	0.026
36	0.028	0.046	0.073	0.097	0.036	0.070	0.042	0.077	0.077	0.039	0.046	0.039
37	0.020	0.107	0.043	0.058	0.085	0.032	0.096	0.148	0.096	0.046	0.063	0.044
38	0.040	0.054	0.052	0.042	0.079	0.063	0.021	0.032	0.029	0.044	0.038	0.055
39	0.037	0.046	0.033	0.033	0.022	0.027	0.079	0.077	0.039	0.060	0.056	0.079
40	0.098	0.012	0.021	0.040	0.048	0.034	0.013	0.148	0.064	0.014	0.040	0.030



## Appendix IV

41	0.054	0.020	0.044	0.053	0.090	0.021	0.039	0.032	0.038	0.044	0.040	0.018
42	0.051	0.022	0.018	0.029	0.019	0.055	0.089	0.024	0.037	0.006	0.036	0.021
43	0.093	0.061	0.050	0.060	0.053	0.067	0.079	0.018	0.083	0.044	0.038	0.072
44	0.042	0.058	0.005	0.029	0.040	0.070	0.013	0.148	0.053	0.034	0.052	0.065
45	0.042	0.016	0.094	0.060	0.043	0.037	0.039	0.032	0.065	0.054	0.032	0.020
46	0.009	0.014	0.040	0.020	0.054	0.032	0.089	0.024	0.047	0.023	0.048	0.154
47	0.039	0.052	0.050	0.026	0.090	0.063	0.154	0.082	0.047	0.046	0.044	0.085
48	0.014	0.042	0.013	0.056	0.085	0.067	0.063	0.044	0.065	0.044	0.035	0.067
49	0.040	0.020	0.032	0.056	0.079	0.026	0.052	0.025	0.063	0.060	0.042	0.009
50	0.037	0.032	0.012	0.020	0.022	0.054	0.086	0.044	0.010	0.014	0.064	0.033
51	0.024	0.035	0.021	0.054	0.048	0.021	0.037	0.077	0.078	0.044	0.042	0.018
52	0.028	0.061	0.043	0.030	0.073	0.055	0.080	0.148	0.038	0.061	0.060	0.021
53	0.020	0.019	0.014	0.010	0.044	0.067	0.164	0.032	0.041	0.030	0.041	0.072
54	0.040	0.058	0.023	0.023	0.050	0.070	0.182	0.024	0.070	0.043	0.056	0.065
55	0.037	0.016	0.033	0.084	0.082	0.032	0.127	0.018	0.021	0.059	0.040	0.020
56	0.098	0.046	0.030	0.050	0.069	0.063	0.110	0.077	0.038	0.085	0.038	0.032
57	0.054	0.052	0.030	0.054	0.090	0.027	0.040	0.148	0.037	0.052	0.052	0.018
58	0.051	0.042	0.026	0.040	0.033	0.034	0.087	0.032	0.083	0.027	0.032	0.021
59	0.093	0.020	0.073	0.010	0.036	0.067	0.044	0.024	0.053	0.013	0.061	0.072
60	0.040	0.019	0.043	0.023	0.085	0.070	0.042	0.018	0.065	0.020	0.046	0.065

**Table 8: The Repeatability of MATT Tiles Measured Under Spectral Component Included Mode By SF-600 Over 60 Weeks**

Week	Pale Grey	Middel Grey	Diff. Grey	Deep Grey	Deep Pink	Red	Orange	Bright Yellow	Green	Diff. Green	Cyan	Deep Blue
1	0.075	0.067	0.073	0.075	0.058	0.036	0.015	0.147	0.100	0.034	0.044	0.071
2	0.025	0.026	0.042	0.051	0.088	0.041	0.089	0.051	0.063	0.053	0.020	0.066
3	0.046	0.044	0.061	0.057	0.020	0.064	0.088	0.097	0.087	0.015	0.038	0.067
4	0.009	0.050	0.011	0.012	0.077	0.022	0.104	0.017	0.013	0.046	0.018	0.013
5	0.025	0.016	0.061	0.081	0.022	0.076	0.037	0.069	0.072	0.047	0.026	0.083
6	0.019	0.019	0.016	0.012	0.032	0.070	0.093	0.055	0.046	0.051	0.023	0.017
7	0.017	0.027	0.009	0.003	0.053	0.091	0.015	0.103	0.062	0.081	0.053	0.047
8	0.029	0.010	0.036	0.022	0.034	0.074	0.089	0.030	0.041	0.057	0.026	0.042
9	0.008	0.038	0.013	0.031	0.076	0.050	0.088	0.096	0.101	0.056	0.040	0.027
10	0.041	0.008	0.057	0.065	0.037	0.038	0.120	0.052	0.027	0.037	0.030	0.075
11	0.008	0.017	0.027	0.027	0.034	0.041	0.056	0.030	0.025	0.056	0.022	0.033
12	0.021	0.036	0.021	0.023	0.059	0.066	0.081	0.113	0.065	0.054	0.035	0.047
13	0.022	0.035	0.043	0.041	0.078	0.060	0.091	0.084	0.068	0.049	0.026	0.049
14	0.013	0.026	0.051	0.061	0.054	0.050	0.042	0.045	0.042	0.024	0.023	0.071
15	0.018	0.024	0.038	0.058	0.072	0.061	0.100	0.057	0.054	0.043	0.015	0.065
16	0.017	0.015	0.040	0.057	0.039	0.017	0.087	0.027	0.034	0.062	0.019	0.063
17	0.016	0.014	0.039	0.032	0.054	0.061	0.025	0.052	0.026	0.044	0.035	0.015
18	0.008	0.027	0.028	0.034	0.060	0.047	0.059	0.048	0.047	0.029	0.056	0.046
19	0.063	0.066	0.037	0.043	0.086	0.055	0.029	0.137	0.094	0.085	0.039	0.054

Appendix IV

20	0.023	0.017	0.087	0.067	0.027	0.047	0.085	0.042	0.035	0.049	0.058	0.073
21	0.023	0.030	0.027	0.033	0.055	0.012	0.058	0.034	0.039	0.071	0.040	0.041
22	0.017	0.026	0.024	0.020	0.054	0.041	0.074	0.039	0.058	0.028	0.033	0.037
23	0.025	0.027	0.046	0.046	0.032	0.091	0.044	0.096	0.046	0.049	0.017	0.057
24	0.019	0.010	0.073	0.081	0.053	0.074	0.059	0.052	0.062	0.024	0.023	0.017
25	0.017	0.038	0.042	0.012	0.034	0.050	0.035	0.030	0.041	0.043	0.053	0.047
26	0.029	0.008	0.061	0.003	0.076	0.038	0.056	0.113	0.101	0.062	0.026	0.042
27	0.008	0.017	0.011	0.022	0.037	0.041	0.081	0.084	0.027	0.044	0.040	0.027
28	0.041	0.036	0.016	0.031	0.034	0.066	0.091	0.147	0.025	0.029	0.030	0.075
29	0.075	0.035	0.009	0.065	0.059	0.066	0.042	0.051	0.065	0.085	0.022	0.033
30	0.025	0.026	0.036	0.027	0.078	0.060	0.100	0.097	0.068	0.034	0.035	0.047
31	0.046	0.024	0.013	0.023	0.054	0.050	0.087	0.017	0.100	0.053	0.026	0.049
32	0.009	0.026	0.057	0.041	0.072	0.061	0.025	0.069	0.063	0.015	0.023	0.071
33	0.025	0.024	0.027	0.075	0.039	0.017	0.059	0.055	0.087	0.046	0.015	0.065
34	0.019	0.015	0.021	0.051	0.054	0.061	0.029	0.137	0.013	0.047	0.044	0.071
35	0.017	0.014	0.043	0.057	0.054	0.047	0.085	0.042	0.072	0.051	0.020	0.065
36	0.029	0.027	0.051	0.012	0.060	0.055	0.058	0.034	0.046	0.056	0.038	0.063
37	0.008	0.066	0.038	0.081	0.086	0.047	0.015	0.039	0.062	0.037	0.018	0.015
38	0.041	0.017	0.040	0.012	0.027	0.012	0.089	0.096	0.041	0.056	0.026	0.046
39	0.008	0.030	0.039	0.003	0.055	0.041	0.088	0.052	0.042	0.054	0.023	0.054
40	0.008	0.026	0.028	0.022	0.054	0.091	0.120	0.030	0.054	0.049	0.053	0.073

## Appendix IV

41	0.021	0.027	0.061	0.031	0.032	0.074	0.056	0.113	0.034	0.024	0.026	0.041
42	0.022	0.010	0.011	0.041	0.053	0.036	0.081	0.084	0.026	0.043	0.040	0.037
43	0.013	0.038	0.061	0.061	0.034	0.041	0.091	0.147	0.047	0.049	0.035	0.057
44	0.018	0.067	0.016	0.058	0.076	0.064	0.059	0.051	0.094	0.024	0.026	0.017
45	0.017	0.026	0.009	0.057	0.037	0.022	0.029	0.097	0.035	0.043	0.023	0.047
46	0.016	0.044	0.036	0.032	0.058	0.076	0.085	0.017	0.039	0.062	0.015	0.042
47	0.008	0.050	0.013	0.034	0.088	0.070	0.058	0.069	0.058	0.044	0.019	0.027
48	0.063	0.016	0.051	0.043	0.020	0.091	0.074	0.017	0.046	0.029	0.035	0.071
49	0.023	0.019	0.038	0.081	0.077	0.074	0.044	0.069	0.062	0.085	0.056	0.066
50	0.008	0.027	0.040	0.012	0.022	0.050	0.059	0.055	0.062	0.049	0.039	0.067
51	0.021	0.010	0.039	0.003	0.032	0.041	0.035	0.103	0.041	0.071	0.058	0.013
52	0.022	0.038	0.028	0.022	0.053	0.066	0.056	0.030	0.101	0.028	0.040	0.083
53	0.013	0.008	0.037	0.031	0.034	0.066	0.081	0.096	0.027	0.049	0.033	0.017
54	0.018	0.017	0.087	0.065	0.076	0.060	0.091	0.052	0.025	0.024	0.017	0.047
55	0.017	0.036	0.027	0.027	0.037	0.050	0.042	0.030	0.013	0.043	0.026	0.042
56	0.025	0.035	0.024	0.023	0.034	0.061	0.056	0.113	0.072	0.062	0.023	0.027
57	0.046	0.027	0.046	0.041	0.059	0.017	0.081	0.084	0.046	0.051	0.053	0.075
58	0.063	0.066	0.073	0.075	0.039	0.061	0.091	0.096	0.062	0.056	0.026	0.033
59	0.023	0.017	0.042	0.003	0.054	0.074	0.042	0.052	0.041	0.037	0.040	0.047
60	0.023	0.030	0.038	0.022	0.054	0.036	0.100	0.113	0.041	0.056	0.030	0.037

**Table 9: The Repeatability of GLOSSY Tiles Measured Under Specular Component Excluded Mode By CE-7000A Over 60 Weeks**

Week	Pale Grey	Middel Grey	Diff. Grey	Deep Grey	Deep Pink	Red	Orange	Bright Yellow	Green	Diff. Green	Cyan	Deep Blue
1	0.014	0.033	0.026	0.120	0.054	0.354	0.141	0.195	0.010	0.028	0.061	0.386
2	0.011	0.019	0.010	0.070	0.005	0.499	0.120	0.207	0.038	0.061	0.081	0.481
3	0.044	0.022	0.019	0.067	0.033	0.327	0.144	0.177	0.047	0.042	0.053	0.526
4	0.019	0.031	0.032	0.075	0.035	0.378	0.062	0.062	0.050	0.059	0.052	0.028
5	0.043	0.034	0.033	0.088	0.038	0.349	0.136	0.209	0.024	0.030	0.065	0.457
6	0.007	0.022	0.020	0.094	0.035	0.347	0.092	0.117	0.050	0.044	0.046	0.333
7	0.011	0.019	0.016	0.106	0.039	0.327	0.088	0.124	0.055	0.080	0.080	0.278
8	0.018	0.017	0.033	0.103	0.066	0.378	0.154	0.147	0.076	0.071	0.037	0.497
9	0.008	0.012	0.036	0.080	0.052	0.202	0.178	0.180	0.066	0.064	0.038	0.425
10	0.022	0.016	0.016	0.070	0.074	0.424	0.096	0.175	0.022	0.048	0.066	0.397
11	0.008	0.026	0.022	0.067	0.052	0.398	0.115	0.117	0.032	0.047	0.038	0.267
12	0.019	0.022	0.021	0.076	0.057	0.181	0.088	0.142	0.067	0.057	0.055	0.546
13	0.029	0.014	0.019	0.100	0.048	0.350	0.133	0.137	0.056	0.060	0.070	0.328
14	0.013	0.022	0.028	0.077	0.029	0.284	0.130	0.202	0.051	0.051	0.065	0.527
15	0.007	0.019	0.018	0.065	0.061	0.260	0.108	0.118	0.054	0.062	0.048	0.398
16	0.031	0.017	0.009	0.092	0.051	0.300	0.087	0.123	0.038	0.026	0.039	0.346
17	0.020	0.012	0.011	0.090	0.038	0.354	0.138	0.120	0.055	0.050	0.031	0.369
18	0.015	0.016	0.015	0.086	0.035	0.499	0.127	0.215	0.043	0.064	0.068	0.398
19	0.013	0.026	0.012	0.073	0.067	0.327	0.089	0.130	0.028	0.054	0.031	0.345

Appendix IV

20	0.017	0.019	0.005	0.082	0.032	0.378	0.074	0.151	0.050	0.050	0.061	0.362
21	0.015	0.017	0.016	0.081	0.048	0.202	0.149	0.112	0.032	0.040	0.036	0.404
22	0.016	0.012	0.016	0.086	0.034	0.240	0.179	0.202	0.095	0.065	0.056	0.404
23	0.019	0.016	0.018	0.106	0.064	0.459	0.141	0.209	0.055	0.088	0.064	0.028
24	0.043	0.026	0.020	0.103	0.066	0.256	0.120	0.117	0.043	0.044	0.039	0.457
25	0.007	0.022	0.016	0.080	0.052	0.301	0.144	0.124	0.028	0.080	0.031	0.333
26	0.011	0.006	0.033	0.070	0.074	0.432	0.062	0.147	0.050	0.071	0.068	0.278
27	0.018	0.032	0.036	0.067	0.052	0.349	0.136	0.180	0.032	0.064	0.031	0.497
28	0.008	0.022	0.016	0.076	0.057	0.347	0.092	0.175	0.055	0.048	0.061	0.425
29	0.022	0.009	0.022	0.100	0.029	0.264	0.127	0.117	0.076	0.047	0.036	0.397
30	0.008	0.019	0.021	0.077	0.061	0.392	0.089	0.142	0.066	0.057	0.056	0.267
31	0.014	0.014	0.019	0.120	0.051	0.343	0.074	0.195	0.022	0.060	0.064	0.546
32	0.011	0.014	0.028	0.070	0.038	0.300	0.149	0.207	0.032	0.051	0.061	0.386
33	0.044	0.033	0.018	0.067	0.035	0.354	0.179	0.177	0.067	0.062	0.081	0.481
34	0.019	0.019	0.009	0.075	0.067	0.499	0.092	0.062	0.056	0.026	0.053	0.526
35	0.043	0.022	0.010	0.088	0.032	0.327	0.088	0.209	0.051	0.050	0.052	0.028
36	0.007	0.031	0.019	0.094	0.005	0.378	0.154	0.202	0.054	0.064	0.065	0.457
37	0.008	0.034	0.032	0.065	0.033	0.459	0.178	0.118	0.010	0.064	0.046	0.346
38	0.019	0.022	0.033	0.092	0.035	0.256	0.096	0.123	0.038	0.054	0.066	0.369
39	0.029	0.019	0.020	0.090	0.038	0.301	0.115	0.120	0.047	0.050	0.038	0.398
40	0.013	0.026	0.016	0.086	0.035	0.432	0.088	0.215	0.050	0.040	0.055	0.345

## Appendix IV

41	0.007	0.022	0.033	0.073	0.039	0.349	0.133	0.130	0.024	0.065	0.070	0.362
42	0.031	0.006	0.036	0.082	0.066	0.347	0.130	0.215	0.043	0.088	0.065	0.404
43	0.007	0.032	0.016	0.081	0.074	0.264	0.108	0.130	0.028	0.044	0.048	0.404
44	0.031	0.022	0.022	0.086	0.052	0.349	0.088	0.151	0.050	0.080	0.039	0.028
45	0.020	0.009	0.018	0.073	0.057	0.347	0.133	0.112	0.032	0.028	0.031	0.497
46	0.015	0.019	0.020	0.082	0.048	0.327	0.130	0.202	0.055	0.061	0.068	0.425
47	0.013	0.014	0.016	0.081	0.029	0.378	0.108	0.175	0.076	0.042	0.031	0.397
48	0.017	0.014	0.033	0.086	0.061	0.202	0.087	0.117	0.066	0.059	0.046	0.267
49	0.015	0.033	0.036	0.106	0.051	0.424	0.138	0.112	0.022	0.030	0.080	0.546
50	0.016	0.019	0.016	0.103	0.038	0.398	0.127	0.202	0.032	0.044	0.037	0.328
51	0.019	0.016	0.022	0.080	0.035	0.347	0.089	0.209	0.067	0.080	0.038	0.527
52	0.043	0.026	0.021	0.070	0.067	0.264	0.074	0.117	0.038	0.071	0.066	0.481
53	0.007	0.022	0.019	0.067	0.066	0.392	0.144	0.124	0.055	0.050	0.038	0.526
54	0.011	0.014	0.028	0.076	0.052	0.343	0.062	0.147	0.043	0.064	0.055	0.028
55	0.031	0.022	0.018	0.100	0.074	0.300	0.136	0.180	0.028	0.054	0.053	0.457
56	0.007	0.019	0.009	0.076	0.052	0.354	0.092	0.175	0.050	0.050	0.052	0.369
57	0.031	0.017	0.010	0.100	0.057	0.499	0.127	0.062	0.032	0.040	0.065	0.398
58	0.020	0.012	0.019	0.077	0.029	0.327	0.089	0.209	0.095	0.065	0.046	0.345
59	0.017	0.016	0.032	0.120	0.061	0.378	0.074	0.202	0.055	0.088	0.066	0.362
60	0.015	0.026	0.033	0.070	0.051	0.424	0.149	0.120	0.043	0.044	0.038	0.546

**Table 10: The Repeatability of GLOSSY Tiles Measured Under Specular Component Included Mode By CE-7000A Over 60 Weeks**

Week	Pale Grey	Middel Grey	Diff. Grey	Deep Grey	Deep Pink	Red	Orange	Bright Yellow	Green	Diff. Green	Cyan	Deep Blue
1	0.022	0.012	0.014	0.050	0.037	0.054	0.081	0.113	0.040	0.060	0.061	0.088
2	0.043	0.034	0.031	0.038	0.053	0.050	0.112	0.091	0.028	0.016	0.032	0.133
3	0.037	0.012	0.037	0.014	0.041	0.037	0.105	0.086	0.018	0.014	0.032	0.096
4	0.007	0.019	0.013	0.038	0.035	0.022	0.014	0.127	0.021	0.028	0.062	0.068
5	0.018	0.017	0.016	0.044	0.020	0.030	0.072	0.115	0.010	0.018	0.027	0.096
6	0.023	0.032	0.013	0.032	0.027	0.019	0.085	0.130	0.027	0.025	0.021	0.104
7	0.021	0.011	0.014	0.048	0.021	0.083	0.077	0.100	0.013	0.012	0.042	0.099
8	0.018	0.015	0.033	0.031	0.045	0.038	0.115	0.121	0.091	0.084	0.032	0.097
9	0.006	0.025	0.015	0.047	0.009	0.076	0.080	0.074	0.018	0.028	0.036	0.098
10	0.014	0.025	0.025	0.047	0.010	0.040	0.103	0.154	0.031	0.027	0.048	0.045
11	0.009	0.019	0.012	0.059	0.039	0.087	0.062	0.091	0.019	0.011	0.062	0.124
12	0.011	0.017	0.028	0.026	0.039	0.030	0.065	0.086	0.052	0.064	0.052	0.125
13	0.033	0.020	0.032	0.052	0.030	0.054	0.087	0.130	0.020	0.033	0.043	0.060
14	0.016	0.010	0.028	0.053	0.043	0.069	0.089	0.091	0.033	0.058	0.039	0.114
15	0.018	0.012	0.033	0.023	0.021	0.011	0.055	0.141	0.014	0.038	0.038	0.100
16	0.007	0.034	0.010	0.048	0.015	0.032	0.099	0.106	0.024	0.023	0.027	0.103
17	0.017	0.012	0.012	0.036	0.020	0.036	0.057	0.074	0.043	0.020	0.046	0.096
18	0.034	0.024	0.008	0.019	0.033	0.046	0.069	0.125	0.048	0.045	0.048	0.098
19	0.027	0.021	0.025	0.044	0.033	0.054	0.093	0.003	0.054	0.048	0.059	0.121



## Appendix IV

20	0.013	0.027	0.023	0.028	0.016	0.035	0.085	0.113	0.023	0.056	0.041	0.096
21	0.004	0.025	0.018	0.037	0.025	0.025	0.098	0.100	0.017	0.032	0.038	0.095
22	0.006	0.025	0.022	0.044	0.032	0.055	0.073	0.085	0.051	0.020	0.046	0.127
23	0.014	0.032	0.017	0.032	0.039	0.038	0.072	0.142	0.031	0.042	0.027	0.068
24	0.021	0.011	0.013	0.048	0.039	0.076	0.085	0.091	0.019	0.033	0.021	0.096
25	0.018	0.015	0.014	0.031	0.030	0.040	0.077	0.086	0.052	0.058	0.042	0.104
26	0.006	0.006	0.033	0.047	0.043	0.087	0.115	0.127	0.020	0.038	0.032	0.099
27	0.014	0.018	0.015	0.047	0.021	0.030	0.080	0.115	0.033	0.023	0.036	0.097
28	0.009	0.021	0.025	0.059	0.020	0.054	0.103	0.130	0.014	0.020	0.048	0.098
29	0.011	0.005	0.012	0.026	0.027	0.069	0.062	0.100	0.024	0.045	0.062	0.045
30	0.033	0.019	0.028	0.052	0.021	0.036	0.099	0.121	0.021	0.048	0.043	0.124
31	0.007	0.012	0.032	0.053	0.045	0.046	0.057	0.113	0.010	0.056	0.039	0.125
32	0.017	0.034	0.028	0.023	0.039	0.054	0.069	0.091	0.027	0.032	0.038	0.088
33	0.034	0.012	0.014	0.048	0.039	0.035	0.093	0.086	0.013	0.060	0.027	0.133
34	0.027	0.024	0.031	0.036	0.030	0.025	0.081	0.127	0.091	0.016	0.046	0.096
35	0.023	0.021	0.037	0.019	0.043	0.055	0.112	0.115	0.018	0.014	0.048	0.068
36	0.021	0.027	0.013	0.044	0.021	0.038	0.105	0.130	0.031	0.028	0.059	0.096
37	0.018	0.025	0.016	0.028	0.015	0.076	0.014	0.100	0.040	0.018	0.061	0.104
38	0.006	0.025	0.013	0.037	0.020	0.040	0.072	0.121	0.028	0.025	0.032	0.114
39	0.022	0.032	0.014	0.050	0.037	0.087	0.085	0.100	0.018	0.012	0.032	0.100
40	0.043	0.011	0.033	0.038	0.053	0.054	0.077	0.085	0.021	0.084	0.062	0.103

Appendix IV

41	0.037	0.015	0.015	0.015	0.014	0.041	0.050	0.115	0.142	0.010	0.028	0.027	0.096
42	0.007	0.025	0.012	0.038	0.035	0.037	0.085	0.091	0.027	0.023	0.021	0.098	
43	0.018	0.019	0.008	0.044	0.033	0.022	0.077	0.089	0.051	0.020	0.042	0.121	
44	0.017	0.017	0.025	0.032	0.033	0.030	0.115	0.130	0.031	0.045	0.032	0.096	
45	0.034	0.020	0.023	0.048	0.016	0.019	0.080	0.091	0.019	0.048	0.036	0.095	
46	0.027	0.010	0.018	0.036	0.025	0.038	0.085	0.141	0.052	0.056	0.048	0.127	
47	0.023	0.012	0.022	0.019	0.021	0.076	0.077	0.106	0.020	0.032	0.062	0.096	
48	0.021	0.006	0.017	0.044	0.045	0.040	0.115	0.074	0.033	0.020	0.036	0.095	
49	0.018	0.018	0.013	0.028	0.039	0.087	0.080	0.091	0.014	0.042	0.048	0.127	
50	0.034	0.021	0.014	0.037	0.039	0.030	0.103	0.089	0.019	0.060	0.062	0.068	
51	0.027	0.005	0.033	0.044	0.053	0.054	0.062	0.130	0.052	0.016	0.043	0.096	
52	0.018	0.019	0.017	0.032	0.041	0.069	0.085	0.091	0.020	0.014	0.039	0.104	
53	0.006	0.012	0.013	0.048	0.025	0.036	0.077	0.141	0.033	0.028	0.038	0.099	
54	0.014	0.034	0.014	0.031	0.032	0.046	0.115	0.086	0.014	0.018	0.027	0.097	
55	0.009	0.019	0.033	0.047	0.039	0.054	0.080	0.127	0.024	0.025	0.046	0.088	
56	0.011	0.017	0.015	0.047	0.039	0.083	0.081	0.115	0.043	0.012	0.048	0.133	
57	0.033	0.020	0.025	0.059	0.030	0.038	0.112	0.130	0.048	0.084	0.048	0.096	
58	0.016	0.010	0.012	0.026	0.043	0.076	0.105	0.100	0.021	0.028	0.059	0.068	
59	0.018	0.012	0.028	0.038	0.021	0.040	0.014	0.121	0.010	0.028	0.061	0.096	
60	0.007	0.034	0.032	0.014	0.015	0.087	0.072	0.130	0.027	0.023	0.032	0.104	

**Table 11: The Repeatability of MATT Tiles Measured Under Specular Component Excluded Mode By CE-7000A Over 60 Weeks**

Week	Pale Grey	Middel Grey	Diff. Grey	Deep Grey	Deep Pink	Red	Orange	Bright Yellow	Green	Diff. Green	Cyan	Deep Blue
1	0.029	0.026	0.049	0.063	0.068	0.064	0.117	0.024	0.054	0.055	0.089	0.054
2	0.014	0.024	0.013	0.068	0.059	0.046	0.098	0.045	0.028	0.029	0.040	0.080
3	0.031	0.010	0.036	0.029	0.055	0.031	0.174	0.030	0.012	0.047	0.075	0.080
4	0.016	0.034	0.015	0.026	0.032	0.017	0.091	0.017	0.026	0.028	0.008	0.100
5	0.077	0.010	0.025	0.019	0.029	0.087	0.137	0.052	0.061	0.035	0.088	0.051
6	0.019	0.023	0.031	0.051	0.046	0.053	0.058	0.086	0.058	0.058	0.042	0.066
7	0.016	0.031	0.028	0.046	0.045	0.068	0.112	0.020	0.019	0.031	0.031	0.061
8	0.019	0.018	0.044	0.055	0.032	0.067	0.072	0.074	0.048	0.047	0.058	0.067
9	0.006	0.024	0.020	0.045	0.068	0.106	0.231	0.067	0.058	0.062	0.042	0.091
10	0.029	0.025	0.052	0.051	0.052	0.062	0.089	0.038	0.049	0.033	0.064	0.054
11	0.014	0.038	0.051	0.059	0.060	0.060	0.092	0.056	0.059	0.040	0.037	0.080
12	0.031	0.038	0.015	0.022	0.040	0.048	0.111	0.023	0.035	0.040	0.046	0.080
13	0.016	0.022	0.017	0.049	0.046	0.047	0.104	0.038	0.048	0.062	0.044	0.100
14	0.012	0.022	0.040	0.041	0.050	0.051	0.107	0.056	0.050	0.018	0.034	0.051
15	0.010	0.024	0.034	0.031	0.032	0.034	0.059	0.050	0.037	0.027	0.056	0.063
16	0.077	0.021	0.040	0.055	0.047	0.066	0.135	0.074	0.079	0.043	0.046	0.064
17	0.019	0.030	0.013	0.028	0.022	0.040	0.079	0.067	0.034	0.056	0.040	0.051
18	0.019	0.005	0.054	0.071	0.062	0.063	0.088	0.077	0.051	0.026	0.041	0.058
19	0.040	0.038	0.018	0.034	0.050	0.041	0.137	0.025	0.059	0.007	0.047	0.077

## Appendix IV

20	0.057	0.012	0.036	0.059	0.050	0.061	0.061	0.091	0.048	0.014	0.033	0.065
21	0.017	0.018	0.030	0.042	0.049	0.056	0.111	0.086	0.051	0.029	0.042	0.066
22	0.008	0.013	0.026	0.047	0.040	0.054	0.120	0.020	0.065	0.028	0.045	0.061
23	0.013	0.028	0.044	0.019	0.052	0.106	0.137	0.074	0.058	0.031	0.064	0.075
24	0.018	0.010	0.020	0.051	0.060	0.062	0.058	0.067	0.019	0.047	0.037	0.066
25	0.038	0.023	0.052	0.046	0.040	0.060	0.112	0.038	0.048	0.062	0.046	0.061
26	0.050	0.031	0.051	0.055	0.046	0.048	0.072	0.056	0.058	0.033	0.044	0.067
27	0.011	0.018	0.015	0.068	0.050	0.047	0.231	0.050	0.049	0.040	0.034	0.091
28	0.025	0.021	0.034	0.029	0.032	0.051	0.089	0.079	0.012	0.040	0.008	0.054
29	0.019	0.030	0.040	0.026	0.047	0.040	0.092	0.040	0.026	0.062	0.088	0.080
30	0.029	0.005	0.013	0.019	0.032	0.063	0.174	0.077	0.061	0.018	0.042	0.051
31	0.014	0.038	0.036	0.051	0.029	0.041	0.091	0.025	0.058	0.027	0.031	0.058
32	0.031	0.012	0.015	0.046	0.068	0.061	0.137	0.091	0.034	0.018	0.058	0.077
33	0.016	0.018	0.025	0.022	0.059	0.047	0.089	0.086	0.051	0.027	0.089	0.065
34	0.012	0.026	0.015	0.049	0.055	0.051	0.092	0.020	0.059	0.043	0.040	0.066
35	0.010	0.024	0.017	0.041	0.032	0.034	0.111	0.074	0.048	0.056	0.075	0.061
36	0.019	0.010	0.040	0.031	0.029	0.066	0.104	0.067	0.051	0.026	0.008	0.087
37	0.019	0.034	0.034	0.055	0.046	0.040	0.107	0.087	0.012	0.007	0.088	0.084
38	0.040	0.010	0.049	0.028	0.040	0.063	0.117	0.048	0.026	0.014	0.058	0.020
39	0.057	0.023	0.013	0.071	0.046	0.064	0.098	0.032	0.061	0.029	0.042	0.060
40	0.017	0.023	0.036	0.063	0.050	0.046	0.174	0.058	0.058	0.028	0.064	0.075

Appendix IV

41	0.008	0.031	0.015	0.068	0.032	0.031	0.091	0.023	0.019	0.058	0.037	0.100
42	0.013	0.018	0.025	0.029	0.047	0.017	0.137	0.038	0.048	0.031	0.046	0.051
43	0.016	0.024	0.031	0.026	0.046	0.061	0.058	0.056	0.058	0.047	0.044	0.063
44	0.019	0.025	0.018	0.019	0.050	0.056	0.120	0.050	0.058	0.062	0.034	0.064
45	0.006	0.038	0.036	0.051	0.032	0.054	0.137	0.024	0.049	0.033	0.056	0.051
46	0.029	0.038	0.030	0.059	0.047	0.106	0.058	0.045	0.012	0.040	0.047	0.058
47	0.014	0.022	0.026	0.022	0.022	0.062	0.112	0.030	0.026	0.055	0.033	0.077
48	0.008	0.012	0.044	0.049	0.062	0.060	0.174	0.017	0.061	0.029	0.042	0.065
49	0.013	0.018	0.044	0.041	0.050	0.048	0.091	0.052	0.058	0.047	0.045	0.077
50	0.018	0.013	0.020	0.031	0.050	0.087	0.137	0.077	0.034	0.028	0.064	0.065
51	0.038	0.028	0.052	0.055	0.032	0.053	0.089	0.025	0.049	0.062	0.037	0.066
52	0.050	0.021	0.051	0.046	0.068	0.068	0.120	0.091	0.059	0.018	0.046	0.061
53	0.011	0.030	0.015	0.055	0.052	0.067	0.137	0.086	0.035	0.027	0.044	0.087
54	0.025	0.005	0.017	0.045	0.060	0.106	0.058	0.020	0.048	0.018	0.034	0.084
55	0.018	0.012	0.040	0.051	0.040	0.061	0.112	0.074	0.050	0.027	0.046	0.020
56	0.038	0.018	0.034	0.049	0.032	0.056	0.072	0.067	0.037	0.058	0.040	0.063
57	0.050	0.010	0.040	0.041	0.047	0.054	0.098	0.087	0.079	0.031	0.041	0.064
58	0.011	0.023	0.013	0.031	0.032	0.106	0.174	0.048	0.026	0.018	0.047	0.051
59	0.025	0.023	0.054	0.055	0.047	0.062	0.091	0.032	0.061	0.027	0.033	0.058
60	0.019	0.031	0.030	0.028	0.022	0.060	0.137	0.067	0.059	0.018	0.042	0.077

**Table 12: The Repeatability of MATT Tiles Measured Under Specular Component Included Mode By CE-7000A Over 60 Weeks**

Week	Pale Grey	Middel Grey	Diff. Grey	Deep Grey	Deep Pink	Red	Orange	Bright Yellow	Green	Diff. Green	Cyan	Deep Blue
1	0.016	0.025	0.021	0.034	0.026	0.134	0.075	0.054	0.061	0.051	0.073	0.071
2	0.059	0.013	0.045	0.032	0.030	0.039	0.044	0.084	0.060	0.027	0.036	0.054
3	0.059	0.034	0.031	0.023	0.032	0.051	0.074	0.059	0.047	0.033	0.079	0.043
4	0.019	0.017	0.014	0.024	0.038	0.054	0.074	0.054	0.024	0.034	0.032	0.024
5	0.052	0.006	0.025	0.031	0.030	0.082	0.067	0.064	0.029	0.011	0.042	0.054
6	0.011	0.017	0.031	0.047	0.034	0.045	0.043	0.036	0.065	0.032	0.053	0.041
7	0.040	0.007	0.021	0.015	0.015	0.067	0.075	0.048	0.046	0.054	0.027	0.055
8	0.015	0.043	0.037	0.043	0.045	0.051	0.077	0.034	0.047	0.045	0.026	0.039
9	0.073	0.028	0.026	0.027	0.055	0.072	0.108	0.060	0.077	0.035	0.045	0.047
10	0.013	0.016	0.040	0.041	0.028	0.134	0.085	0.041	0.038	0.033	0.029	0.048
11	0.013	0.026	0.011	0.043	0.036	0.048	0.021	0.061	0.043	0.021	0.021	0.044
12	0.046	0.014	0.019	0.003	0.019	0.054	0.021	0.085	0.035	0.025	0.056	0.038
13	0.020	0.015	0.047	0.037	0.040	0.082	0.102	0.069	0.074	0.021	0.052	0.036
14	0.019	0.025	0.024	0.022	0.032	0.045	0.084		0.042	0.051	0.024	0.088
15	0.023	0.013	0.017	0.046	0.046	0.085	0.044		0.076	0.043	0.065	0.049
16	0.016	0.034	0.016	0.046	0.044	0.085	0.102		0.056	0.061	0.042	0.072
17	0.022	0.017	0.017	0.044	0.052	0.085	0.045		0.073	0.031	0.058	0.072
18	0.030	0.033	0.020	0.046	0.046	0.048	0.090		0.073	0.061	0.053	0.071
19	0.025	0.010	0.025	0.059	0.058	0.054	0.059		0.070	0.041	0.057	0.073

## Appendix IV

20	0.023	0.017	0.035	0.043	0.040	0.082	0.059	0.085	0.053	0.037	0.053	0.084
21	0.040	0.006	0.017	0.026	0.029	0.045	0.046	0.069	0.054	0.044	0.031	0.070
22	0.031	0.017	0.026	0.048	0.036	0.067	0.063	0.085	0.065	0.018	0.041	0.062
23	0.015	0.007	0.021	0.027	0.046	0.051	0.021	0.034	0.047	0.036	0.053	0.080
24	0.073	0.012	0.026	0.041	0.044	0.072	0.021	0.019	0.077	0.032	0.027	0.054
25	0.013	0.030	0.040	0.043	0.052	0.134	0.102	0.046	0.038	0.054	0.026	0.041
26	0.013	0.009	0.011	0.003	0.046	0.039	0.084	0.076	0.043	0.045	0.045	0.055
27	0.046	0.020	0.019	0.037	0.045	0.051	0.044	0.056	0.035	0.035	0.029	0.039
28	0.059	0.013	0.047	0.022	0.055	0.054	0.102	0.075	0.074	0.033	0.021	0.047
29	0.019	0.033	0.024	0.037	0.028	0.068	0.045	0.085	0.070	0.025	0.056	0.048
30	0.052	0.010	0.020	0.022	0.036	0.076	0.090	0.034	0.053	0.021	0.052	0.044
31	0.011	0.017	0.025	0.046	0.026	0.072	0.067	0.019	0.054	0.051	0.024	0.038
32	0.040	0.006	0.035	0.046	0.030	0.078	0.043	0.046	0.065	0.043	0.036	0.049
33	0.015	0.017	0.017	0.044	0.032	0.067	0.075	0.060	0.035	0.061	0.079	0.072
34	0.073	0.007	0.014	0.031	0.038	0.089	0.077	0.041	0.074	0.031	0.032	0.072
35	0.020	0.012	0.025	0.047	0.030	0.081	0.108	0.061	0.042	0.051	0.042	0.024
36	0.019	0.030	0.031	0.015	0.034	0.072	0.085	0.048	0.076	0.027	0.053	0.054
37	0.023	0.009	0.021	0.043	0.015	0.062	0.044	0.034	0.056	0.033	0.027	0.041
38	0.016	0.013	0.021	0.034	0.045	0.079	0.102	0.060	0.073	0.034	0.056	0.055
39	0.022	0.034	0.045	0.032	0.040	0.067	0.045	0.041	0.073	0.011	0.052	0.071
40	0.030	0.017	0.031	0.023	0.032	0.051	0.090	0.061	0.061	0.051	0.024	0.054

Appendix IV

41	0.025	0.006	0.014	0.024	0.046	0.072	0.059	0.085	0.060	0.043	0.065	0.043
42	0.023	0.017	0.025	0.003	0.044	0.134	0.059	0.069	0.047	0.061	0.042	0.024
43	0.040	0.007	0.026	0.037	0.052	0.039	0.046	0.085	0.029	0.031	0.058	0.054
44	0.019	0.043	0.021	0.022	0.046	0.051	0.063	0.034	0.065	0.061	0.053	0.080
45	0.052	0.043	0.026	0.046	0.058	0.054	0.044	0.019	0.046	0.041	0.057	0.054
46	0.011	0.028	0.040	0.046	0.040	0.068	0.074	0.046	0.047	0.037	0.053	0.041
47	0.040	0.016	0.026	0.044	0.029	0.076	0.074	0.076	0.077	0.044	0.031	0.055
48	0.015	0.026	0.040	0.046	0.036	0.076	0.067	0.056	0.038	0.031	0.041	0.044
49	0.073	0.014	0.011	0.059	0.046	0.072	0.043	0.075	0.043	0.061	0.026	0.038
50	0.013	0.015	0.019	0.043	0.046	0.078	0.075	0.054	0.035	0.041	0.045	0.049
51	0.025	0.033	0.011	0.031	0.044	0.067	0.021	0.084	0.074	0.037	0.029	0.072
52	0.023	0.010	0.019	0.047	0.052	0.089	0.102	0.059	0.042	0.044	0.021	0.072
53	0.040	0.017	0.021	0.015	0.046	0.081	0.084	0.054	0.076	0.018	0.056	0.024
54	0.031	0.006	0.045	0.043	0.045	0.072	0.044	0.064	0.056	0.027	0.052	0.055
55	0.015	0.030	0.031	0.027	0.055	0.134	0.102	0.036	0.074	0.033	0.024	0.039
56	0.073	0.009	0.014	0.041	0.032	0.039	0.045	0.048	0.070	0.034	0.065	0.047
57	0.020	0.020	0.025	0.043	0.038	0.051	0.090	0.069	0.053	0.011	0.042	0.048
58	0.019	0.013	0.031	0.031	0.030	0.054	0.067	0.085	0.054	0.032	0.058	0.044
59	0.023	0.033	0.021	0.047	0.034	0.068	0.043	0.034	0.065	0.054	0.053	0.038
60	0.016	0.010	0.037	0.015	0.015	0.076	0.077	0.019	0.035	0.041	0.057	0.049